On The Biophysical Factors That Control Under-Ice Phytoplankton Bloom Onset in the Central Canadian Archipelago

By

Matthew A. Gale

A thesis submitted to the Faculty of Graduate Studies of

The University of Manitoba

In partial fulfilment of the requirements of the degree of

MASTER OF SCIENCE

Department of Environment and Geography

University of Manitoba

Abstract

Sporadic reports of significant under-ice phytoplankton production indicate a critical knowledge gap of a key component of the Arctic ecosystem. In this thesis I examine the following research objectives in an effort to improve the understanding of under-ice phytoplankton production: (1) to determine the biophysical processes controlling the timing of under-ice phytoplankton production, and (2) to compare and contrast both the timing of the under-ice bloom and the controlling processes between multiple years of data.

Data for objective (1) were collected during the three-year Arctic-ICE field campaign (2010-2012) near Resolute Bay, NU in the central Canadian Arctic. Additional data from the region were collected from open source databases and peer-reviewed literature for a dataset that spanned from early 1960 to the present, supporting the analysis to meet objective (2). Two separate under-ice phytoplankton blooms were observed during the three-year Arctic-ICE campaign. It was found that phytoplankton blooms conformed well to the critical depth hypothesis in the Canadian Archipelago under first-year ice, where snow and ice melt both increased light transmission and shoaled the surface mixed layer which, in turn, placed phytoplankton within a favourable light environment for positive net production underneath the ice cover. Factors such as timing of melt water drainage and water column mixing greatly affected bloom onset.

From the historical analyses, I was able to show that under-ice phytoplankton blooms have regularly occurred under landfast ice from at least the 1960's. Significant correlations between the timing of bloom onset with melt onset related variables (i.e., air temperature reaching 0 ºC and complete snow melt) suggested a strong link to climate change. In fact, the

analysis supported that since the mid 1990s bloom onset has been occurring earlier, and is likely related to decreasing trends in day of complete snow melt, maximum ice thickness, and snow depth.

Overall, this thesis has helped improve our understanding of the under-ice spring phytoplankton bloom, showing that under-ice production has been a regular occurrence in the Canadian Arctic. The results also support that timing of the spring phytoplankton blooms could be shifting earlier in response to the warming Arctic and its changing icescape. Such a shift could also have important consequences on the Arctic marine food web, influencing the transfer of energy through the food chain. Therefore, it is of utmost importance to continue future observational programs of the under-ice pelagic environment focussed on the late spring melt period to better understand how the system could change with further perturbations.

Acknowledgements

I would like to thank my advisor Dr. CJ Mundy, who gave me direction and encouragement during the entirety of this difficult project, as well as my committee members Drs. Andrea Niemi and Mark Hanson for their insight and suggestions. My wife Lauren who is a constant source of inspiration, and who is ever present when I need her; my mother Marsha who spent countless hours reading early editions of chapters and teaching me grammar rules.

I would also like to express my gratitude to those people who were involved in the collection of the data during the Arctic-ICE campaigns, particularly, Karley Campbell, Marjolaine Blais, Virginie Galindo, and Margaux Gourdal and all the others who made working in such a remote region, feel like home, for our extended stay.

My thanks also goes to the organizations which have supported me during this project: Polar Continental Shelf Program, Aboriginal Affairs and Northern Development Canada, University of Manitoba and the Centre for Earth Observation Science, Manitoba Government, Nunavut Government, Arctic Science Partnership and Dr. Michel Gosselin at Institut des sciences de la mer de Rimouski.

Finally I would like to extend an extra special thanks to the CEOS support staff members Linda Chow and Fei Fei Zhao, for guiding me throughout the never ending paperwork of conducting science and being a graduate student. Without the both of you reminding me about deadlines, and your thorough explanations of how to fill things out properly I surely would have been lost.

- - - I dedicate this to the concept of friendship - - -

Table of Contents

List of Figures

List of Tables

Chapter One: **Introduction**

The Arctic marine environment is experiencing warming at an unprecedented pace (Comiso et al., 2008). There has been a rapid loss of thick multiyear ice (Maslanik et al., 2007; Barber et al., 2009, Stroeve et al., 2012) and a growing summer melt season (Polykov et al., 2005; Markus et al. 2009). The result is a thinner and less opaque Arctic Ocean ice cover (Nicolaus et al., 2012), with an earlier melt onset (Markus et al., 2009). Water mass characteristics and distribution are also being altered through changes to freshwater input (river run-off and ice melt) and enhanced atmosphere-ocean coupling (McLaughlin et al., 2002). These changes are influencing the Arctic ice-covered marine ecosystem; however, to an unknown extent.

In the face of this rapidly changing climate, we lack an understanding of crucial components of the ecosystem. Two papers in particular highlight a critical gap in knowledge with respect to under-ice phytoplankton production (Mundy et al., 2009; Arrigo et al., 2012); whereas previous studies in the Arctic (Grebmeier et al., 1995; Sakshaug, 2004) have assumed negligible under-ice production due to the strong light attenuation properties of snow, sea ice, and ice algae. It is significant to note that phytoplankton play a multi-faceted role in biogeochemical cycles. They not only sustain life in food webs, but also sequester greenhouse gases into the deep ocean for extended periods of time (Falkowski, 1994). This process of deep sequestration of organic carbon is known as the carbon pump. Surface ocean circulation and regional environmental characteristics influence primary production, and thus the carbon pump in different regions (Takahashi et al., 2009). Understanding the role of primary production and the regionally dependent carbon pump in the global oceans is of principal importance due to the current anthropogenically induced rise in atmospheric CO_2 levels. However, in the face of a

rapidly changing climate, we lack an understanding of important components of the ecosystem. It has been common in the Arctic to assume negligible under-ice production due to the strong light attenuation properties of snow, sea ice, and ice algae (Grebmeier et al., 1995; Sakshaug, 2004). However, a critical gap in knowledge with respect to under-ice phytoplankton production has been recently highlighted (Mundy et al., 2009; Arrigo et al., 2012).

In the Arctic, phytoplankton blooms likely conform to the critical depth hypothesis (Figure 1.1). The critical depth hypothesis states that the depth where phytoplankton growth equals net biomass losses must be greater than the surface mixed layer depth for a bloom to develop. During the Arctic spring, ice melt contributes to a shoaling of the surface mixed layer, resulting in phytoplankton becoming confined within the upper water column. Furthermore, because of sub-ice winter mixing processes that infuse nutrients into surface waters, nutrients are typically in ample supply in the spring water column (Prinsenberg and Ingram, 1991; Carmack et al., 2006; Bourgault et al., 2011). These two factors, combined with a rapid increase in transmitted light to the under-ice water column associated with ice melt and the formation of melt ponds (Frey et al., 2011; Ehn et al., 2011), provide favourable conditions for positive net primary production to occur under the ice cover (Mundy et al., 2009).

Bays, channels, and inlets of the Canadian Arctic Archipelago with their shallow basins, limited atmospheric driven mixing events, and annual formation of a landfast first-year ice cover should conform quite well to the critical depth hypothesis for under ice blooms. Additionally, first-year ice transmits three times more light than multi-year ice (Nicolaus et al., 2012). This increase in transmission is due to a higher spatial melt pond coverage associated with less surface topography on first-year ice (Polashenski et al., 2012; Nicolaus et al., 2012). It has been suggested that these conditions present an ideal environment for an early spring bloom to

develop under landfast first-year sea ice prior to ice-break-up (Mundy et al., 2009). Indeed, previous reports have shown that significant under-ice blooms have been observed across the Arctic, such as in the Barents Sea (Strass and Nöthig, 1996), Chukchi Sea (Arrigo et al., 2012), Beaufort Sea (Mundy et al., 2009), and the Canadian Archipelago (Fortier et al., 2002; Apollonio and Matrai, 2011; Mundy et al., 2014).

My thesis research will seek (1) To determine the biophysical processes controlling the timing of under-ice phytoplankton production in Resolute Bay, NU; and (2) To compare and contrast the timing of the under-ice bloom and controlling processes between different years. While investigating objective (1), I hypothesize that critical depth theory plays a vital role in the mitigation of the under-ice phytoplankton blooms in the Canadian Archipelago as a function of increasing light transmission and melt water stratification associated with snow and ice melt in spring. For objective (2), an underlying hypothesis of my thesis is that under-ice pelagic primary production has been a regular, yet under-documented phenomenon in the Arctic. Additionally, as the deepening of the euphotic zone in spring is linked to an increasing earlier sea ice melt onset (ACIA, 2005; Markus et al., 2009), I further hypothesize that the timing of under-ice phytoplankton production is occurring earlier in the Arctic. My thesis will seek to test these hypotheses using recent and historical datasets collected in the central Arctic region with a specific focus on Resolute Passage, NU, Canada.

My thesis is separated into five chapters. The first chapter provides an introduction to the significance of the research, the thesis objectives, and a background on relevant theory required for a better understanding of the thesis' field of research. In the second chapter, I describe the datasets collected in support of the research, which include a field and an historical dataset, and the analysis used to meet the posed objectives. Chapter three describes the pertinent results

observed in the datasets and chapter four discusses these results in the context of the thesis' objectives. The thesis is concluded with a fifth chapter, including a discussion of recommendations for future work in the research field.

1.0 Background

1.0.1 Phytoplankton

Primary producers are organisms that can convert inorganic carbon to organic carbon through either photosynthesis or chemosynthesis, with the majority using photosynthesis. These organisms include plants, bacteria, and phytoplankton. The word phytoplankton is based on the Greek terms, *phyton*, meaning plant, and *planktos*, meaning passive drifter. Phytoplankton are microscopic autotrophs that range in size from approximately 0.2 to 200 μm and are found in both freshwater and marine environments (Jeffrey et al., 2005). Marine phytoplankton account for >40% of total primary production on a global scale; however, their total standing stock at any one time is less than 1% global biomass (Falkowski, 1994). This highlights the rapid turnover time of phytoplankton relative to the large standing stocks associated with terrestrial plants. In order to provide a general overview of phytoplankton, this sub-section describes the process of photosynthesis, the main limiting factors that determine phytoplankton growth in seawater (light and nutrients), what is meant by a phytoplankton bloom and how critical depth theory can be applied to help describe why blooms typically develop in springtime temperate through sub-polar oceanographic regions.

1.0.1.1 Photosynthesis

Photosynthesis is the chief process by which carbon dioxide (CO_2) is fixed into chemical energy. The process of photosynthesis results in the production of biomass and the rate of change in the amount of biomass is defined as primary production (Falkowski and Raven, 1997). Biomass can be defined in many ways, typically represented by one of the main elements fixed into organic matter during growth of a primary producer (e.g., C, N, P, Si,). However, due to its essential role in photosynthesis, chlorophyll *a* (Chl *a*) is commonly used as a proxy of photosynthetic biomass.

Reviews of photosynthesis can be found in numerous texts and articles and the process itself is relatively well-understood (e.g., Lehninger, 1970; Kirk, 1994; Jeffrey et al., 2005; Falkowski and Raven, 1997; Nelson and Cox, 2000). The process can be represented through the following general chemical equation 1.1:

$$CO_2 + 2H_2O \xrightarrow{\text{LIGHT}} (CH_2O) + H_2O + O_2 \qquad (1.1)$$

Photosynthesis takes place in organelles called chloroplasts of eukaryotic algae and higher plants. The chloroplast contains a number of flat vesicles (pockets) known as thylakoids. Embedded along the thylakoid membranes are sets of two photosystems linked by electron transport complexes, known collectively as photosynthetic apparatuses. Pigments, namely Chl *a*, are the main components of the photosystems as they absorb light that is then used to catalyze a series of reactions that oxidize water molecules and generate chemical reducing agents (reductants). This first stage of the photosynthetic process is known as light-dependent reactions,

as light is the catalyst for the process. The freed H^+ ions evolved from the oxidation of water also create a gradient across the thylakoid membranes. The ion is then harnessed through enzymes to produce further reductants.

The reductants produced by the photosynthetic apparatuses are found in the stroma, an aqueous solution surrounding the thylakoids. It is here that the light-independent reactions take place, reliant upon the reductants of the light-dependent reactions. Coupled to particular enzymes in the stroma, namely RuBisCO (Ribulose-1, 5-bisphosphate carboxylase/oxygenase), the reductants are used to reduce CO_2 and ultimately fix carbohydrates.

The carbohydrates are essential energy stores used for other metabolic reactions in phytoplankton, which in turn result in necessary cellular components such as: lipids, pigments for photosynthesis, enzymes, carriers of electrons, amino and nucleic acids, etc. These additional cellular components are essential for organism growth and reproduction. It is through these latter steps that other essential elements are fixed into organic molecules.

1.0.1.2 Light and Nutrients as Limiting Factors

Although many factors play a role in the rate of phytoplankton growth, a considerable amount of variability can be explained by access to light and nutrients in their environment. Both light and nutrients are essential for photosynthesis to take place. Therefore, limiting access to either of these resources will limit production. Because of the need for both resources, phytoplankton production is constantly in a relative balance between access to light and nutrients.

Sunlight at the top of the atmosphere is a constant. However, energy reaching the earth and ocean surfaces fluctuates with a sun angle that varies with time of day and season, according

to the Earth's rotation and revolution around the sun, respectively (Kirk, 1994). Light is attenuated in the atmosphere by water vapour (clouds) and a variety of aerosols and gases (e.g., CO_2). Most of the sun's energy transmitted through the atmosphere is in the visible (VIS) portion of the spectrum with tails of the spectrum into high wavelength ultraviolet (UV) and low wavelength infrared (IR). Roughly 50% of the sun's energy is lost before it even hits the ocean's surface due to reflection, scattering, and absorption associated with the atmosphere and clouds (Lalli and Parsons, 1997). Upon penetrating the ocean, approximately 50% of the surface incident radiation is reflected and attenuated within the uppermost metres of the water column, although most of this attenuation occurs at UV and IR wavelengths, leaving mostly photosynthetically active radiation (PAR; 400-700 nm) to penetrate to depth (Pope and Fry, 1997). Additionally, attenuation is altered in both quantity and spectral quality by other substances found in the water, such as chromophoric dissolved organic matter (CDOM), suspended organic matter, and phytoplankton (Prieur and Sathyendranath, 1981; Kirk, 1994). Therefore, phytoplankton growth is restricted to the upper layers of the water column known as the euphotic zone. The euphotic zone is typically defined as the surface layer down to the level where light is reduced to 1.0 (Kirk, 1994) to 0.2% (Knap et al., 1996) surface levels.

In terms of nutrients, the cellular components of phytoplankton require not only C, H, and O, but additional macronutrients such as N, S, P, Si, K, Na, Ca, Mg and Cl, as well as some micronutrients Fe, Mn, Cu, Zn, Co and Mo (Lalli and Parsons, 1997). Nitrogen is perhaps the most likely limiting nutrient in temperate and more northerly marine regions of the northern hemisphere (Falkowski, 2002), although some regions of the global oceans can be limited by micronutrients such as Fe, leading to so-called HNLC (High-Nitrate, Low-Chlorophyll) waters (Falkowski, 1997). For the most part, phytoplankton can only utilize fixed forms of nitrogen,

such as nitrate, nitrite, and ammonia, although cyanobacteria are capable of fixing N_2 (McCarthy, 2002). Therefore, once used up through primary production in surface waters, fixed nitrogen can become limiting, accessible through either remineralisation by microbes or by mixing, upwelling, and/or diffusion from deeper waters.

1.0.1.3 Spring Phytoplankton Bloom

Changes in biomass of phytoplankton in the upper layers of any marine body can be summarized by the following equation:

$$\frac{\Delta B}{\Delta t} = P - [R + G + S] \quad (1.2)$$

Where *B* is biomass, t is time, *P* is gross primary production, *R* is community respiration, *G* is grazing by large herbivores and production of faecal pellets and *S* is sedimentation of intact cells (Lalli and Parsons, 1997). Equation (1.2) shows that for a bloom to occur, *P* needs to be much greater than the sum of loss terms in between the square brackets. Holligan (1987) stated that a bloom of phytoplankton is defined as an abnormally high concentration of cells due to division of the phytoplankton cells and active or passive aggregations. Legendre (1990) took this same approach and defined blooms as a rapid increase in biomass caused by local driving factors that result in abnormally high cell counts.

The marine spring bloom refers to an exponential growth of primary producers, which characteristically takes place during early spring and lasts until early summer (approximately April to June). This annual event is typical in the North Atlantic as well as sub-polar waters (Miller and Wheeler, 2012). Duration, extent, and magnitude of the bloom depend on various environmental inputs and conditions, including light, nutrients, and temperature, as well as seasonal surface stratification of the water column (Miller and Wheeler, 2012).

In the North Atlantic, the spring bloom is preconditioned by winter events, such as wind and temperature driven turbulent convection that degrade surface stratification of the water column. This degradation mixes nutrients from depth into surface waters (Miller and Wheeler, 2012). The reduced incoming solar radiation during winter months limits the growth of phytoplankton, while bacteria continue to remineralize nutrients, further replenishing the surface water nutrient stock (Miller and Wheeler, 2012).

During spring, turbulent convective forces driving surface mixing weaken as temperatures reach above freezing (Taylor and Ferrari, 2011). Eventually, the water thermally stratifies, while incoming solar radiation increases light availability at the same time (Miller and Wheeler, 2012). Thermal stratification inhibits further mixing between the surface mixed layer and waters below the pycnocline, confining phytoplankton to the nutrient-replete surface layer that rests within the euphotic zone (Miller and Wheeler, 2012). With a deepening euphotic zone and nutrients available in sufficient quantities, primary production undergoes exponential growth with doubling of cells up to once per day (Miller and Wheeler, 2012). Furthermore, zooplankton grazing classically lags behind the spring bloom (Falk-Petersen et al., 1990), permitting phytoplankton biomass to exponentially accumulate in the euphotic zone (Miller and Wheeler, 2012).

Both the pelagic and benthic food webs largely rely on the spring bloom. In particular, some zooplankton species time their spawning to coincide with the annual bloom (Cushing, 1990). Generally, in the late spring or early summer, spring blooms can collapse due to nutrient depletion and/or grazing pressure from zooplankton, (Miller and Wheeler, 2012).

At more northern latitudes that remain relatively ice-free, a delayed timing in the bloom is observed due to the shift in the seasonal incoming solar radiation (insolation) cycle with

latitude (Leu et al., 2010). The result is a longer period of light limitation and a delay in thermal stratification of the upper water column. In addition, the shorter warm season slows zooplankton grazing pressures as their metabolism is dependent on water temperatures (Sherr et al., 2009).

1.0.1.4 Critical Depth Hypothesis

Critical depth (Gran and Braarud, 1935) has been defined as the depth at which respiration and production integrated over the upper water column are balanced. That is, it is the depth at which the water column integrated net growth rate becomes zero (Figure 1.1). Net growth is defined as the total growth rate minus respiration losses. The hypothesis, developed by Sverdrup (1953), assumes that the loss rate for the phytoplankton community is a relatively constant rate at all depths and times.

Sverdrup (1953) hypothesized that shoaling of the mixed layer depth above the critical depth is the cause of annual spring blooms in temperate oceans. This hypothesis suggests that if the mixed layer depth exceeds the critical depth, a bloom cannot develop (Figure 1.1). Alternatively, if the mixed layer depth was shallower than the critical depth, the phytoplankton community would experience a positive mixed layer integrated net growth rate. Originally, critical depth theory was developed to explain the timing of annual spring blooms in the mid-latitudes Atlantic Ocean. Stratification in this region is based predominantly on temperature gradients. The concept followed that the increase of insolation during spring both deepened the euphotic zone while thermally stratifying the surface ocean through increased light absorption. The result was a rapid switch to a surface mixed layer that was less deep than the critical depth and therefore, a spring bloom ensued. As described in detail by Lalli and Parsons (1997) gross

photosynthesis declines at an exponential rate in accordance with Beer's law as a function of water column light attenuation:

$$I_z = I_0 e^{-kz} \quad (1.3)$$

where k is the attenuation coefficient (m^{-1}) due to absorption and scattering properties of the water, z is water column depth (m), and I_0 and I_z are the light intensities (μmol m^{-2} s^{-1}) penetrating the surface water and transmitted to z, respectively. Using Beer's law, the average water column light intensity over z, $\overline{I_z}$ (μmol m^{-2} s^{-1}), can be calculated as follows:

$$\overline{I_z} = \frac{I_0}{kz}(1 - e^{-kz}) \quad (1.4)$$

Compensation depth (z_C) is defined as the depth where photosynthesis is equal to respiration. The transmitted light intensity at this point is called the compensation light intensity (Ic). Therefore, above z_C net primary production is positive and below it is negative. Sverdrup (1953) demonstrated that the depth at which $\overline{I_z}$ equals I_C is the critical depth. That is, replacing $\overline{I_z}$ with I_C in equation (2), z becomes the critical depth (z_{Cr}). Then, through minor adjustments to equation (2), you can obtain:

$$z_{Cr} = \frac{I_0}{kI_C}(1 - e^{-kz_{Cr}}) \quad (1.5)$$

Finally, given z_{Cr} as a large number, the exponent in equation (1.5) becomes large, resulting in the following approximation:

$$z_{Cr} \approx \frac{I_0}{kI_c} \quad (1.6)$$

This approximation provided in Lalli and Parsons (1997), represents a useful tool to calculate the critical depth using light measurements and a value for I_C obtained from the literature. However, it may not work for sea ice as the critical depth is not as deep.

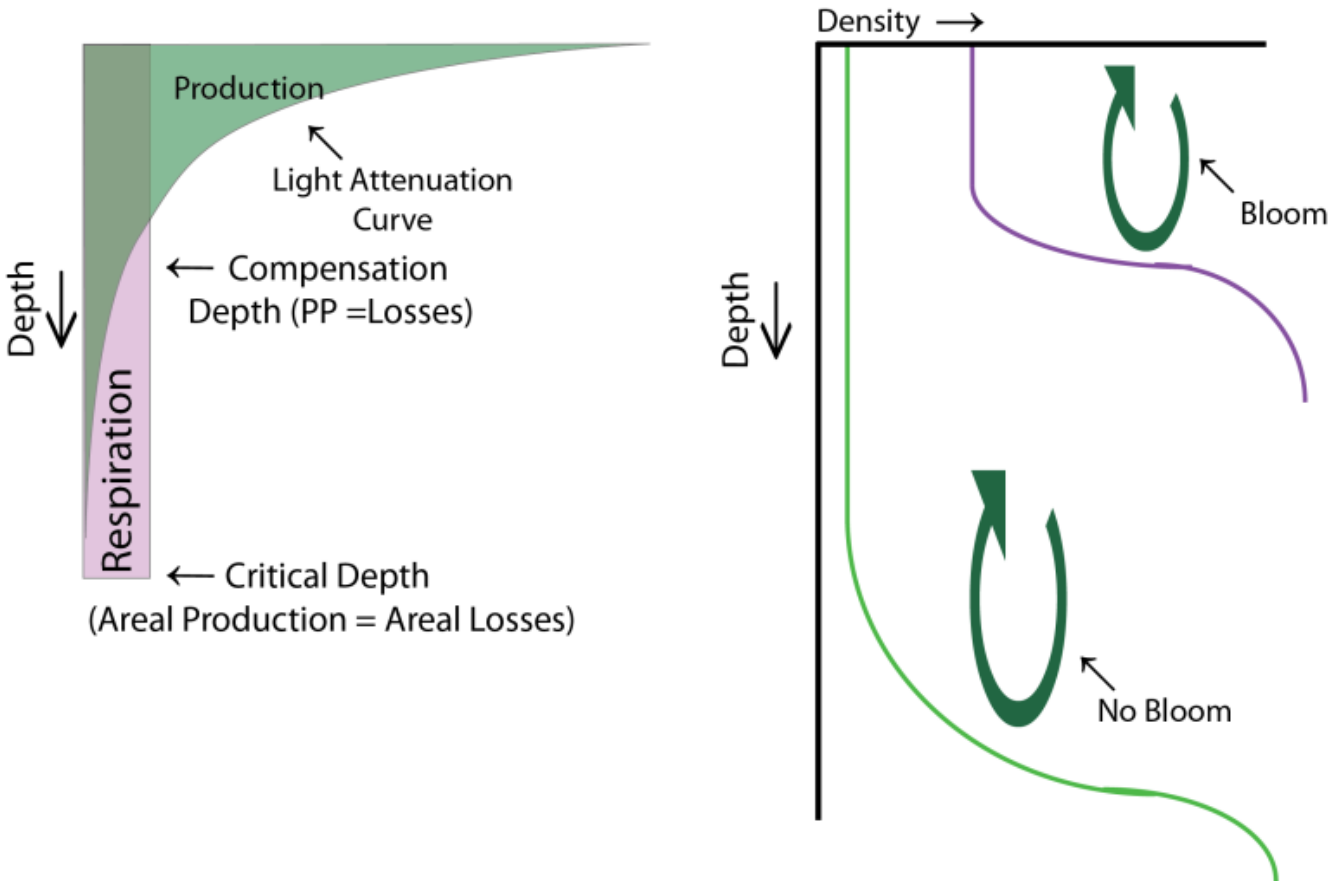

Figure 1.1: A schematic of the critical depth hypothesis [left side] (adapted from: Miller and Wheeler, (2012)). Right side schematic showing how the shoaling of the mixed layer (green [mixed to depth] and purple [shoaled] lines) allows for a bloom to occur or not take place based on density and depth.

1.0.2 Under-ice Phytoplankton Blooms

In the Arctic, the spring (May) bloom is a major contributor to annual primary production and is important for fuelling secondary production (Sakshaug, 2004). Most of the Arctic Ocean has at least a seasonal ice cover that influences a much different set of season spring processes affecting the spring bloom. Due to the presence of sea ice and the numerous major North American and Eurasian rivers that drain into the Arctic Ocean, the role of salinity in stratification and convective mixing is dominant over that of temperature (Carmack, 2007). Furthermore, sea ice strongly attenuates the transmission of light to the pelagic environment, and thus plays a critical role in primary production of the Arctic Ocean. In this sub-section, I review existing observations and evidence for the occurrence of under-ice Arctic spring phytoplankton blooms, and in particular, I review pertinent processes operating in ice-covered marine environments that could influence timing of the bloom.

1.0.2.1 Historical Observations of Under-Ice Phytoplankton Blooms

The Arctic has seen a significant rapid decline in its sea ice cover in recent years (Comiso et al., 2008; Kwok et al., 2009) with some models predicting an ice free summer as early as 2037 (Wang and Overland, 2009). Sea ice melt is not only associated with a rapid increase in light transmission to the water column (Sakshaug, 2004), but also provides low salinity melt water that rapidly stratifies the upper water column. Earlier salinity stratification in turn will affect the duration and timing of the phytoplankton growing season (Rysgaard et al., 1999; Sakshaug, 2004; Arrigo et al., 2008; Mundy et al., 2009).

Rysgaard et al., (1999) suggested that annual primary production in the Arctic was directly correlated to the length of the growth season due to the main control of light limitation (Glud et al., 2007). In contrast, additional reviews and studies have suggested that variability in annual primary production across the Arctic could have a greater dependence on dissolved nitrogen supply (Sakshaug, 2004; Tremblay and Gagnon, 2009). It is likely that both factors play a significant role in the Arctic spring bloom but at different stages, and to different communities within the bloom.

Due to the high albedo and attenuation properties of sea ice, snow, and ice algae, primary production in the under-ice water column has been assumed and measured to be negligible in previous investigations and reviews (Smith and Sakshaug, 1990; Grebmeier et al., 1995; Sakshaug, 2004; Michel et al., 2006). However, many past studies have provided evidence to the contrary. Using fluorescence data from a mooring, Fukuchi et al., (1989) observed a bloom in the southern most region of sea ice in the northern hemisphere. The bloom took place under landfast ice in the Lagoon Saroma, Ko. Measurements were taken every two hours over a total of 161 days. The measurements showed that prior to the bloom there was less than 1 μg L^{-1} of chlorophyll in the water column. Bloom onset started in the middle of March and lasted until mid-April when the ice was still present. During this time Chl *a* concentrations reached peak concentrations of 5 μg L^{-1} in the under-ice water column.

Strass and Nöthig (1996) observed a bloom in the Barents Sea under substantial ice cover in the early to late summer of 1991. They associated it with the stability of the water column during the transition period from early to late summer. The movement of the bloom transitioned for a month over ~ 400 km and was associated with the retreat of the ice edge. The bloom terminated with maximum chlorophyll concentrations 100 to 300 km north of the meltwater lens

where substantial ice cover was still in place. Strass and Nöthig (1996) concluded that the bloom started at the onset of stabilization, which was initiated by meltwater under the ice cover. Strass and Nöthig (1996) also stated that an increase in temperature associated with seasonal warming did not come into play as a factor for the bloom.

Fortier et al., (2002) also observed two notable blooms and the potential commencement of a third bloom under landfast ice in the Resolute Bay, NU, region. Under 100% ice cover, the two observed blooms were substantial with one reaching upper water column integrated concentrations of >400 mg m^{-2}. The years 1994 and 1995 were triggered by the snow cover diminishing early as a result of an early rain event and a heat wave, respectively. These results suggested a link to possible climate changes. The year 1992 additionally showed evidence of a bloom onset prior to ice breakup in the region.

Mundy et al., (2009) observed a large bloom under the ice, but in close proximity to an ice-edge in the Beaufort Sea region. The bloom was attributed to an upwelling event in the area. The upwelling event brought nutrient replete water to the surface under the ice allowing for a substantial bloom of new production to take place. Unfortunately, due to the Ekman spiralling nature of an upwelling event, they were unable to conclude from the measurements that the observed increase in biomass was strictly associated with under-ice production and not the open water adjacent to the ice-edge. However, through measurements of transmitted light levels and a photosynthesis-irradiance relationship for the under-ice phytoplankton, they were able to provide a conservative estimate that the under-ice portion of the bloom contributed at least 22% of the daily ice-edge production. This estimate confirmed that enough light was penetrating under a melted ice cover to support phytoplankton growth, which led to the hypothesis therein that under-ice blooms may be an under-documented phenomenon, particularly within the Canadian

Arctic Archipelago.

However, it was not until Arrigo et al. (2012) observed a significant under-ice bloom in 2011 in the western Arctic Ocean that major attention was paid by the scientific community to the possibility of under-ice phytoplankton blooms. In contrast to the observed under-ice bloom in surface waters, the adjacent open water region showed maximum phytoplankton biomass at depths of 20 to 50 meters. Arrigo et al. (2012) suggested that these deep chlorophyll maxima (DCM) were the remnant of a previous under ice bloom. Furthermore, they showed that ample light required by the under-ice bloom had penetrated the pack-ice. Light transmission was enhanced by a first-year ice cover coupled with high surface melt pond fractionation (25 to 50%). Furthermore, due to a stronger shade-acclimated state of the under-ice phytoplankton, cells grew twice as fast at the same low light conditions as that in adjacent open oceans. From the above studies, it is apparent that under-ice phytoplankton blooms have occurred in the Arctic and that light transmission through sea ice and its relationship to a melting ice cover is of prime importance to the development of an under-ice bloom.

1.0.2.2 Sea Ice and Oceanographic Processes Affecting Blooms

The Arctic Ocean differs from other oceans as it is encased by land, with only 3 relatively confined marine inputs, namely Barents Sea, Fram Strait, and Bering Strait. Furthermore, Fram Strait is the only deep ocean connection to the global ocean network. The Arctic Ocean is also fed by major freshwater inputs from Canadian and Siberian rivers and streams. In addition to being a major inflow (up to 5 times higher than the Bering Strait; Schauer et al., 2002; Woodgate et al., 2005; Carmack and Wassmann, 2006), the Fram Strait is the largest and deepest marine

outflow of the Arctic Ocean. Other outflows include the Canadian Arctic Archipelago and the west coast of Greenland.

It is important to note that the Arctic Ocean is considered as a beta ocean, where stratification is predominately a function of salinity rather than temperature (Carmack, 2007). A major halocline exists in the Arctic Ocean that is located between 50 and 200 m and is arguably the most important characteristic in maintaining the ice cover and influencing biology (Carmack and Wassmann, 2006). The halocline identifies the transition between the major water masses: the cold and fresh polar surface water (PSW), the more saline Pacific waters (PW), and the warmer and more saline Atlantic waters (AW; Thomas and Dieckmann, 2003). The density of cold waters is directly related to the salinity creating a sharp pycnocline between the PSW and the underlying water mass. This pycnocline inhibits mixing from depth and the nutrients that would normally come with it (Thomas and Dieckmann, 2003). In turn, this reduces the transfer of heat from the underlying PW and AW masses to the surface and helps to promote the growth and maintenance of the sea ice cover.

In the case of PW, the water mass is fresher and higher in nutrient concentration than the AW mass and has a predominant influence on water observed in the Canadian Arctic Archipelago (Jones et al., 2003; Carmack and Wassmann, 2006). A program to continuously monitor the flow and hydrography in Barrow Strait (centre of the Archipelago) — started in 1998 by the Department of Fisheries and Oceans of Canada (Prinsenberg et al., 2005) — determined that the majority of water through Barrow Strait originated in the Beaufort Sea. The Beaufort Sea is fed by the Mackenzie and the Bering Strait. Water moving through the Bering Strait and eventually to Barrow Strait is considered to be the oldest and some of the most nutrient rich water in the world (Sakshaug, 2004). As these waters traverse the Archipelago, shoals and

tidally driven currents can act to mix the underlying PW into surface waters (McLaughlin et al., 2004).

Mixing of the upper water column with underlying waters is further augmented during the fall and winter. That is, water mass characteristics in the Arctic are strongly affected by growth and melt processes associated with sea ice (Prinsenberg and Ingram, 1991). Arctic seawater typically has a salinity of 32 to 34 with a freezing point of ~ -1.76 to -1.86 ^{o}C, respectively (Fofonoff and Millard, 1983). As surface layers are exposed to the rapidly cooling atmosphere in fall, convection is induced due to the fact that colder waters at these salinities are denser than warmer waters. Eventually the surface layer reaches its freezing point, resulting in the formation of sea ice. As sea ice forms, it further increases the density of the upper water column by freeze-segregation and desalination of brines. Gravity drainage of brines from the thickening sea ice cover destabilizes the water column and allows for increased vertical mixing. In contrast, as the ice melts in spring and summer, lower salinity melt water acts to stratify surface waters, reducing vertical mixing (Prinsenberg and Ingram, 1991).

It is through these general formation and melt processes that the sea ice is intimately linked to primary production in the Arctic. That is, the cycle of sea ice growth and melt provide ideal conditions during spring for primary production: high nutrient availability due to winter mixing processes (Michel et al., 2006), optimal illumination once the ice starts to melt (Mundy et al., 2014), as well as minimal grazing pressure due to low temperatures (Sherr et al., 2009). However, under-ice spring phytoplankton blooms have been understudied and as a result are not well-understood (Sakshaug, 2004). It has been hypothesized that the occurrence of the spring bloom is triggered by sea ice break-up (Gran 1931; Braarud 1935; Alexander and Niebauer, 1981; Sakshaug and Skjoldal, 1989; Sakshaug, 2004), combined with a freshening of the surface

layer stratifying the water column. More recently, evidence suggests that this bloom might be occurring earlier than originally thought and could have significant effects on pelagic-benthic coupling in the Arctic marine ecosystem (Mundy et al., 2009; Arrigo et al., 2012; Palmer et al., 2013).

1.0.2.3 Stages of Melt Evolution

Sea ice formation is relatively well-understood in the Arctic (Weeks and Ackley, 1982; Thomas and Dieckmann, 2009). However, the progression of sea ice melt and its radiative transfer properties remain a topic of investigation (e.g., Eicken et al., 2004; Ehn et al., 2011; Polashenski et al., 2012; Landy et al., 2014). During spring, sea ice undergoes a rapid transition from a highly reflective snow cover to a relatively dark melt pond cover.

Early melt onset stages in the snowpack and eventually ice is annually variable (Zhang et al., 1996). It is characterized by a warming atmosphere (Perovich et al., 2002a) and increased incoming solar radiation (Perovich et al., 2002a). Notably, Else et al., (2014) found that melt onset for landfast ice was a function of a combination of variables. The driving variables appeared to be a low loss value of longwave radiation coupled with seasonal bursts of shortwave radiation. The key to the low loss of longwave radiation was associated with the feedback process of counter-radiation by clouds. This feedback loop was also discussed in depth in Jin et al., (1994) and Curry et al., (1996). Melt onset as a whole function typically lasts about 2-3 weeks (Horner, 1985; Else et al., 2014). The quantity of snow on the ice, air temperature, and precipitation events help determine the timing of early melt onset (Zhang et al., 1996). Snow depth directly affects the melt progression by acting as a thermal insulator, while the snow surface contributes to a high albedo (Zhang et al., 1996). Once the snowpack has reached a

thermal “tipping-point”, snow grains begin a wet metamorphic change. At this point, growth of snow grains contributes to a rapidly decreasing albedo, and increasing transmission properties of the snowpack. This metamorphic change is initially caused by conductive heat flux into the system. The surface warms first, while the bottom layer has higher temperatures than the middle of the pack due to temperature gradients prior to melt onset, resulting in a c-shape temperature profile (Papakyriakou, 1999). Water found within the snowpack alters the physical characteristics and transmission properties of the snow (Colbeck, 1982). Colbeck (1982) noted that under wet snow metamorphism, snow grain size increases by grains clustering together. This allows for greater drainage of water by increasing the pore size between grain clusters. In turn, water can connect snow grains together and diurnal atmospheric changes result in a thaw-freeze cycle causing grains to grow at a much more rapid rate (Colbeck, 1982). As the grains grow in size and melt water collects at the base of the snowpack, the surface albedo rapidly drops, causing the snowpack to absorb more solar radiation. This in turn advances the melt state (Eicken et al., 2004).

During the early melt stage, the ice cover also warms, causing brine volume inside the ice to increase. The previously separated brine inclusions open up as the sea ice attains a critical threshold around 5% brine volume (Golden et al., 1998). Following this early melt progression, the ice undergoes more advanced stages of melt. Polashenski et al., (2012) suggested there are four stages of advanced melt progression as a function of surface melt pond coverage.

Stage 1 begins when ponds start to form. Initial pond formation is categorized by a swift increase in pond coverage due to the accumulation of melt water on the surface of the sea ice. The ice is impermeable to percolation during this period (Polashenski et al., 2012). Typically melt pond coverage is highly variable inter-annually and seasonally due to topographic

differences and atmospheric changes (Romanov, 1995; Tschudi et al., 2001; Perovich et al., 2002a; Eicken et al., 2004). Due to the impermeable ice cover, melt water does not immediately drain into the underlying ocean, thus forming ponds above sea level. Melt drainage can be categorized into two groupings: (a) through macroscopic flaws (e.g., seal holes, leads, cracks, etc.) that drain the surface with horizontal flow over the ice surface and into the ocean; and (b) the ice becomes permeable, which allows percolation of melt water through the sea ice and into the ocean. Melt ponds forming above sea-level create a hydrostatic head of water that flows laterally according to topographic relief over the sea ice into surface cracks and flaws in the ice (i.e., drainage state (a); Polashenski et al., 2012). First-year ice normally shows the highest pond fraction of all ice types (Derksen et al., 1997; Fetterer and Untersteiner, 1998; Hanesiak et al., 2001; Eicken et al., 2004). This greater fraction is a function of diminished topography and deformation on first-year ice relative to that of multiyear ice (Polashenski et al., 2012).

Stage 2 is triggered by melt water draining from the surface ice. This drainage causes melt ponds to drop towards sea level, decreasing the hydrostatic melt water head. Furthermore, the drop in water level is associated with a decrease in the spatial coverage of melt ponds (Polashenski et al., 2012). Pond area, and its resulting control on albedo, is driven by the hydraulic head for both multiyear and first-year ice (Eicken et al., 2004). Eicken et al., (2004) noted that this control is true for both diurnal variations and the seasonal melt progression. The lateral movement of water is reduced as the hydraulic head reaches equilibrium (Eicken et al., 2004). This in turn reduces the ponds shrinking and expanding and steepens the walls of ponds (Eicken et al., 2004).

Stage 3 of sea ice melt is distinguished by melt pond levels that are near or at sea level with vertical drainage no longer being limited. That is, the ice cover is highly permeable and melt

drainage falls within grouping (b), allowing water to flow freely should a hydraulic head re-develop. Melt pond spatial coverage has the potential to increase during this stage due to loss of buoyancy caused by the thinning ice as well as lateral melt of pond walls (Polashenski et al., 2012). Numerous melt ponds decay through to the ocean and the ice has the potential to break-up and decay entirely during this stage.

Stage 4 of sea ice melt can be observed within any one of the previously mentioned advanced melt stages and is not restricted to a specific timeframe. This change is a result of refreezing and is caused by atmospheric forcing. The refreezing forms a skim on ponds, which prevents melt water inflow in addition to the potential outflow. The skim can also rapidly raise the surface albedo (Polashenski et al., 2012).

1.0.3 Snow and Ice - Albedo and Transmission

A photon transferring through a medium such as snow and sea ice — containing a mixture of air, ice, liquid, solid salts, and biotic and abiotic dissolved and particulate material — can either: a) be absorbed and the energy transformed and emitted at another wavelength (e.g., via radiated heat or fluorescence) or harnessed as photochemical energy (e.g., photosynthesis); or b) it can be scattered. It is these two properties that determine the attenuation of light as it passes through a material. For example, the high scattering and strong absorption properties of snow and sea ice cause these materials to have strong attenuation properties (Perovich, 1996).

The growth and decay of sea ice is directly affected by the surface radiation budget, which has a strong seasonal cycle in the Arctic. The peak value of daily averaged insolation incident on a horizontal surface over 22 years was 508 W m^{-2} in the summer (June) and 0 W m^{-2}

in the winter months (74.6975° N, 94.8322° W) (Figure 1.2) (Source: NASA Surface meteorology and Solar Energy).

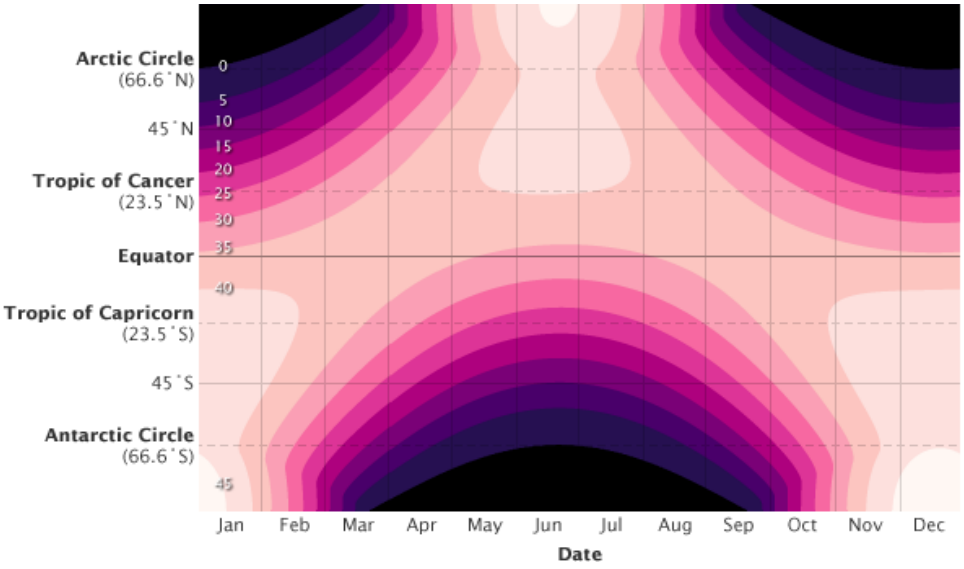

Figure 1.2: Daily averaged insolation at the top of the atmosphere as a function of latitude versus date. The largest values of incoming energy (pale pink) are at high latitudes in summer. During winter some areas receive no light (black). Figure used with permission from: NASA (http://earthobservatory.nasa.gov/ImageUse/)

Clouds also exert a substantial influence on the radiation balance of the surface (Curry et al., 1996; Walsh and Chapman, 1998; Minnett, 1999). During the summer and fall, clouds reflect and absorb some of the insolation (the dominant radiation during this period) and keep the surface cooler than on a clear day. Conversely, during the spring, although cloud cover blocks incoming shortwave radiation, it also traps longwave radiation below the cloud, thus warming the surface (Jin et al., 1994; Curry et al., 1996). Similarly, during winter months, clouds act to warm the surface by trapping longwave surface emission. Hence, cloud cover affects changes in ice properties and thickness (Jin et al., 1994; Schweiger, 2004). This extreme between the two seasons, partially offsets the variations in the longwave cooling of the atmosphere. Both longwave and shortwave radiation peak in July (Curry et al., 1996). Curry et al., (1996) found

that peak cooling occurs in the fall and minimum cooling occurs during the spring due to a series of complex interactions between atmospheric temperatures and cloud properties.

It is important to note that the radiative energy balance is affected by the thickness of the ice present. Albedo is related to the scattering properties of the surface layer. Therefore, sea ice albedo is not a constant value across space and time. Clear water has very few impurities that can scatter light, causing a very low albedo for water around 0.05 (Grenfell and Maykut, 1977). During initial ice growth surface albedo increases as the ice thickens until it becomes optically thick such that the water column below no longer contributes to the surface albedo (Perovich, 1996). Albedo increases due to increased scattering of light to a maximum value of ~0.52. Once the ice provides a contiguous platform; however, snowfall usually accumulates on the surface and due to its strong scattering properties, surface albedo rapidly becomes solely due to the snow (i.e., the ice cover below the snow no longer contributes to the surface albedo). During melt, the snow cover disappears, exposing a variegated surface of melt ponds and drained white ice (Ehn et al., 2011), which again affects the surface albedo.

The presence or absence of snow on the sea ice is potentially the most important variable controlling light transmission to the water column. During winter, snow-covered ice can have a very high albedo, typically ranging between 0.8 to >0.9 (Langleben, 1967). As little as 1 cm of fresh snow can result in an albedo that is independent of the underlying surface (Petzold, 1977). Albedo is mainly affected by snow grain size, liquid water content, and presence of impurities. Smaller grain sizes increase scattering, thus increasing albedo, whereas liquid water and impurities such as soot can increase absorption and reduce albedo (Perovich et al., 1998).

New snow can have an albedo of approximately 0.9 or greater (e.g., Allison et al., 1990; Perovich et al., 1998), but due to aging of the snowpack, surface albedo steadily drops with time

to an average of approximately 0.8 to 0.85 (Barber et al., 1995; Mundy et al., 2005). For example, as snowflakes fall on existing snow their structure partially breaks down. The multiple fragments of tiny snow spread over the surface, increasing albedo. Given time, dry metamorphism and gravity compaction cause snow grain size and density to increase, respectively.

Due to the high snow albedo, transmission of light prior to any significant melt is very low. Perovich (1996) observed <1% transmission under a snow cover of 25 cm, 3% under 12 cm, and 7% under surface drained ice. A drained ice cover (also referred to as white ice) is actually not snow, representing a surface that forms after the snow cover has melted away and thus is only observed during advanced melt stages.

Once temperatures rise towards freezing, the sun's energy can act to start snow-melting processes. Horner (1985) suggested that the snow cover can melt as fast as 2 to 3 weeks after air temperatures reach 0 ^{o}C, producing melt ponds. This transition from snowpack to melt ponds greatly influences the quantity of surface light transmitted to the underlying water column. During this time, the liquid water content of snow rapidly increases causing a further drop in albedo to <0.8 (Barber et al., 1995; Perovich 1996; Mundy et al., 2005). Rainfall can dramatically accelerate this melt process, which is a driving concern with respect to timing of snow and sea ice melt and the current increasing trends in rain events (IPCC 1995, Simmonds et al., 2008).

With a period of sustained temperatures above freezing, melt ponds begin to form on the ice surface with the first ponds forming in regions of low snow covers (Iacozza and Barber, 2001). Water-covered sea ice has a lower albedo causing the surface to absorb and transmit more insolation (Ehn et al., 2011; Polashenski et al., 2012). This increase in absorbed and transmitted

radiation helps to hasten ice melt (Polashenski et al., 2012) and potentially activate primary production in the water column (Mundy et al., 2009; 2014). However, the albedo of melt ponds is highly variable, with ranges of 0.2 to 0.4 (Perovich et al., 2002b Eicken et al., 2004; Ehn et al., 2011). Ehn et al., (2011) found that the PAR albedo of advanced melt stage melt ponds and white ice were 0.22 ± 0.04 and 0.70 ± 0.06, respectively. Furthermore, this highly variable surface of melt ponds and white ice greatly affects the transmission of light through the sea ice, which is controlled by ice thickness and proximity to other surface types (Ehn et al., 2011).

PAR transmission through the sea ice has been estimated at 38 to 67% and 5 to 18% under melt ponds and white ice (Perovich, 1996; Ehn et al., 2011; Arrigo et al., 2012). When ponds become stable and deep, they show a relatively consistent PAR transmission to the underlying water column that is 4-5 times higher than through surrounding white ice.

The attenuation properties of ice biota are also important to the transmission of light through ice. In particular, ice algae preferentially absorb wavelengths at 440 nm (blue light) and around 665-675 nm (red light), further decreasing the quality and quantity of the light being transmitted to the underlying ocean (Legendre and Gosselin, 1991; Mundy et al., 2007).

Chapter Two: **Methods**

In this chapter, I explain the methods used to collect and analyze the data, which were obtained during the three Arctic-ICE field campaigns from 2010 - 2012. Additionally, I briefly discuss methods used to standardize the data and where the historical data was obtained from.

2.0 Study Sites

The central dataset contributing to this study was collected as part of the 2010, 2011, and 2012 Arctic-ICE (Ice Covered Ecosystem) field campaigns (Brown et al. 2010; Campbell et al. 2011; Landy et al. 2012). These campaigns were based on landfast first-year ice sites within the vicinity of Resolute Passage (Figure 2.1; Table 2.1). During the 2010 campaign, sampling occurred over a 3-day schedule. During the 2011 and 2012 campaigns, sampling occurred over a 4-day schedule. Water column sampling occurred the day prior to ice core sampling in all campaigns.

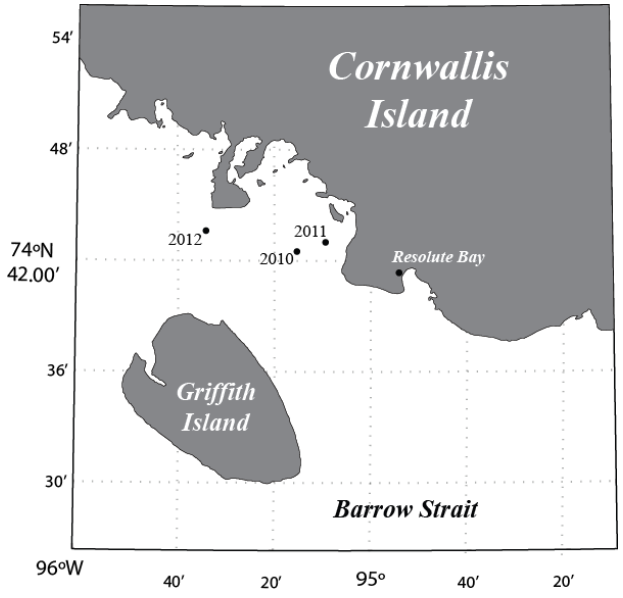

Figure 2.1 Arctic-ICE field study sites in Allen Bay area near barrow Strait. All sites took place on landfast first-year ice

Table 2.1: Sampling dates, coordinates, and bottom depths for each Arctic-ICE field sampling location.

Year	Start Date	End Date	Depth (m)	Latitude (°N)	Longitude (°W)
2010	08/05/2010	21/06/2010	141	74.7085	95.248
2011	08/05/2011	26/06/2010	60	74.7167	95.15
2012	18/05/2012	22/06/2012	80	74.7269	95.5583

2.1 Environmental Measurements

During each of the three years, a meteorological station was established within 0.5 – 1 km of the main sampling tent and monitored on a regular basis. The measurements collected include: air temperature, shortwave surface albedo, incident photosynthetically active radiation (PAR; 400-700 nm), and relative humidity (Brown et al. 2010; Campbell et al. 2011; Landy et al. 2012). Air temperature data was collected using a Vasailla, model HMP45C212 sensor. Surface albedo was determined using the ratio of upwelling to downwelling shortwave (0.3-2.8 μm) irradiance, measured using a Kipp & Zonen, model CNR1 sensor. Incident PAR was collected during the 2010 and 2011 campaigns using a Kipp & Zonen PAR-Lite sensor. In addition to the on-ice meteorological site, daily rain precipitation data was obtained from Environment Canada's (EC) meteorological station located near the Resolute Bay airport. The EC station was approximately 8, 5 and 20 km east of the 2010, 2011 and 2012 field sites, respectively. Precipitation totals calculated at the station were consistent with on-ice weather observations and are considered a best-estimate of on-ice totals. Snow depth and ice thickness were measured on a scheduled basis using a measuring stick and a Kovacs Enterprises ice thickness gauge, respectively. For comparison purposes and the historical data analyses, snow depth data were also obtained from the EC station dataset.

Water column profiles of temperature and salinity were obtained by use of a Sea-Bird SBE 19plus V2 conductivity-temperature-depth (CTD) sonde. The CTD additionally housed an *in vivo* Chlorophyll *a* (Chl *a*) fluorometer sensor (Wet Labs, ECO-FL (RT)) and a scalar PAR sensor (Biospherical QSP-2300L). Casts of the CTD sensors were obtained daily through the main sampling hole within a heated tent on the sea ice. The casts included an equalization period where the sonde was held at a 2 m water depth from the water-atmosphere interface for 90 s for instrument environmental equilibration. The CTD was then lowered at a speed of approximately 0.9 m s^{-1} until the maximum depth was attained and only the downcast are presented hereinafter. Calibration of the CTD fluorometer sensor was accomplished each year via quadratic regressions against extracted Chl *a* concentrations measurements (Trembley et al, 2008). Figure 2.2 shows the best-fit calibration curves for all years together. Individually, results were: 2010 (n = 83; R^2 = 0.98), 2011 (n = 74; R^2 = 0.9), and 2012 (n = 46; R^2 = 0.32).

Variability in the under-ice light field as a function of surface cover inconsistencies (e.g., snow drifts, melt ponds and white ice patches, and the sampling tent) caused problems with the interpretation of under-ice light measurements. To examine this problem further, I tested multiple techniques that included: moored sensors, water column profiles with the CTD light sensor, and a combination of the two. Another difficulty with the dataset was the use of planar (cosine corrected) irradiance sensors for surface downwelling and albedo measurements, and scalar (4π) irradiance sensors for transmitted light measurements. Following Mundy et al. (2014), I assumed negligible upward irradiance from the water column and multiplied the under-ice scalar data by an average cosine to estimate a potential range in percent transmittance. The range used includes the use of an average cosine of 0.5 (diffuse light field) and 1.0 (downward

directed light field) in order to encompass the possible light fields encountered under the ice cover.

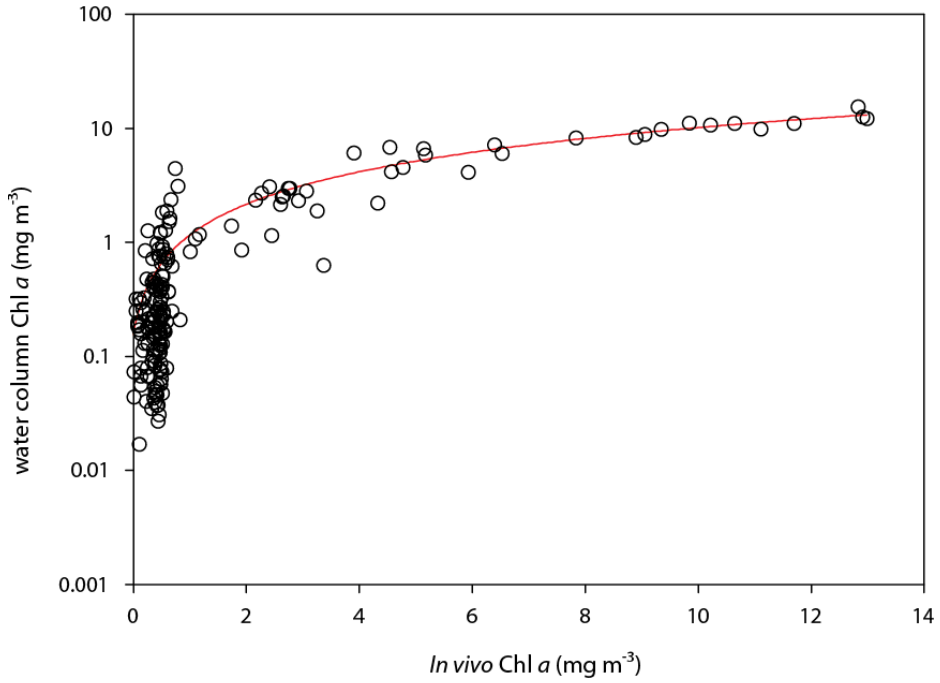

Figure 2.2: Relationship between discrete depth water samples of chlorophyll (Chl) *a* versus CTD-based in vivo Chl *a* during Arctic-ICE. The red line represents a least square fitted regression with the following equation f=0.156 + 1*x^1 (*n* = 203; R^2 = 0.9384; *p* = 0.05).

Scalar PAR in the water column under the ice was measured using two independent tethers with ALEC MKV-L sensors mounted at discrete depths during the three field campaigns (Table 2.2). The scalar sensors had to be adjusted for the underwater immersion effect. This was accomplished by multiplying by the calibration values provided in the manual (~1.6). Each year these PAR tethers were moored to the sea ice under "high" and "low" snow depths. The defining "highs" and "lows" were variable depending on the snow cover each year (Table 2.2). Additionally, a large weight of 8 pounds was positioned at the lowest point of each tether to ensure a mostly vertical orientation of the tethers throughout the field campaigns.

Table 2.2: Tether depths of ALEC MKV-L sensors and overlying averaged snow depths for each year prior to melt onset.

Year	High (cm)	Low (cm)	Depths (m)
2010	42.6	12.6	2, 5, 7.5, 10, 20, 30, 40
2011	18	10	2, 5, 7.5, 10, 20, 30, 40
2012	15	3	1.5, 2.5, 5, 7.5, 10, 20

Snow depth has a strong influence on the quantity of transmitted light under the ice cover (Legendre and Gosselin, 1991; Perovich, 1996; Eicken et al., 2004; Mundy et al., 2007; Ehn et al., 2011; Arrigo et al., 2012;). This fact made it difficult to compare between years of transmitted PAR data from the tether data described above (Table 2.2). Therefore, I attempted two separate methods to estimate under-ice transmitted PAR using data from the CTD casts. However, profiles of transmitted light were difficult to obtain from the CTD data due to shading effects of the main sampling hole and tent. Frey et al. (2011) found transmitted light to become spatially homogenous under the sea ice at depths greater than 20 m due to enough variability of the overlying ice surface being captured in the light sensor's field of view. Therefore, I used this finding to estimate under-ice transmitted light through two main methods. (1) Light was averaged over the maximum intensity every day for each of the PAR sensor tethers at discrete depths. Light attenuation coefficients (K_{PAR}) were calculated between each of the sensors using Beer's law:

$$K_{PAR} = \frac{\ln(\frac{Lz1}{Lz2})}{\Delta z} \qquad (2.1)$$

The daily values of K_{PAR} were then used to extrapolate transmitted light data from the CTD starting at a 20 m depth. (2) The second method involved the use of a relationship between K_{PAR} (i.e., tether-based light attenuation estimates) *versus* CTD-based *in vivo* Chl *a* concentrations to extrapolate the transmitted light data from 20 m depth using the CTD profiles of *in vivo* Chl *a*

concentrations. Prior to examining the relationship, the *in vivo* Chl *a* concentrations were averaged over the depths from which each K_{PAR} was calculated. A significant 2nd order polynomial regression was found to best fit the relationship between K_{PAR} (i.e., tether-based light attenuation estimates) versus *in vivo* Chl *a* concentration (Figure 2.3). This relationship was then used to extrapolate transmitted PAR from 20 m depth up to the ice-water interface using the Chl *a* concentration data from the CTD casts. This second method proved to be a better choice due to the attenuation of different spectra associated with biomass in the water column.

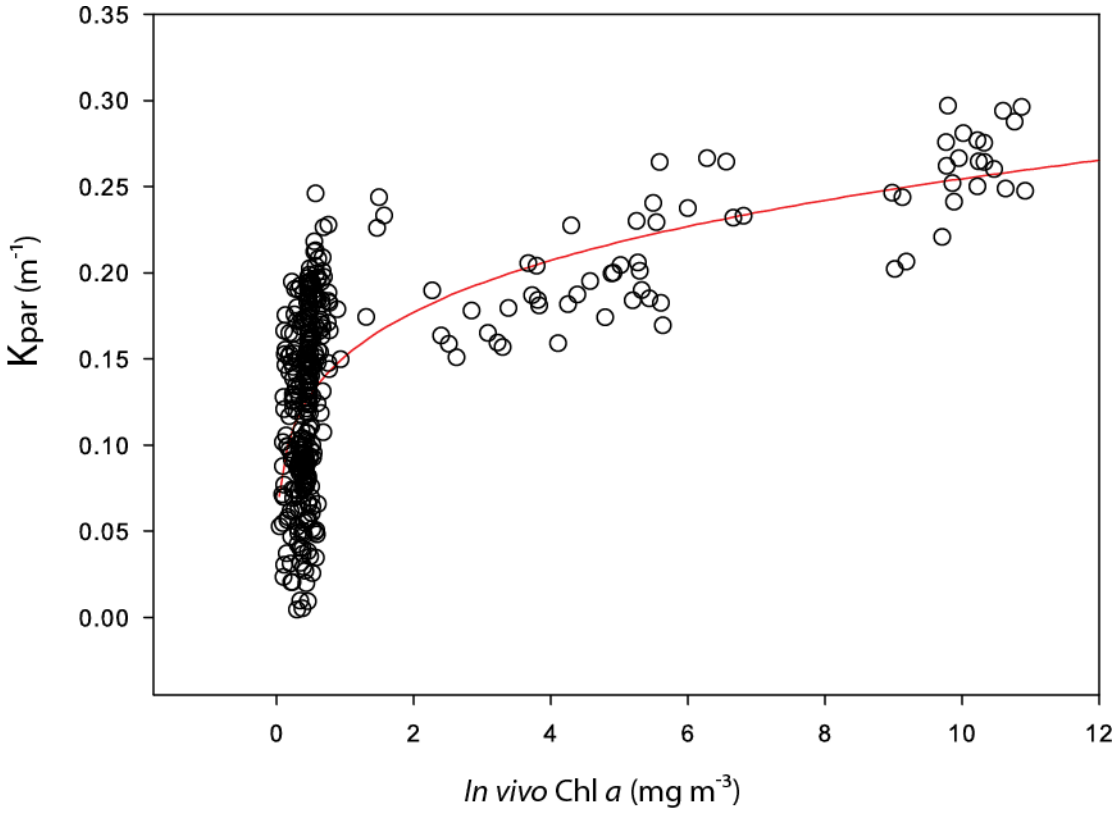

Figure 2.3: K_{PAR} calculated from the PAR tether data versus *in vivo* Chl *a* concentration from the calibrated CTD data averaged to the PAR tether intervals. The red line represents a least square fitted regression with the following equation f= 0.147 * x$^{0.229}$ (n = 358; R^2 = 0.505; p = 0.05).

2.2 Nutrients and Phytoplankton Biomass

Niskin sampling bottles (5-L) were deployed to collect water samples at discrete depths during each field season (3 or 4-day sampling interval depending on year). Each discrete depth had samples collected in pseudo-duplicate for determination of nutrient (nitrate+nitrite; phosphate; silicic acid) and Chl *a* concentrations (see Table 2.3).

Table 2.3: Discrete sampling depths listed by year for water column nutrients and Chl *a* concentrations.

Year	Sampling Depth (m)
2010	2, 5, 10, 25, 50, 130
2011	2, 5, 10, 25, 40
2012	2, 5, 10, 25, 50, 80

Nutrient samples in pseudo-duplicate were analysed for silicic acid, phosphate, and nitrate+nitrite concentrations. To collect the samples, water was filtered through a pre-combusted (5hrs @ 450^{o}C) Whatman GF/F glass fiber filter with the filtrate collected into 15 mL falcon tubes that had previously been sterilized by acid cleaning. Samples were placed immediately into a -20 ^{o}C freezer until analysis at Institut des Sciences de la Mer (Rimouski, QC) for 2010 samples and Universitie Laval (Vachon Laboratoire Jean-Éric Tremblay, Quebec City, QC) for 2011 and 2012. In both labs, nutrient concentrations were measured using a Bran-Luebbe 3 autoanalyzer (adapted from: Grasshoff et al., 1999).

Chlorophyll *a* concentration was determined from pseudo-duplicate subsamples filtered onto Whatman GF/F 25 mm filters (0.7 µm nominal pore size). Acetone extraction was conducted as indicated by Parsons et al. (1984). The filters were soaked in separate vials filled with 10 ml of 90% acetone at 4 ^{o}C in the dark over a minimum of 18 hours to a maximum time of 24 hours. A 10-005R Turner Designs fluorometer was utilized to measure fluorescence of

extracted Chl *a*. Prior to use, the fluorometer was allowed to warm up and stabilize, and regularly zeroed with 90% acetone. Measurements were taken prior to and after acidification with 5% hydrochloric acid (HCl) in order to account and correct for fluorescence by phaeopigments, a non-photosynthetic degradation product of algal Chlorophyll pigments. Chl *a* concentrations were then computed using equations found in Holm-Hansen et al. (1965).

2.3 Historical Data Sets

Historical data were collected from a variety of sources. Air temperature, snow depth, ice thickness, and precipitation were obtained through the Environment Canada historical data website (http://goo.gl/UuQ5mJ and http://goo.gl/VPvdPX). Water column Chl *a* concentrations were obtained from a number of previous projects and publications, and their locations are presented in Figure 2.4. When actual data were not directly available, they were digitally extracted from published figures using the freeware program, Data Thief III (http://datathief.org). Chlorophyll *a* concentrations were integrated over depths as near to 25 m as possible. Additionally, if needed a basic conversion from m^{-3} to m^{-2} was made as necessary. Datasets for the years 1961, 1962, 1963 were obtained from Apollonio and Matrai (2011). Chl *a* concentrations for the years 1983, 1984, 1985, 1986, 1987, 1988, 1989, 1990, and 1991 were obtained through the NOAA World Ocean Database (2013). Data were obtained from a published data report by Michel et al. (2003) for the year 2001. Chl *a* data from 1992, 1994, and 1995 were obtained from Fortier et al. (2002). Additional historical data for nutrients were obtained through Cota-Pomeroy Arctic Nutrient Database (2013) (ArcNut). The 2011 Arctic-ICE campaign was similar in location to the years 1983, 1985, and 1988 in the ArcNut studies, while the 2012 Arctic-ICE campaign was similar in location to 1994.

A limitation of the historical data is that Chl *a* measurements were not standardized in any way including sampling methods. I was only able to collect the raw concentrations from the sources and no inference can be made beyond the concentration values, their collection date, and the depth or integrated depth associated with the concentration.

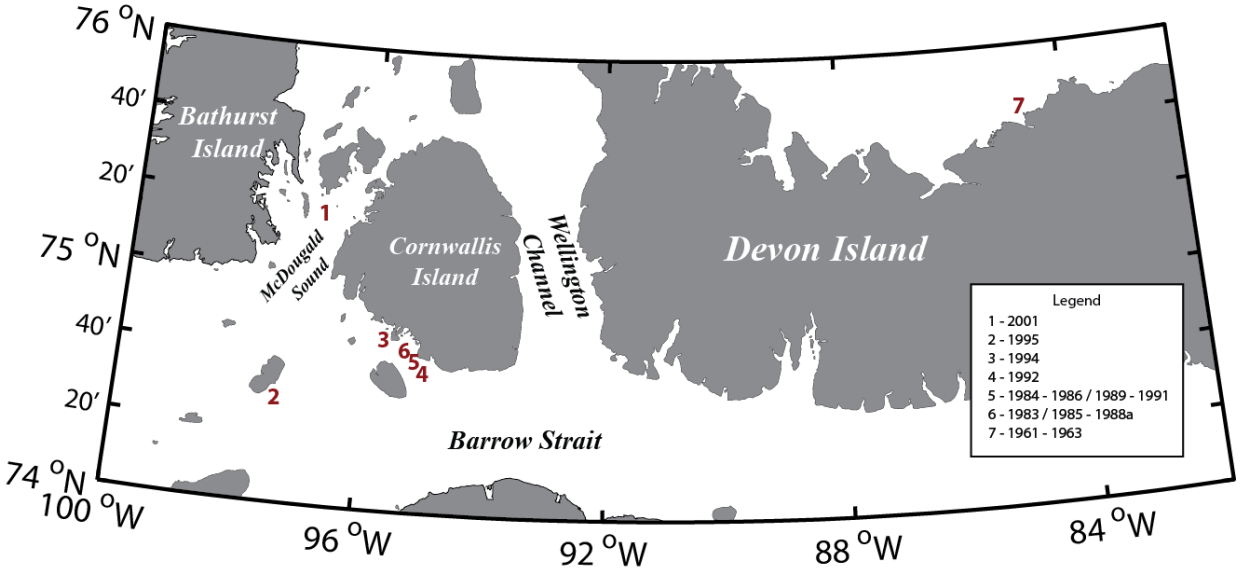

Figure 2.4: Map showing historical data sites.

Chapter Three: **Results**

In this chapter, I describe results from the data collated for this thesis over two sections. The first section describes in detail the conditions observed during the three Arctic-ICE field campaigns from 2010-2012. In the second section, I describe results for the entire historical dataset, including the three-year Arctic-ICE dataset discussed in the first section. It is noted that day of year (DOY) is used in graphs instead of calendar date. To assist interpretation, a DOY-calendar date look-up-table is provided in Appendix A.

3.0 Arctic-ICE Environmental Conditions

3.0.1 Meteorological, Ice, and Snow Time Series

Over the sampling period of 2010 (May 7 to June 21; DOY 127 to 172), mean daily air temperature showed a steady rise from approximately -13.0 ^{o}C to a maximum of about 1.2 ^{o}C. Mean daily temperature reached and remained near 0 ^{o}C following June 8 (Figure 3.1a). On June 10 the area experienced a minor rain event of 0.4 mm (Figure 3.1b). Average snow depth around the sampling sites was ~13 cm until June 6, the start of a successive decline in the snow cover until 0 cm was reached at low snow depths on ~ June 14 (Mundy et al., 2014; Figure 3.1c). Sea ice thickness averaged 140 cm (± 2.34 SD; Figure 3.2) over the sampling period, only decreasing under the low snow/melt pond cover sites towards the end of the period (data not shown).

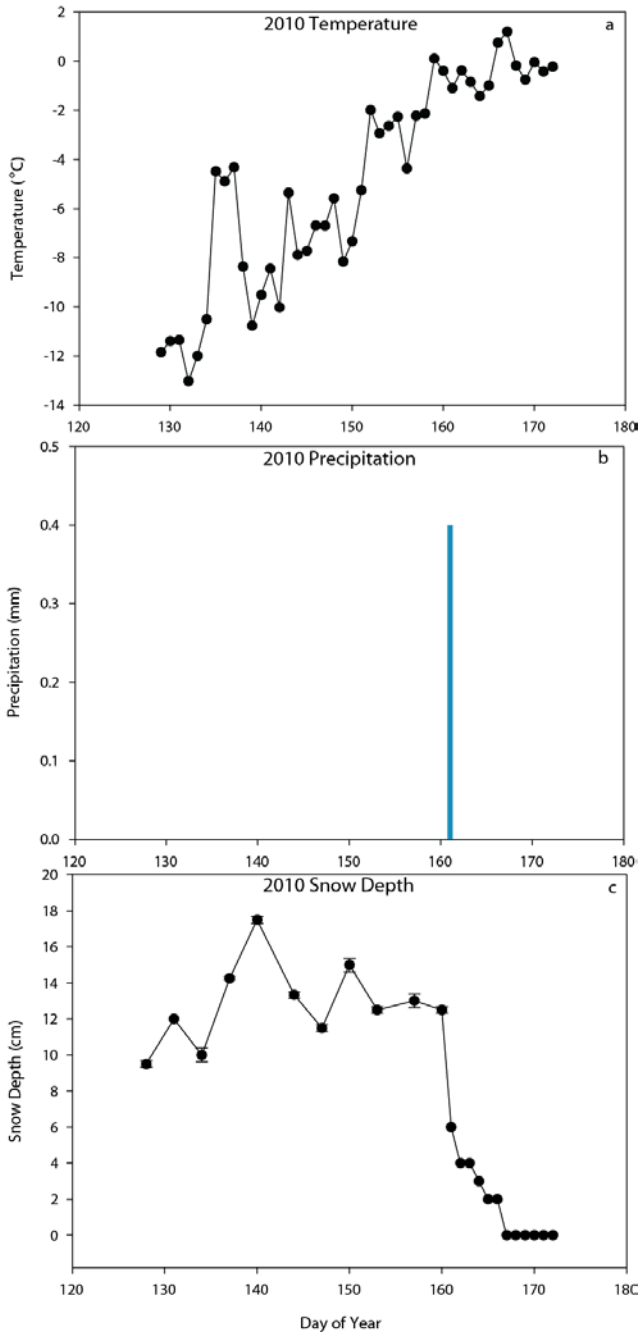

Figure 3.1: a) Daily averaged air temperature during 2010 Arctic-ICE sampling campaign (data were collected from the Arctic-ICE meteorological tower). b) Total rain precipitation during 2010 Arctic-ICE field campaign (data were collected from Environment Canada). c) Average snow depth (± standard error bars) on ice between medium high and low snow sites during the 2010 Arctic-ICE field campaign (data were collected at the Arctic-ICE meteorological station until June 9 (DOY 160), then following June 9, data were from Environment Canada).

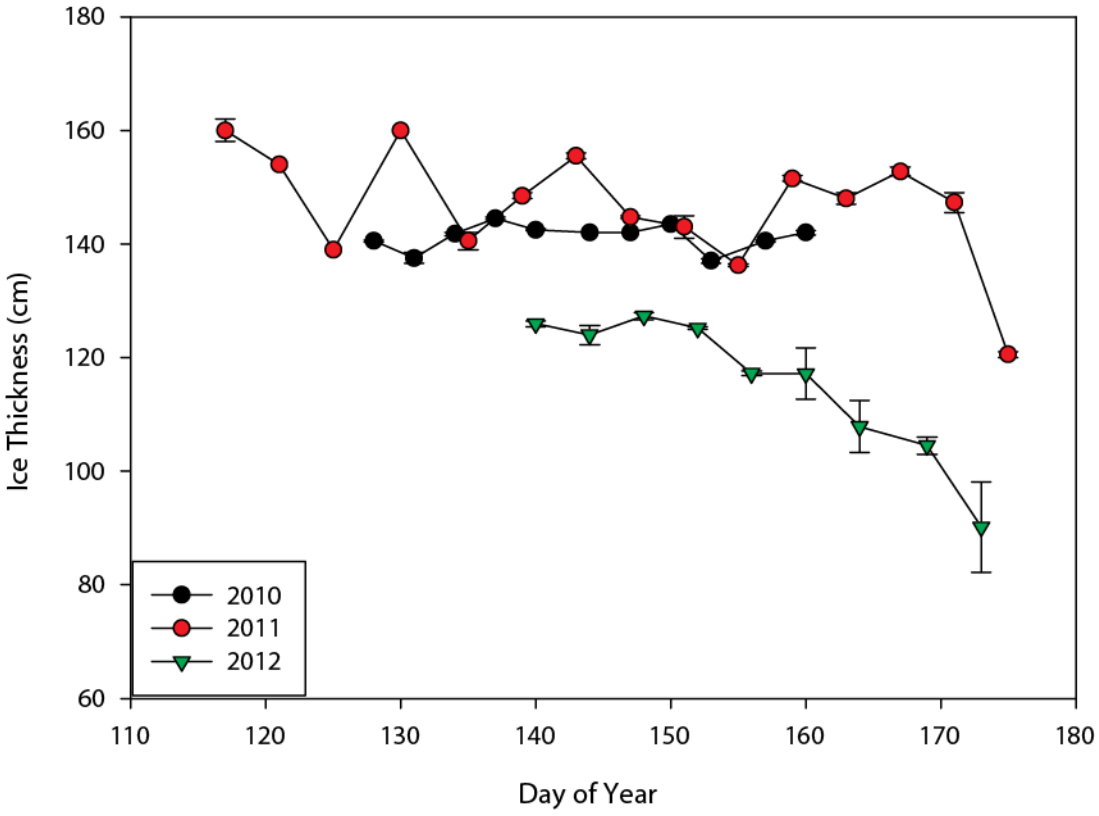

Figure 3.2: Times series of averaged ice thickness (± standard error bars) from high, low, and medium (if applicable) snow depth sites during the three years of the Arctic-ICE program.

During the sampling period of 2011 (April 24 to June 26; DOY 114 to 177), mean daily air temperature showed a steady rise from approximately -21.8 ^{o}C to a maximum of about 4.1 ^{o}C, reaching 0 ^{o}C on June 6 and averaging near or above 0 ^{o}C thereafter (Figure 3.3a). Two rain events took place in close proximity to each other (June 10 [1 mm] and 12 [0.8 mm]; Figure 3.3b). Three additional rain events of 6.2, 1, and 0.4 mm took place on June 24, 25, and 26, respectively. Snow depth averaged ~15 cm until June 5, when a decrease commenced from approximately 15 to ~3 cm by June 12 (Figure 3.3c). A comparison with EC snow depth data shows a similar pattern, but with much deeper snow cover of about double the thickness until the

beginning of June. Ice thickness averaged ~ 140 cm until the end of the sampling period where a loss of thickness was observed to ~ 121 cm (Figure 3.2).

In 2012 (May 19 to June 23; DOY 140 to 175), mean daily air temperature increased in a near linear fashion from -12.8 to 3.6 ºC (Figure 3.4a). Mean daily temperatures exceeded 0 ^{o}C on May 30, dipped back down, then remained above 0 ^{o}C following June 2. The sampling campaign during 2012 had a single major rain event of 6.2 mm on June 14 (Figure 3.4b). Snow depth showed a steady decline from May 23 until June 9 when it reached ~0 cm (Figure 3.4c). Ice was constant at 125 cm until June 12, when ice thickness declined slightly to 116 cm (Figure 3.2). By June 15 the ice had declined to ~100 cm and continued to slowly decline until the end of the sampling period.

3.0.2 Light

In 2010, shortwave surface albedo was relatively constant, ranging from 0.8 to 0.9, until a slight decline commenced following June 6 (Figure 3.5). Albedo continued a steady decline until June 14 when snow melt at low snow sites became 0 cm and melt ponds formed shortly thereafter causing surface albedo to drop to ~0.3 by June 16. The minor rain event on June 10 had no notable effect on albedo. PAR transmitted through the ice cover was a function of incident PAR (data not presented), snowmelt progression, and the decrease in albedo (Figure 3.6) until June 16 according to Figure 3.6. With the formation of surface melt ponds substantially more light was transmitted through the sea ice; however, the amount of transmitted PAR decreased after this point due to water column attenuation associated with the accumulation of Chl *a* in the upper water column (*see section* 3.1.5).

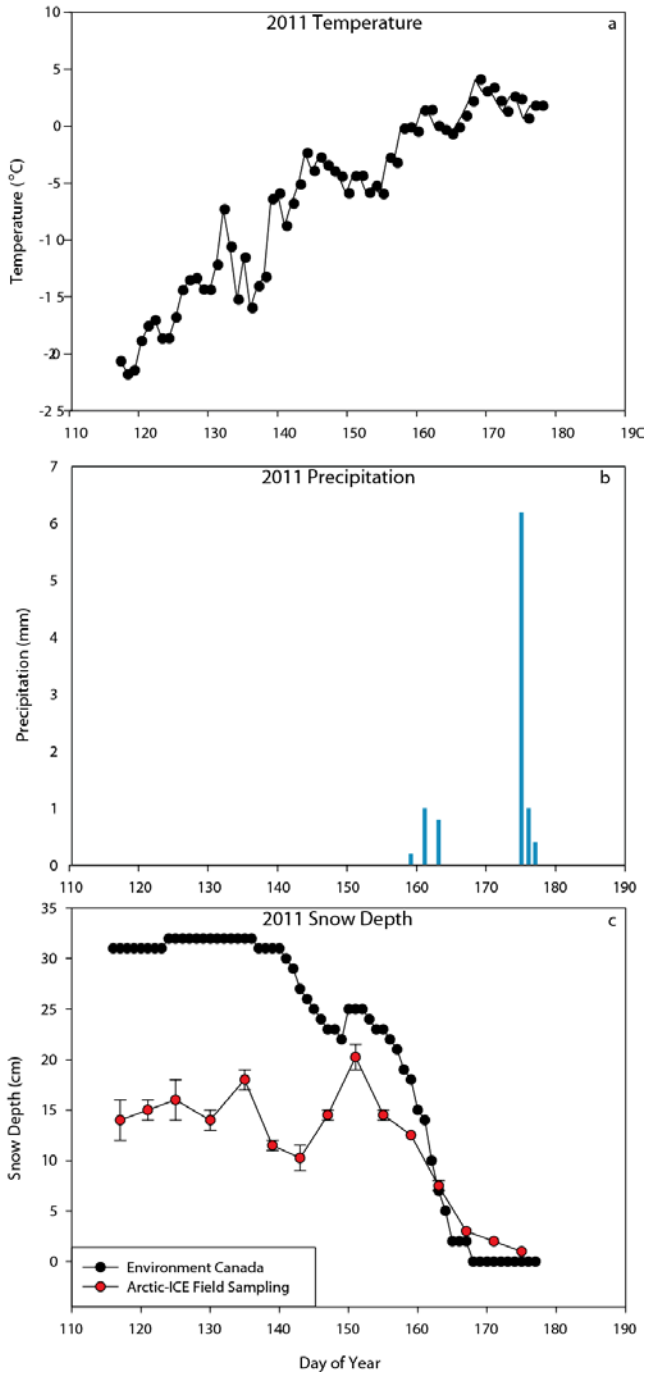

Figure 3.3: a) Daily averaged air temperature during the 2011 Arctic-ICE sampling campaign (data were collected from the Arctic-ICE meteorological tower). b) Total rain precipitation during 2011 Arctic-ICE field campaign (data were collected from Environment Canada). c) Average snow depth (± standard error bars) on ice between high, medium, and low snow sites during the 2011 Arctic-ICE field campaign. On-ice snow depth data were also collected from Environment Canada for comparison purposes.

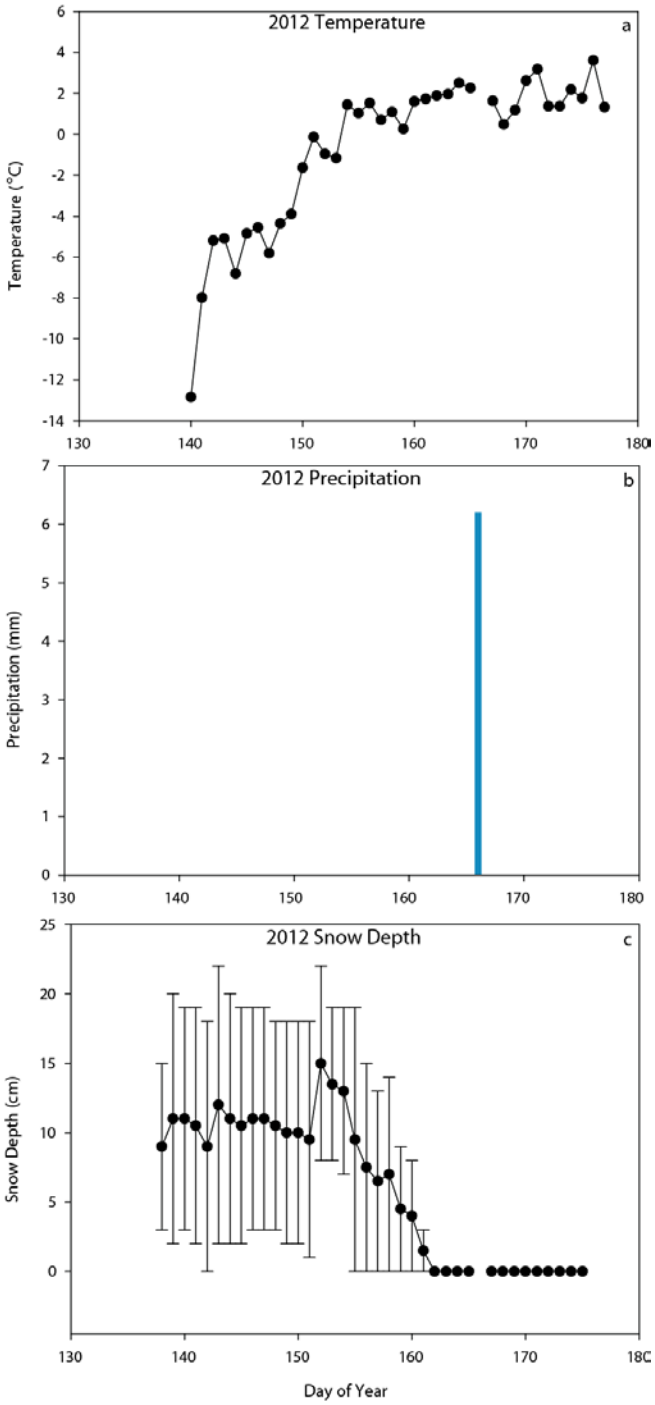

Figure 3.4: a) Daily averaged air temperature during 2012 Arctic-ICE sampling campaign (data were collected from the Arctic-ICE meteorological tower). b) Total rain precipitation during 2012 Arctic-ICE field campaign (data were collected from Environment Canada). c) Average snow depth (± standard error bars) on ice between high and low snow sites during the 2012 Arctic-ICE field campaign.

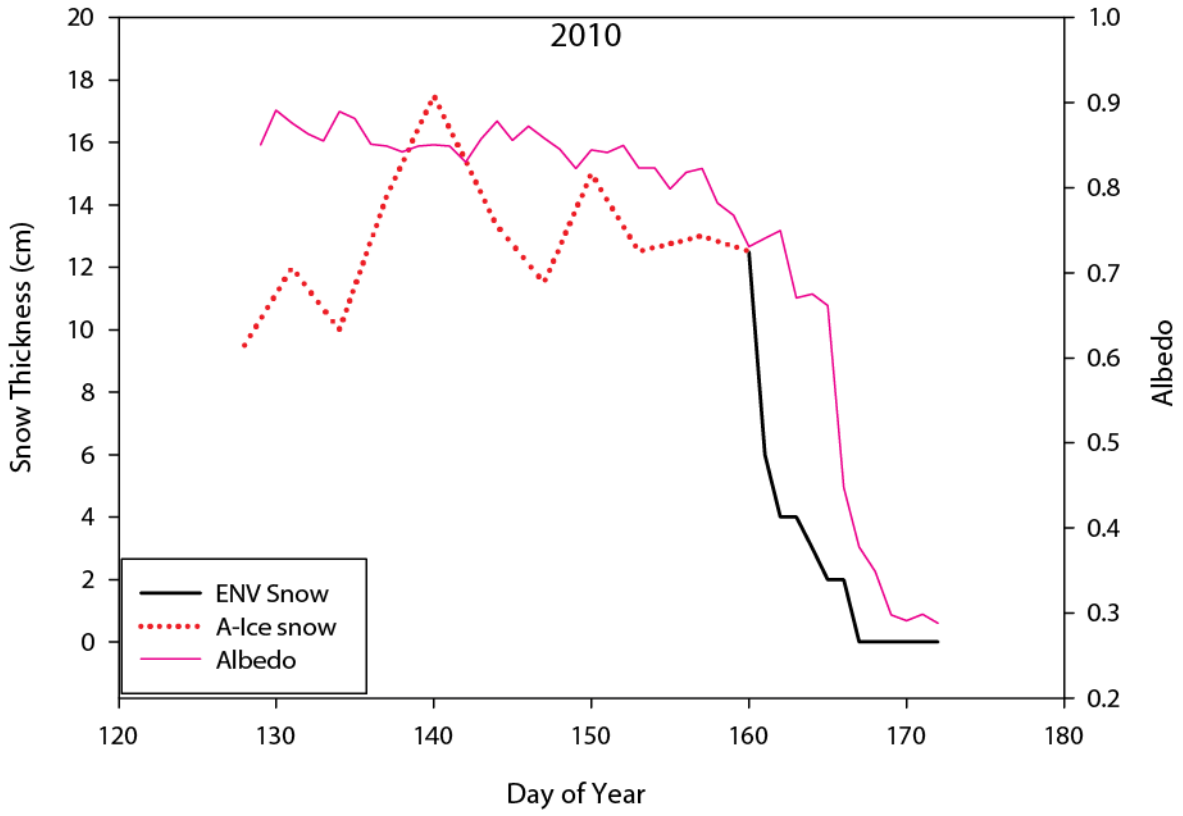

Figure 3.5: Mean daily albedo measurements contrasted against measured snow cover over the 2010 Arctic-ICE field campaign. Data were collected at the Arctic-ICE meteorological station until June 9 (DOY 160), then following June 9, snow data were from Environment Canada.

Recorded by the upper most tether PAR sensors at 2 m on June 19, transmitted PAR showed a maximum of 444 (20 to 39% incident PAR) and 286 (13 to 25% incident PAR) µmol m^{-2} s^{-1} under melt pond (low snow) and white ice (high snow) covers, respectively. Applying the attenuation-Chl *a* relationship described in chapter 2, I estimated PAR transmitted to the bottom of the ice from the upper most sensor located on the tether. Estimated values were 588 (26 to 52% incident PAR) and 378 (17 to 33% incident PAR) µmol m^{-2} s^{-1} under melt pond (low snow) and white ice (high snow) covers, respectively.

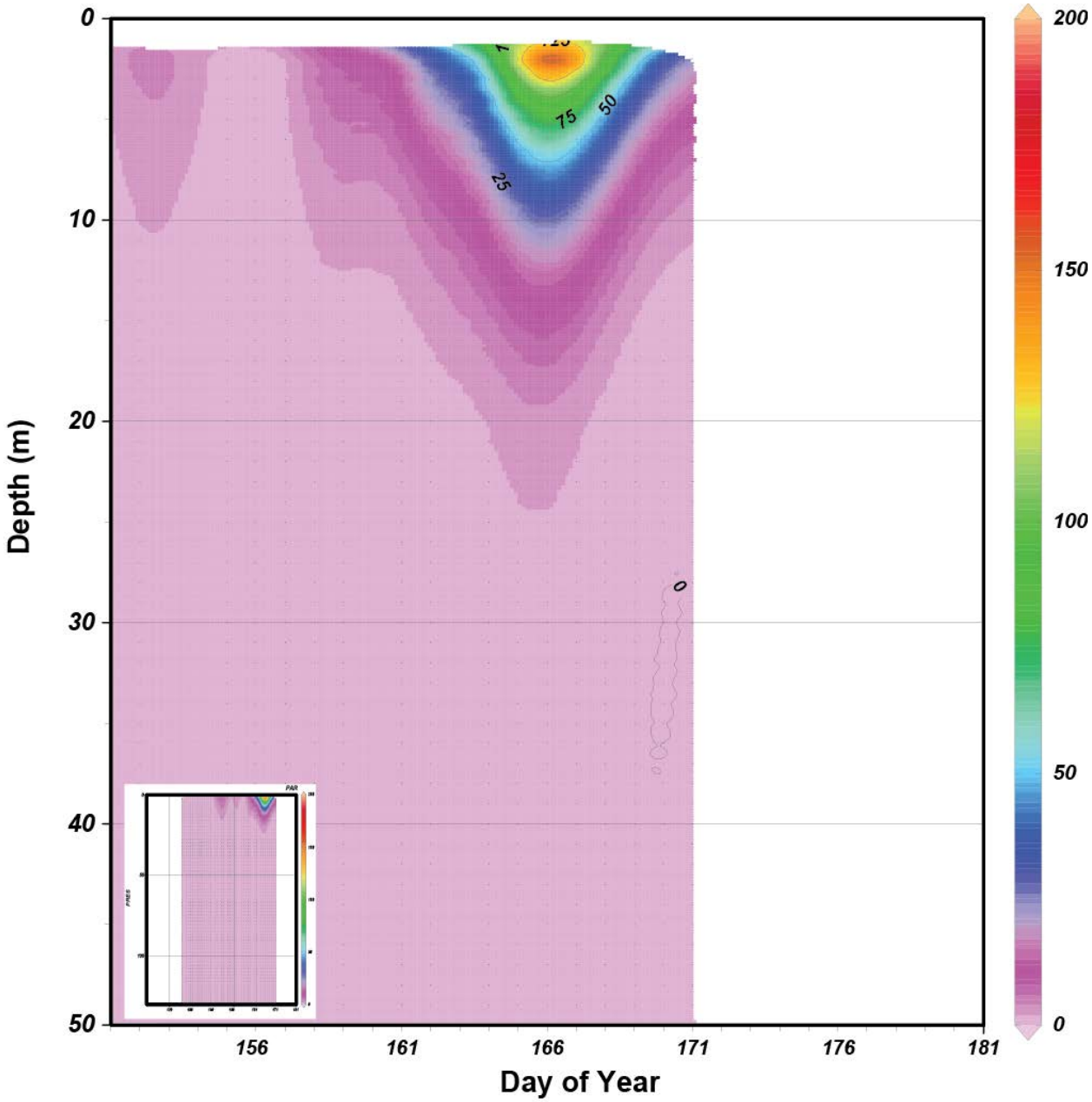

Figure 3.6: Estimated transmitted PAR (µmol m^{-2} s^{-1}) in the upper 50 m water column during the month of June. Estimates are from the 2010 Arctic-ICE campaign calculated by extrapolating the 20 m depth CTD-based PAR measurement to the surface using *in-vivo* Chl *a* data and the derived K_{PAR}-Chl *a* relationship (see Chapter 2). The inset on the lower left shows the 140 m water column and covering the entire 2010 sampling period.

In 2011, surface albedo was consistent at ~0.84 until June 9 when a strong decrease took place (Figure 3.7). The swift decrease in albedo can be partly attributed to the increased air temperature above 0 °C, contributing to the initial melt of the snow cover that decreased from 31 to 20 cm depth prior to June 9. Additionally, two major rain events took place on June 10 and 12 that rapidly melted the snow cover causing the observed decrease in albedo which reached ~0.3 by June 11. A minimum value was observed on June 15 at 0.23. Following this minimum, albedo increased to ~0.56 and remained at this point until end of sampling. The increase in albedo can be attributed to the drainage of ponds within the down looking sensor's field of view (Landy et al., 2014). Transmitted PAR appeared to increase much more gradual in comparison to that observed in 2010, but penetrated deeper into the water column by the end of the period (Figure 3.8). Recorded by the upper most tether PAR sensors at 2 m under the low snow and 5 m under the high snow on June 20, hourly transmitted PAR peaked at 851 (27 to 54% incident PAR) and 312 (10 to 20% incident PAR) μmol m^{-2} s^{-1} under the melt pond (low snow) and white ice (high snow) sites, respectively. Bottom ice estimated values were 1037 (33 to 65% incident PAR) and 685 (22 to 43% incident PAR) μmol m^{-2} s^{-1} under melt pond (low snow) and white ice (high snow) covers, respectively.

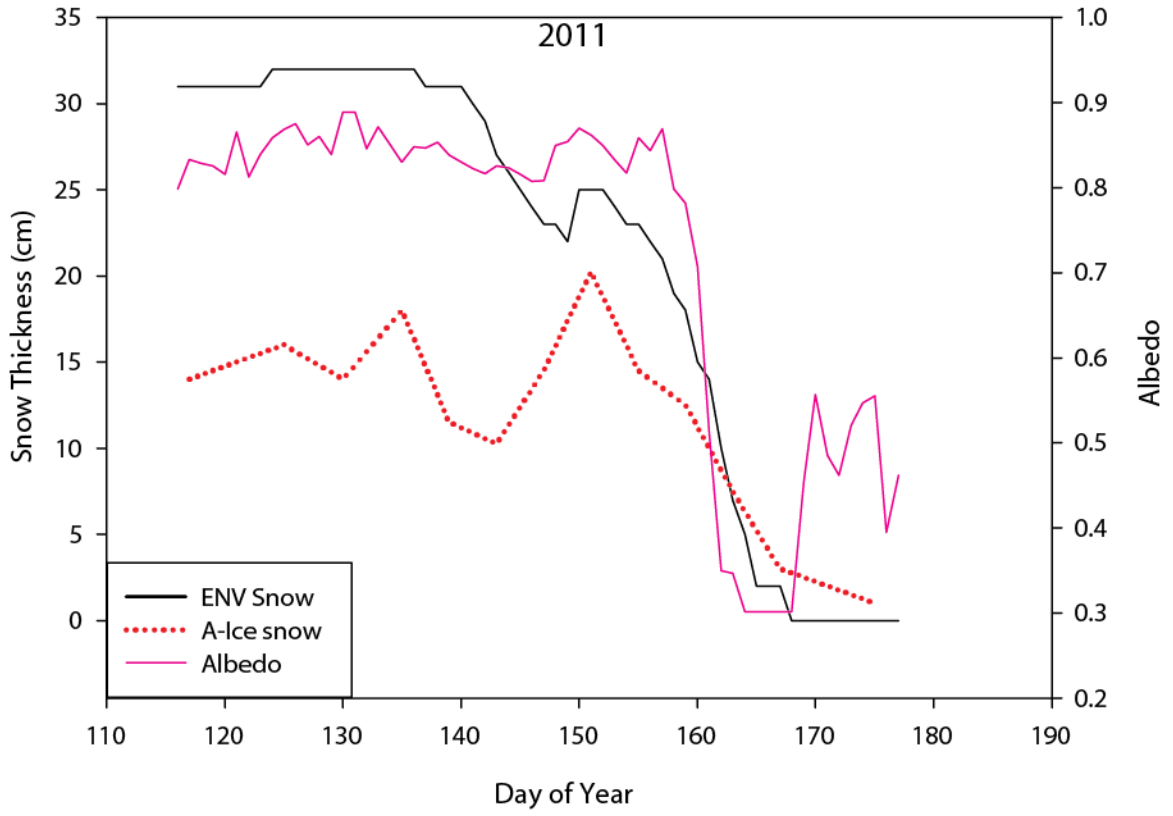

Figure 3.7: Mean daily albedo measurements contrasted against snow thickness over the 2011 Arctic-ICE field campaign. Snow data were from Environment Canada and Arctic-ICE field camp.

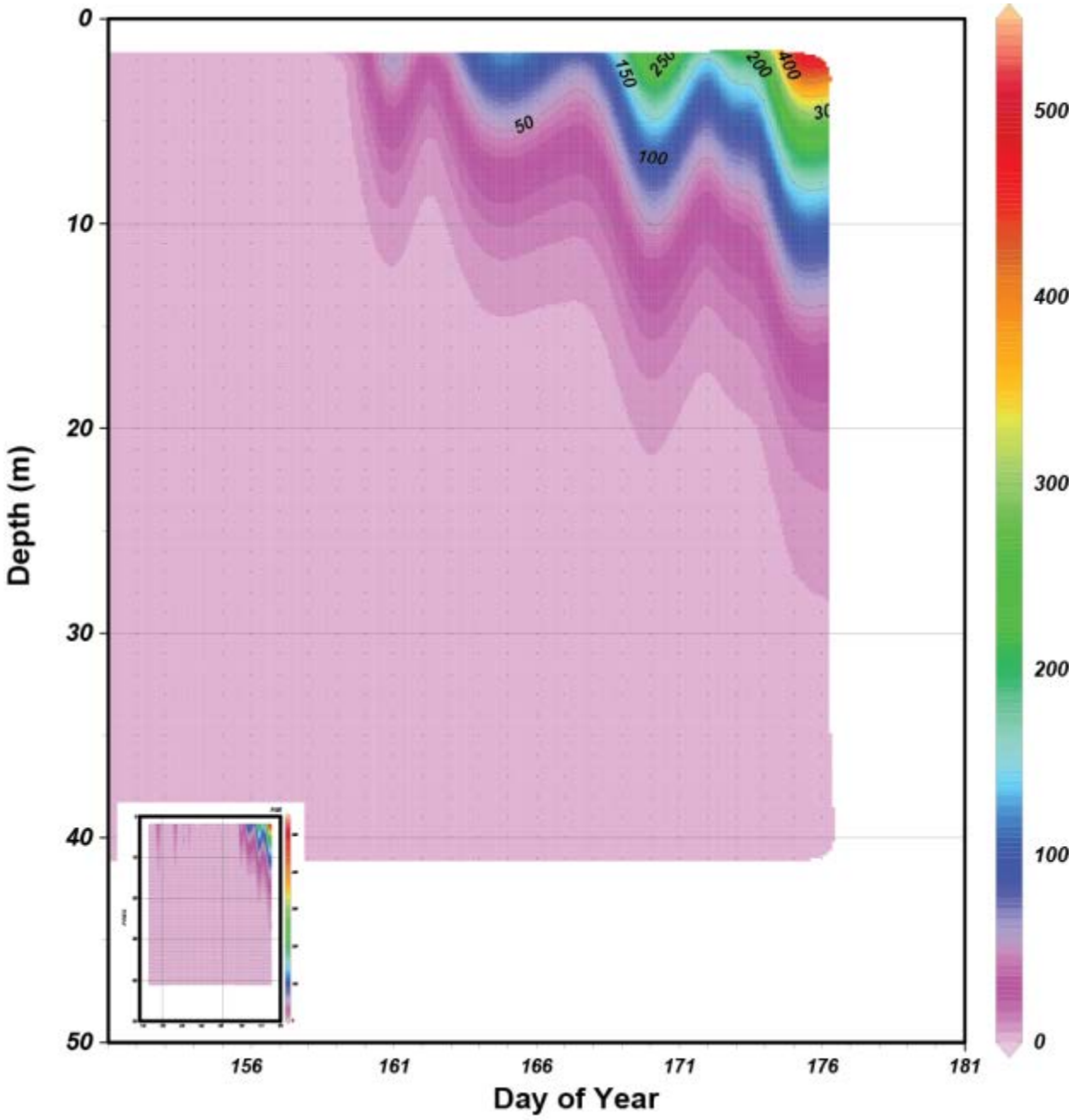

Figure 3.8: Estimated transmitted PAR (μmol m^{-2} s^{-1}) in the water column during the month of June. Estimates are from the 2011 Arctic-ICE campaign calculated by extrapolating the 20 m depth CTD-based PAR measurement to the surface using *in-vivo* Chl *a* data and the derived K_{PAR}-Chl *a* relationship (see Chapter 2). The inset on the lower left shows the entire 2011 sampling period.

In 2012, surface albedo ranged from 0.75 to 0.90 prior to melt onset on June 4 (Figure 3.9). Albedo decreased slowly relative to the two previous years, reaching ~0.30 on June 13. Increased air temperatures melted the average snow cover from ~19 to 0 cm depth by June 9. A major rainfall event took place on June 14 that flooded the ice surface; however, the snow cover already was nearly absent under the meteorological station prior to the rain event. Following the rain event on June 14 the albedo continued to decrease until it reached ~0.1 on June 25. The decrease in albedo can be attributed to the flooding of the ice surface and slow drainage, which caused a deepening of the melt pond underneath the albedo sensor (Landy et al., 2014). The albedo remained at this point until end of sampling. Similar to 2010, transmitted PAR increased quite rapidly, then appeared to stabilize following June 14 (Figure 3.10). Recorded by the upper most tether PAR sensors at 1.5 m depths, hourly averaged transmitted PAR peaked at 644 (25 to 50% incident PAR at 1.5 m depth) and 460 (18 to 36% incident PAR at 1.5 m depth) μmol m^{-2} s^{-1} under the melt pond (low snow) and white ice (high snow) sites, respectively. Bottom ice transmitted PAR were estimated at 726 (28 to 57% incident PAR) and 518 (20 to 40% incident PAR) μmol m^{-2} s^{-1} under melt pond (low snow) and white ice (high snow) covers, respectively.

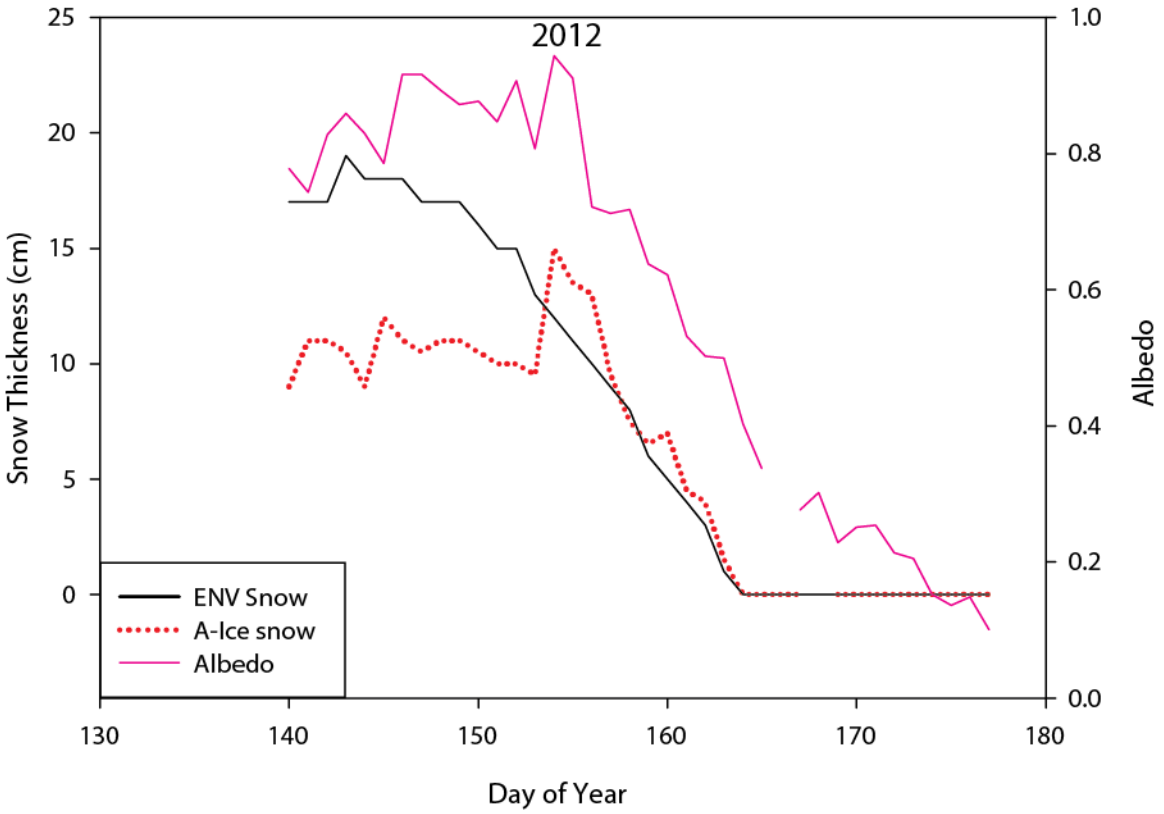

Figure 3.9: Mean daily albedo measurements contrasted against the snow thickness over the 2012 Arctic-ICE field campaign. Note: the gap in data is due to the sensor not working during a storm event (June 14). Snow data collected on site during Arctic-ICE field campaign and Environment Canada.

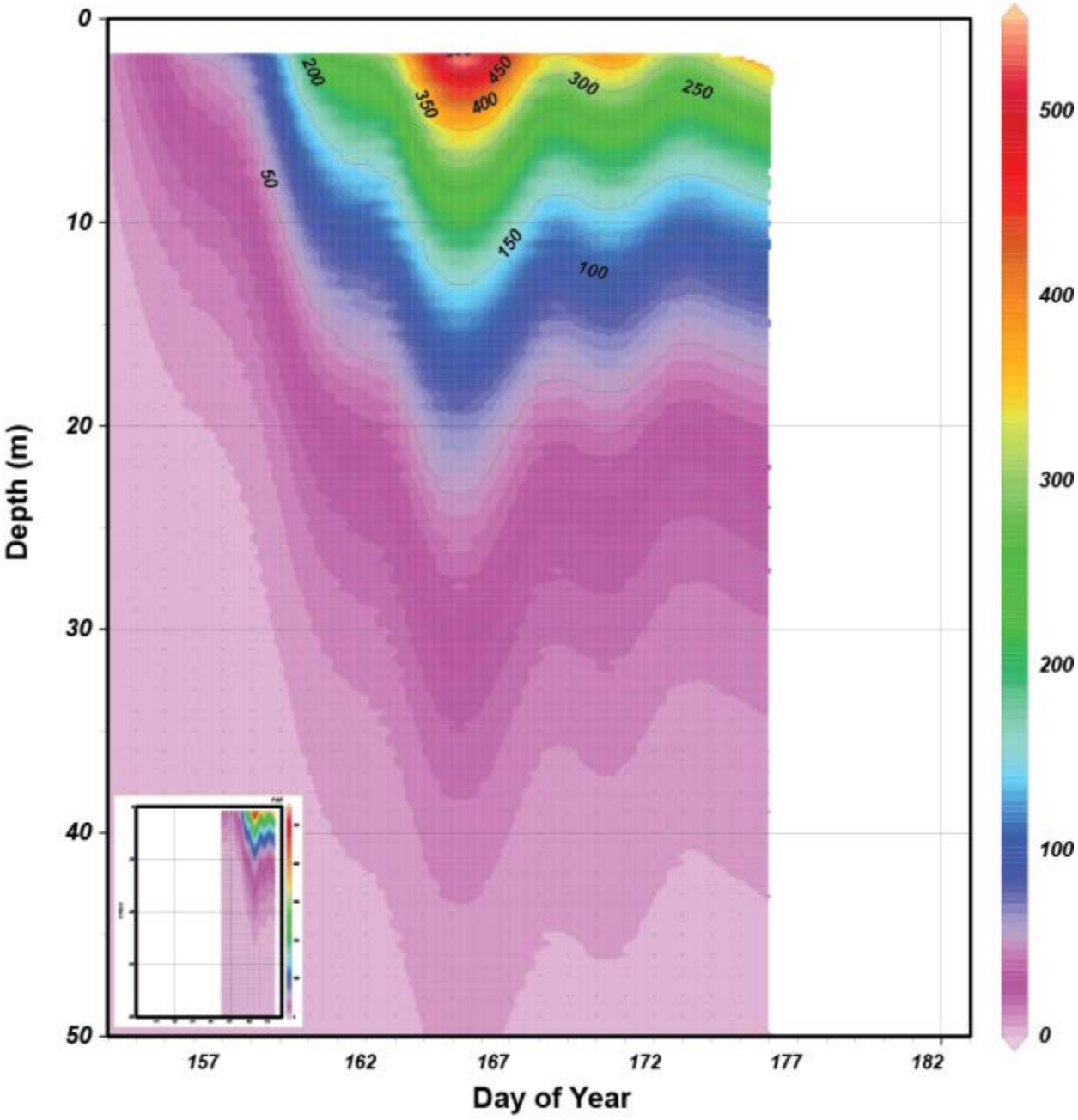

Figure 3.10: Estimated transmitted PAR (μmol m^{-2} s^{-1}) in the upper 50 m water column during the month of June. Estimates are from the 2012 Arctic-ICE campaign calculated by extrapolating the 20 m depth CTD-based PAR measurement to the surface using *in-vivo* Chl *a* data and the derived K_{PAR}-Chl *a* relationship (see Chapter 2). The inset on the lower left shows the entire 80 m water column and covering the entire 2012 sampling period.

3.0.3 Nutrients

In 2010 nitrate+nitrite (Figure 3.11A), silicic acid (Figure 3.12A), and phosphate (Figure 3.13A) at a 2 m water depth averaged 7.3, 14.7, and 1.3 µmol L^{-1}, respectively, prior to June 8 (i.e., prior to any substantial biomass accumulation in the water column). Nutrient concentrations decreased to 0.1, 2.1, and 0.6 µmol L^{-1} for nitrate+nitrite, silicic acid, and phosphate, respectively, by the end of the period at a 2 m water depth. Furthermore, concentrations were depleted to similar low concentrations down to a depth of at least 25 m (0.2, 3.9, and 0.8 µmol L^{-1}).

In 2011 nutrient concentrations at 2 m averaged 9.31, 14.19 and 1.0 µmol L^{-1}, respectively, for nitrate+nitrite (Figure 3.11B), silicic acid (Figure 3.12B), and phosphate (Figure 3.13B) prior to June 7 when biomass began to accumulate in the water column. Towards the end of the period (June 23), nutrient concentrations within the upper 2 m water column averaged 0.70, 2.07, and 0.65 µmol L^{-1}, respectively for nitrate+nitrite, silicic acid, and phosphate. As with 2010, nitrate+nitrite showed a considerable decrease down to at least a 10 m depth towards the end of the period on June 23 (1.1, 4.6, 0.6 µmol L^{-1}).

In 2012 nutrient concentrations at 2 m over the entire study averaged 7.6, 14.9 and 1.1 µmol L^{-1}, respectively, for nitrate+nitrite (Figure 3.11C), silicic acid (Figure 3.12C), and phosphate (Figure 3.13C). Only a slight decrease was observed in the nutrient concentrations over the course of sampling.

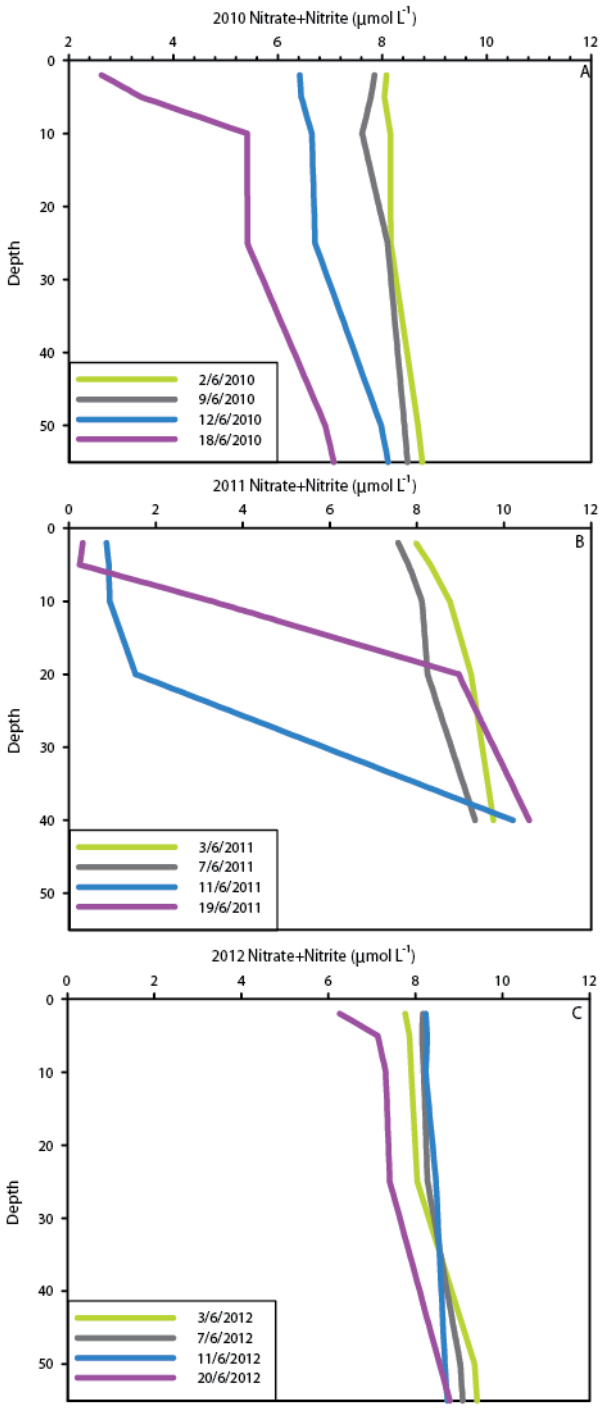

Figure 3.11: Discrete water column samples of nitrate+nitrite over the three field campaigns of Arctic-ICE (2010-A; 2011-B; 2012-C). Final sampling dates for 2010/2011 – June 22; 2012 – June 23.

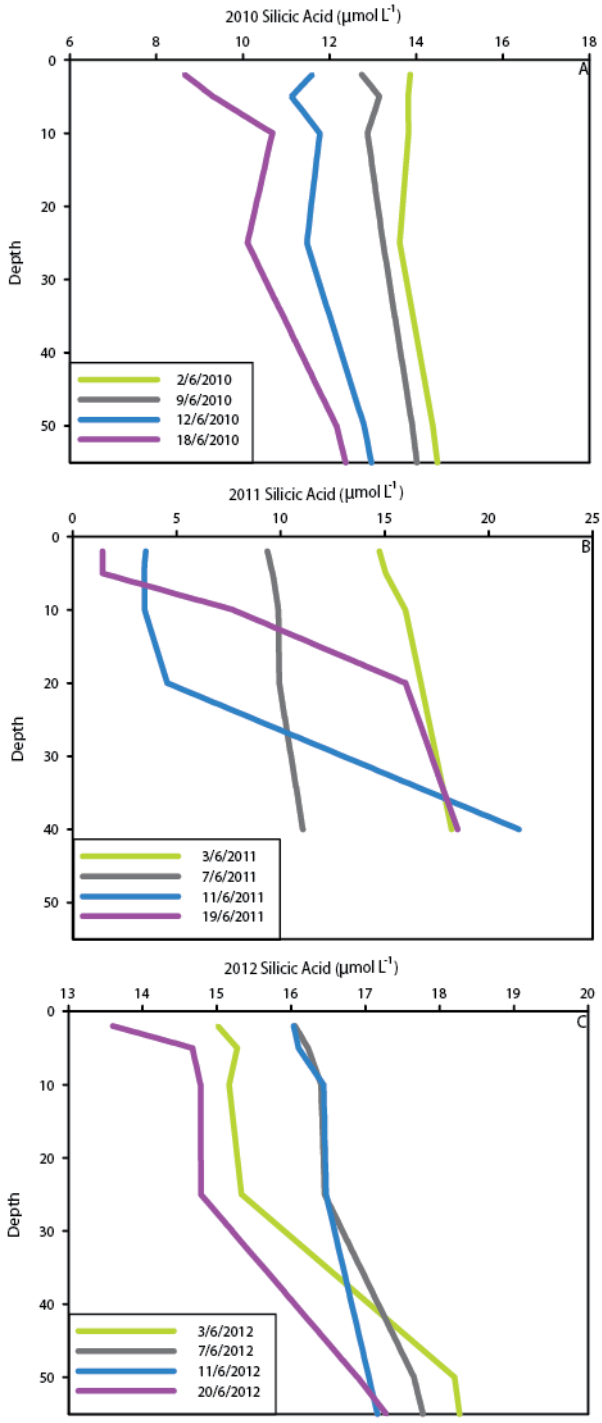

Figure 3.12: Discrete water column samples of silicic acid over the three field campaigns of Arctic-ICE (2010-A; 2011-B; 2012-C). Final sampling dates for 2010/2011 – June 22; 2012 – June 23.

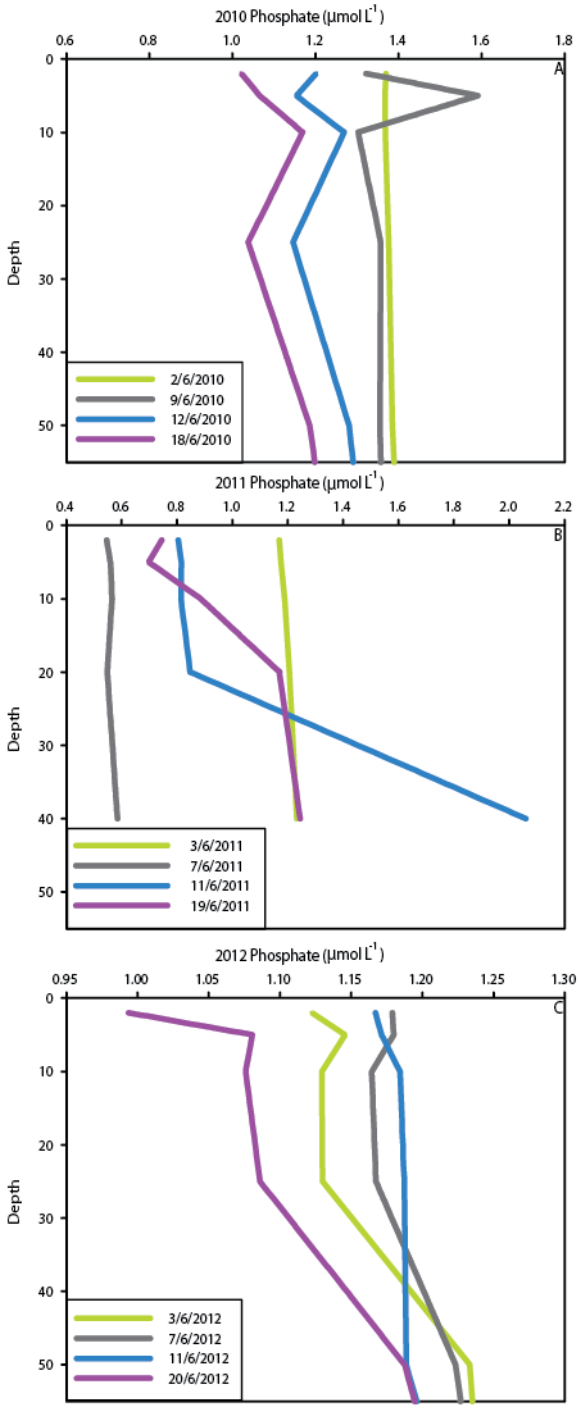

Figure 3.13: Discrete water column samples of phosphate over the three field campaigns of Arctic-ICE (2010-A; 2011-B; 2012-C). Final sampling dates for 2010/2011 – June 22; 2012 – June 23.

3.0.4 Water Column Structure

The CTD data from the three years each demonstrated a distinct seasonal pattern, but varied considerably between years. In 2010 temperatures were consistently near freezing at <-1.7 ^{o}C over the top 30 m of the water column until June 9 (Figure 3.14). Following June 9, temperatures in the upper water column increased substantially through to the end of the study (approximately 0.4 ^{o}C). From the beginning of the study, a salinity gradient existed throughout the upper water column, implying consistent stratification (i.e., no surface mixed layer). Snow and ice melt resulted in a slight freshening of the upper 2 to 10 m layer of the water column following June 11. By the end of the sampling period (June 21), surface waters down to >40 m were slightly less saline with approximately a 1.1 salinity change (Figure 3.15).

The 2011 water column data showed a variety of differences during the sampling season. Temperatures remained consistent around -1.75 to -1.65 ^{o}C over most of the 40 m water column until June 10 (Figure 3.16). On June 10 the entire column abruptly warmed to about -1.5 ^{o}C and continued to warm to -1.25 ^{o}C in the upper 20 m through to the end of the sampling period. The abrupt warming was associated with a decrease in surface salinities (Figure 3.17), which was likely influenced by the major precipitation events on June 10 and 12. By mid June, the pulse of freshwater into the surface layers relaxed, strongly stratifying the upper 5 to 10 m of the water column. Towards the end of the period, the low salinity layer had mixed down to greater than a 30 m depth.

During 2012, water column temperatures were around -1.7 to -1.6 ^{o}C over the entire 80 m water column until June 12 when the upper 2 to 5 m layer started to show a slightly increasing temperature (Figure 3.18). This warming was associated with a very small decreasing trend in

salinity over time (Figure 3.19). The gradual freshening and warming trend continued, reaching a depth of ~10 m until June 16, after which the surface freshening trend increased its rate mixing further down into the water column and affecting depths up to 30 m by the end of the study period.

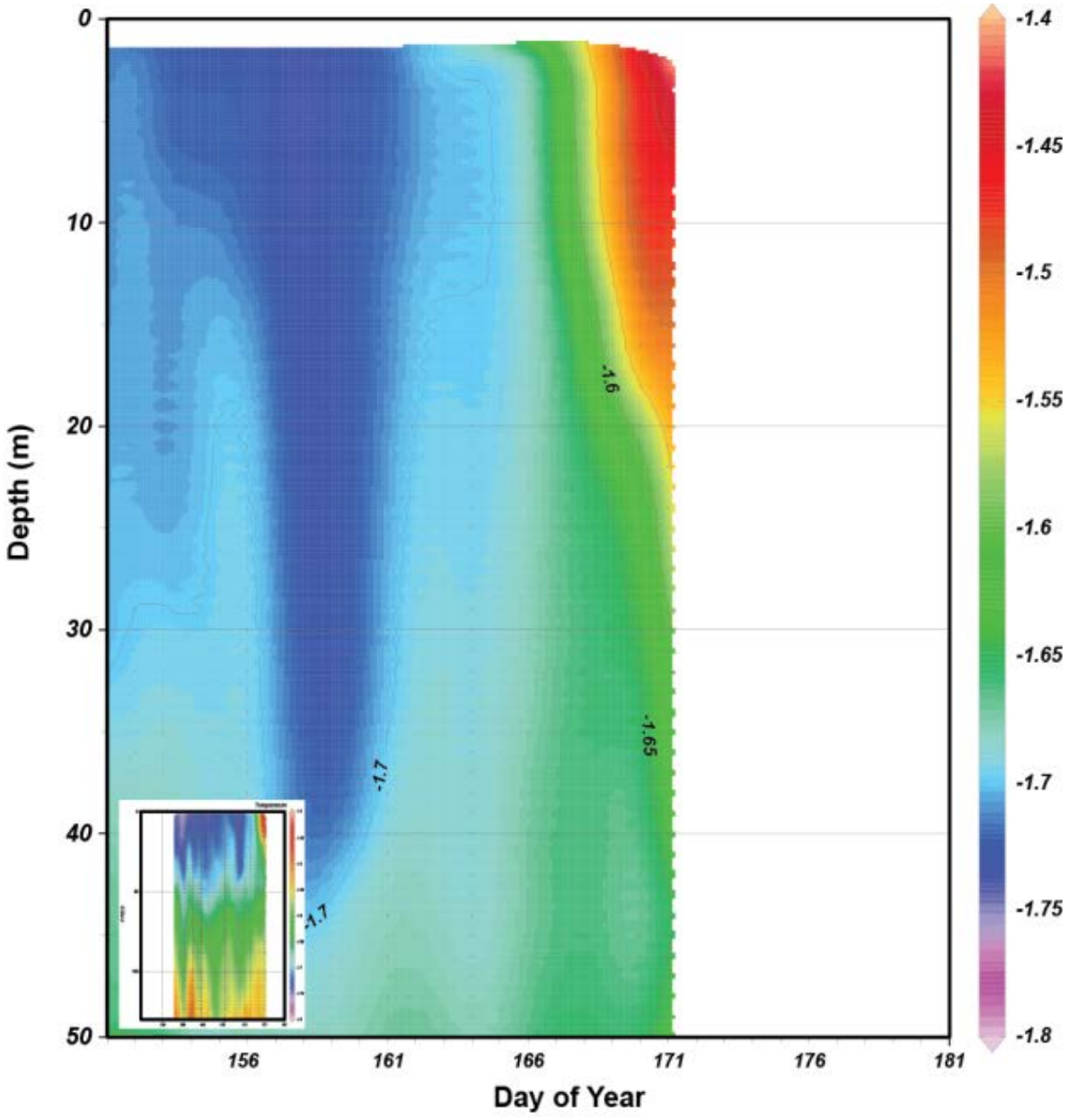

Figure 3.14: Time series of water column temperatures (°C) from daily CTD casts during the month of June (Arctic-ICE 2010). Inset in lower left is of the entire water column and data series.

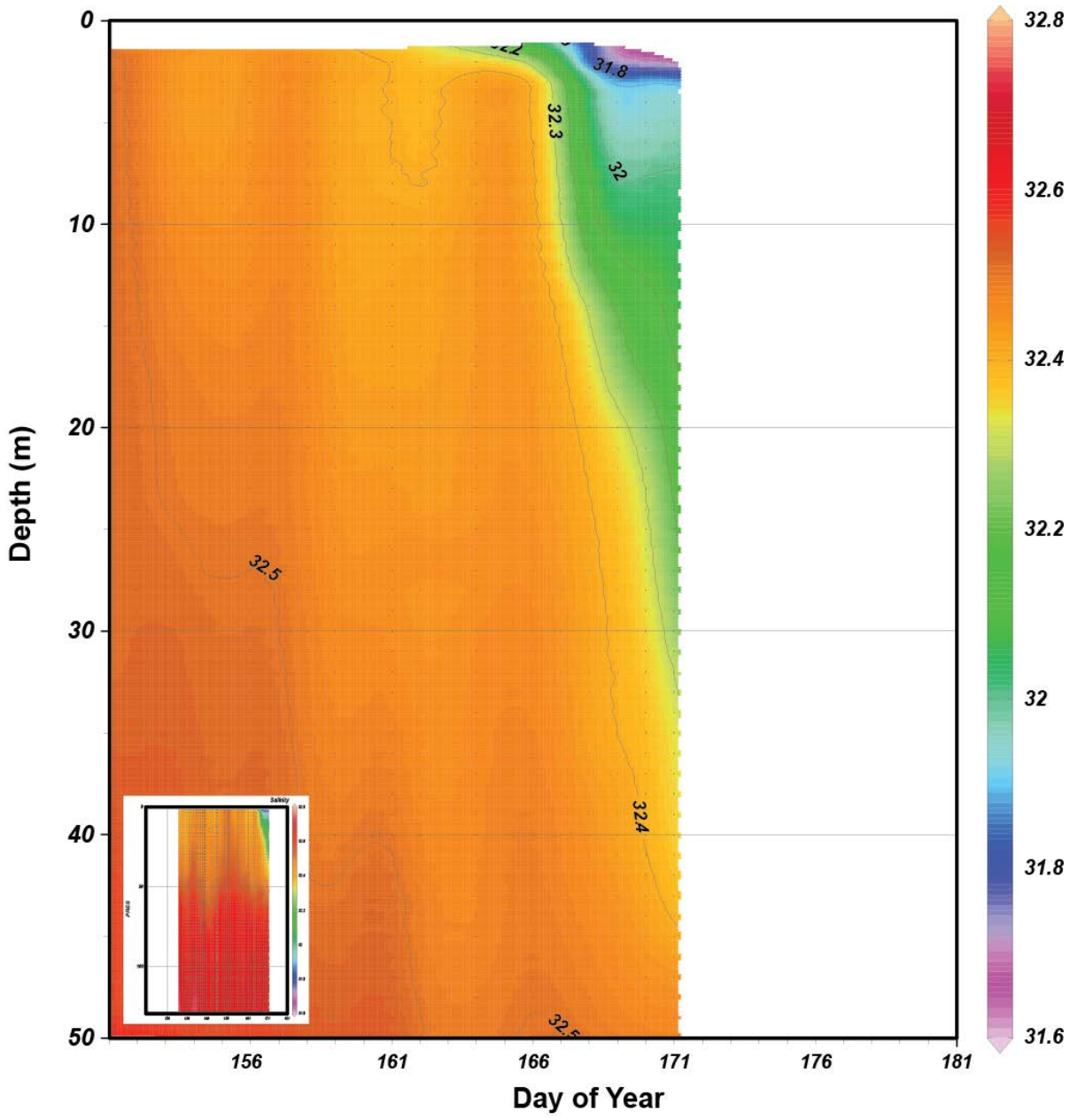

Figure 3.15: Time series of water column salinity from daily CTD casts during the month of June (Arctic-ICE 2010). Inset in lower left is of the entire water column and data series.

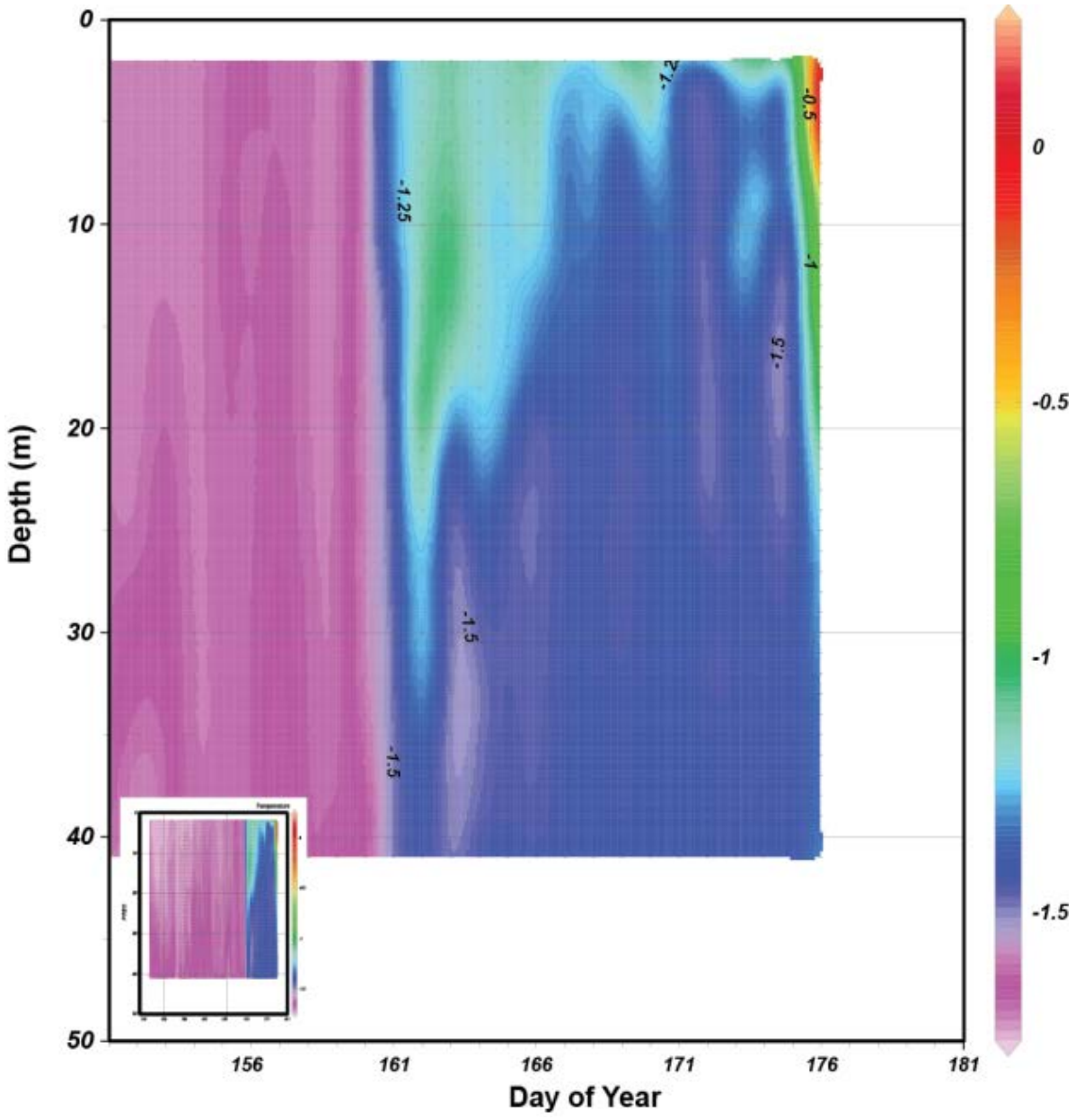

Figure 3.16: Time series of water column temperatures (°C) from daily CTD casts during the month of June (Arctic-ICE 2011). Inset in lower left is of the entire water column and data series.

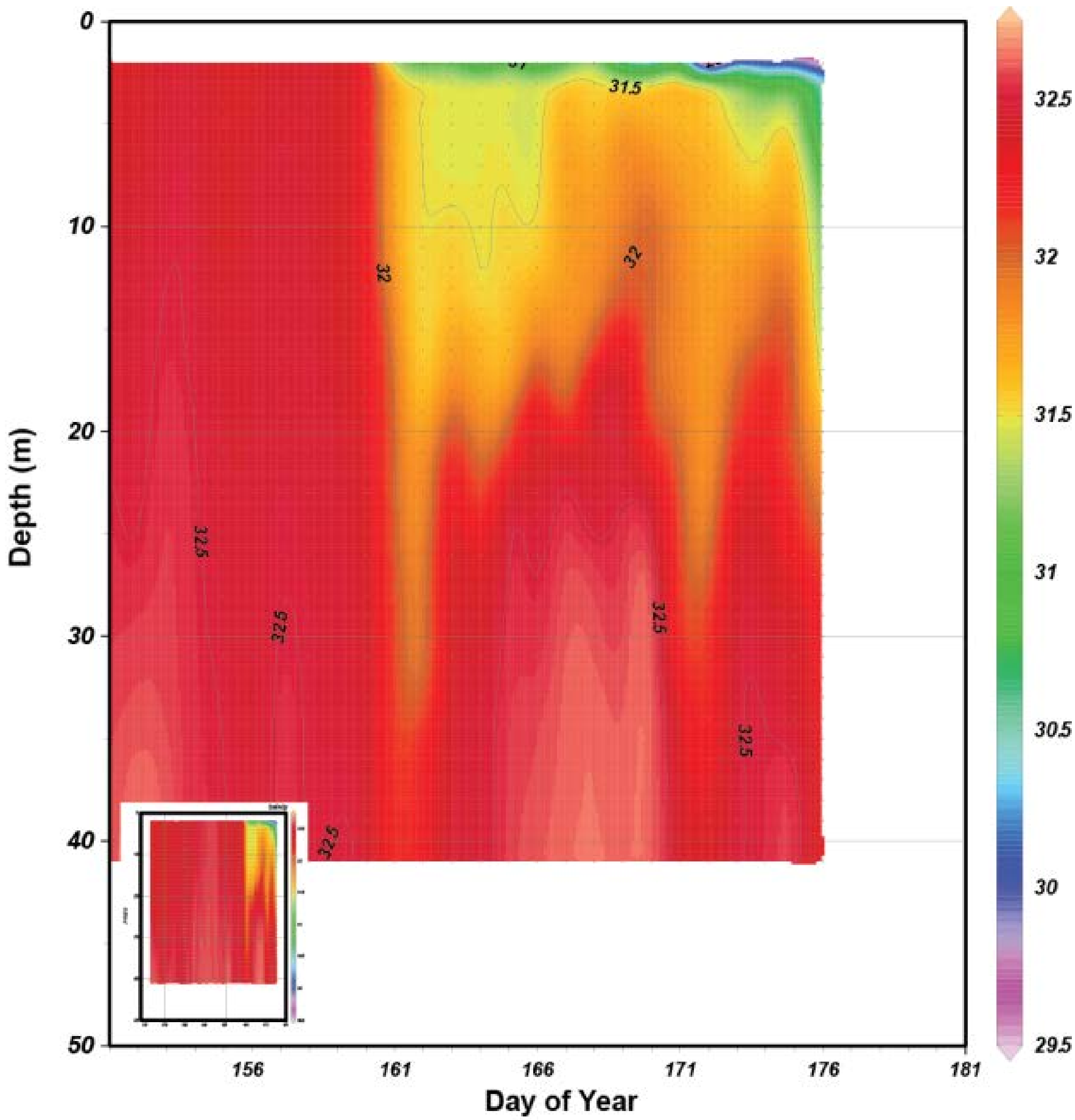

Figure 3.17: Time series of water column salinity from daily CTD casts during the month of June (Arctic-ICE 2011). Inset in lower left is of the entire water column and data series.

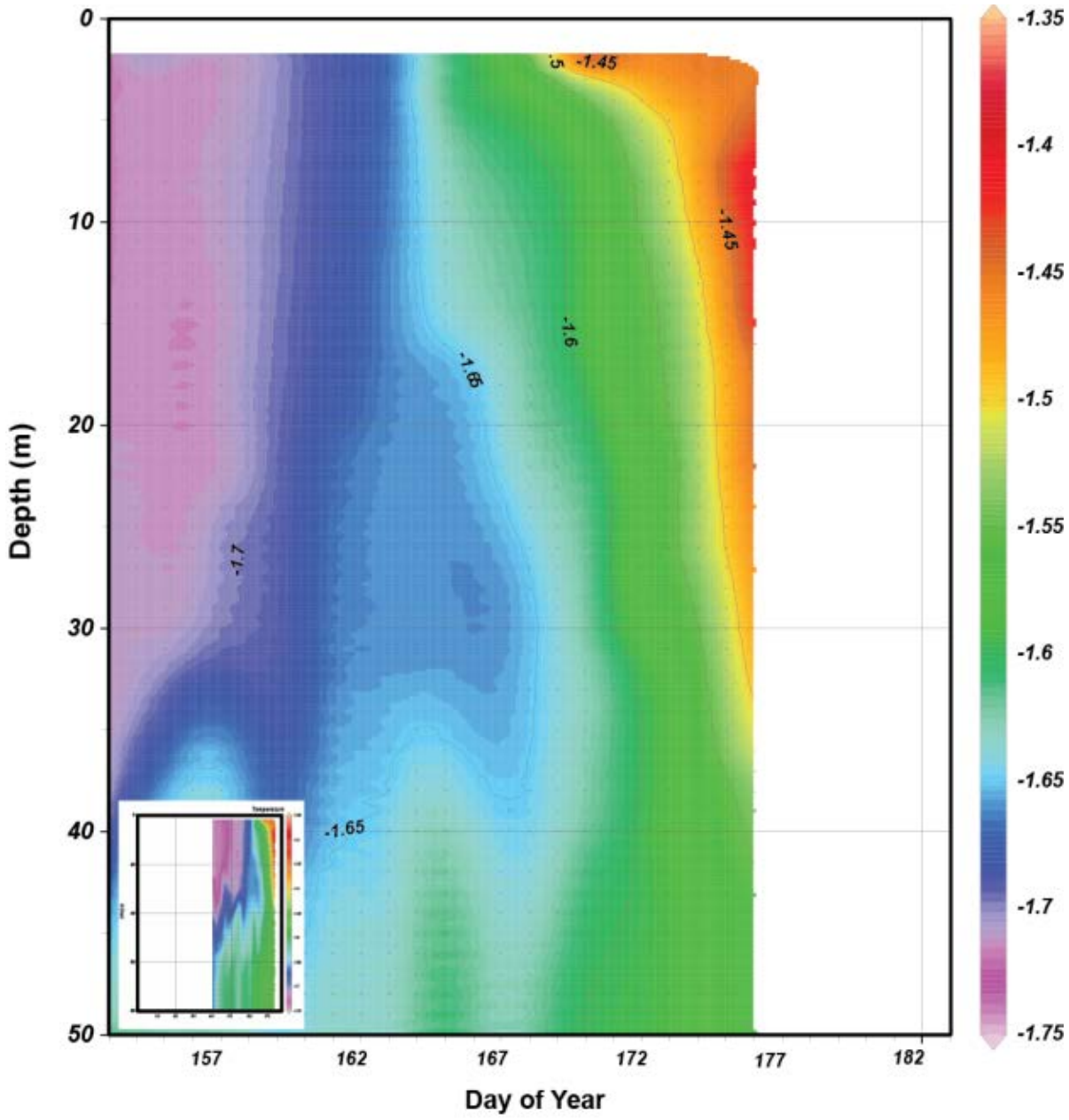

Figure 3.18: Time series of water column temperatures (°C) from daily CTD casts during the month of June (Arctic-ICE 2012). Inset in lower left is of the entire water column and data series.

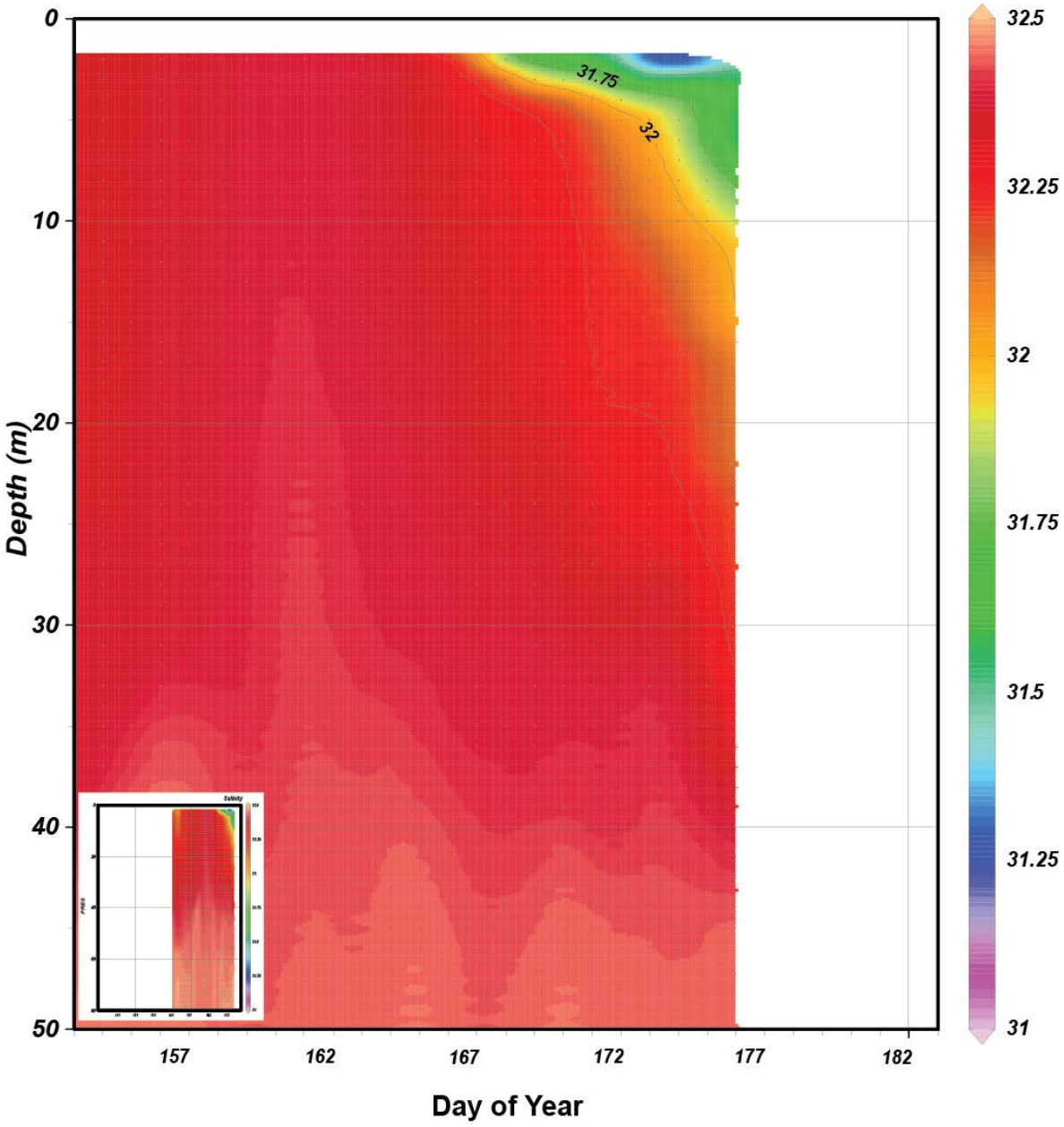

Figure 3.19: Time series of water column salinity from daily CTD casts during the month of June (Arctic-ICE 2012). Inset in lower left is of the entire water column and data series.

3.0.5 Chlorophyll a

Both the 2010 (Figure 3.20A) and 2011 (Figure 3.20B) campaigns were marked by a notable increase in Chl *a* within the upper water column towards the end of the period

(maximums of 445 and 319 mg m^{-2} integrated over the upper 50 m water column, respectively). However, 2012 (Figure 3.20C) showed no substantial increase in Chl *a* concentration during the study.

Prior to June 9 in the 2010 season, Chl *a* concentrations slowly increased in the top 50 m of the water column with integrated values increasing from ~ 5 to 28.0 mg m^{-2} (Figure 3.21). Starting June 9, Chl *a* concentrations rapidly increased in the upper water column, denoting the beginning of an under-ice phytoplankton bloom (Mundy et al., 2014). By the end of the period on June 21, Chl *a* concentrations had increased over the entire water column with peak recorded values within the upper 15 m, reaching its maximum *in vivo* Chl *a* concentration of 445 mg m^{-2} (Figure 3.21).

Generally, the 2011 season showed relatively constant values of Chl *a* concentration in the water column over the first half of the study (Figure 3.22). On May 28, Chl *a* concentrations started to increase slightly to water column integrated values of ~ 22 mg m^{-2}. An abrupt increase took place between June 8-11 where water column integrated concentrations reached a maximum of 319 mg m^{-2}. Following this date, surface Chl *a* concentrations decreased, causing a distinct subsurface Chl *a* maximum (SCM) to develop. The SCM deepened and decreased in concentration through to the end of the study period.

The 2012 season showed no substantial increase in Chl *a* concentration during our sampling season (Figure 3.23). However, water column integrated concentrations over the top 50 m did slightly increase at the end of the study period from a minimum of 15.2 mg m^{-2} on June 9 to a maximum of 23.4 mg m^{-2} on June 23.

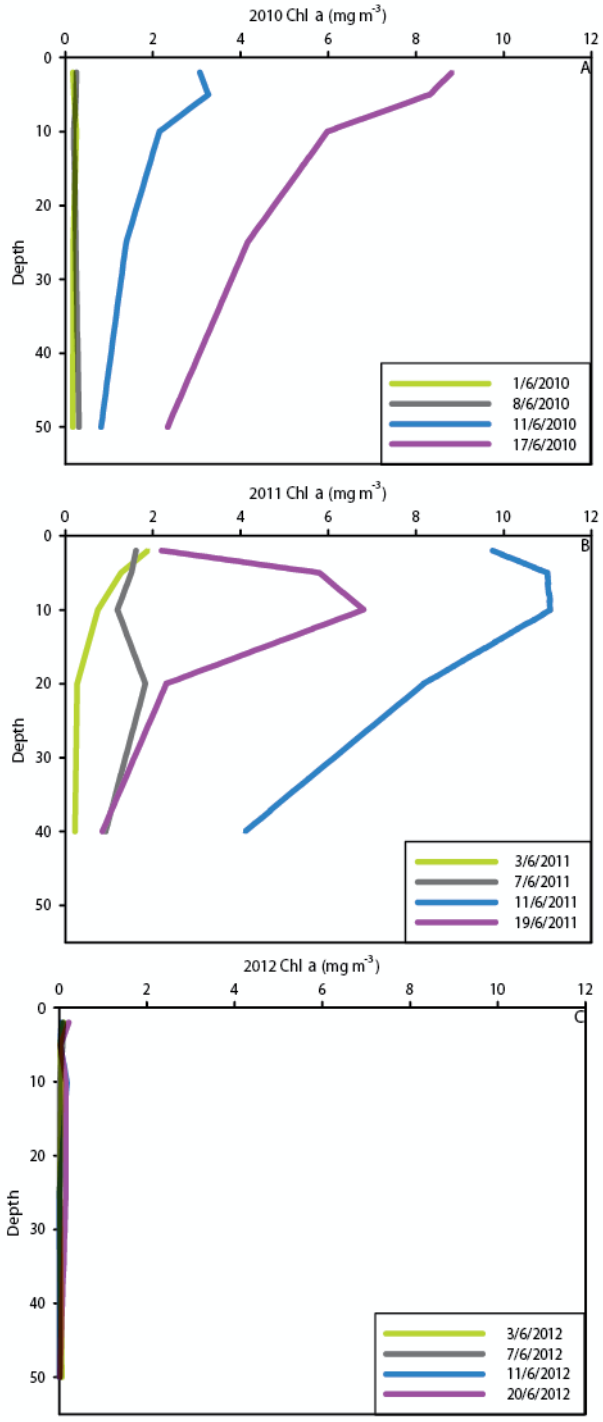

Figure 3.20: Discrete water column samples of Chl *a* over the three field campaigns of Arctic-ICE (2010-A; 2011-B; 2012-C). Final sampling dates for 2010/2011 – June 22; 2012 – June 23.

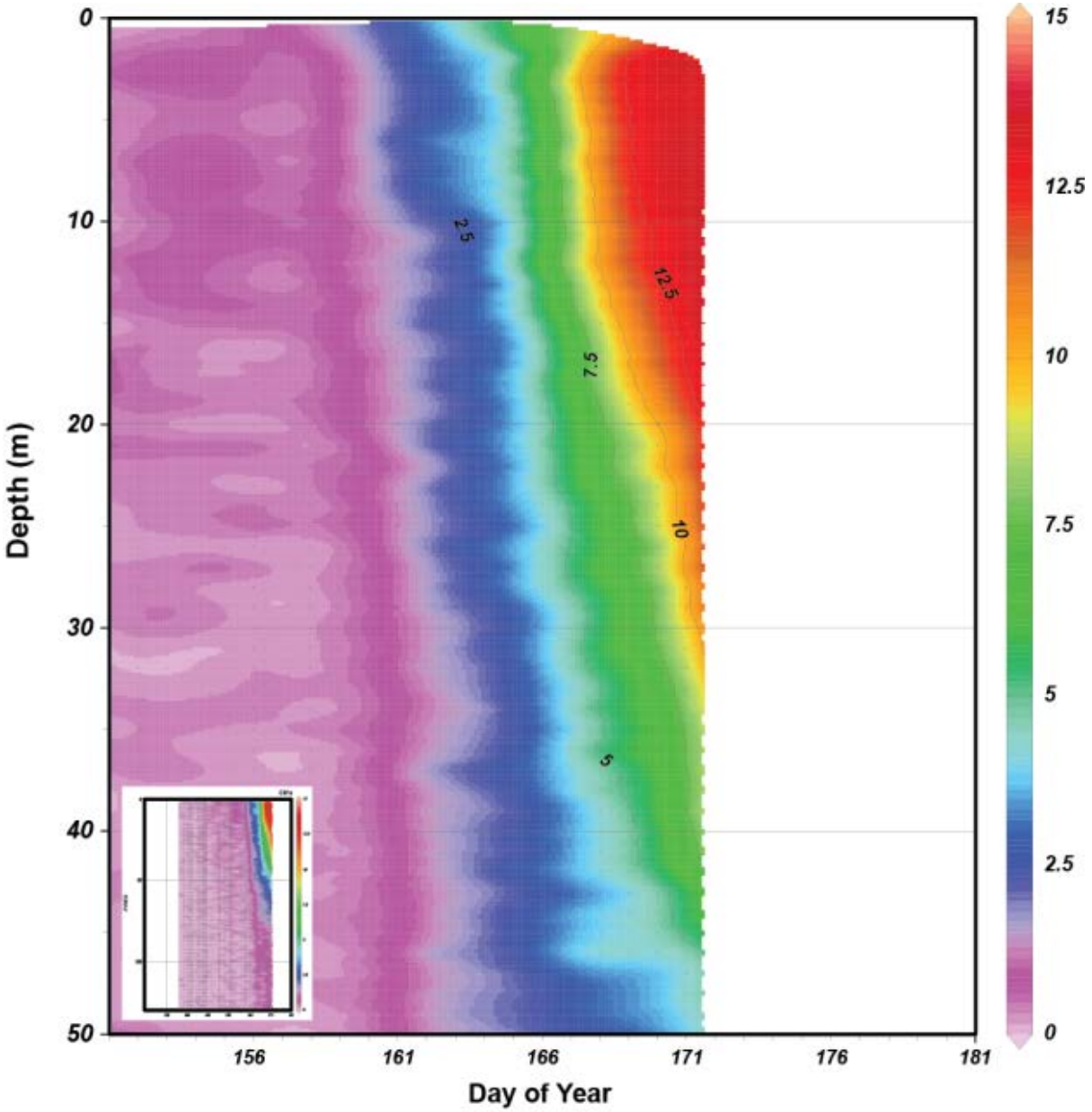

Figure 3.21: Time series of water column Chl *a* concentration (mg m^{-3}) from daily CTD casts during the month of June (Arctic-ICE 2010). Inset in lower left is of the entire water column and data series.

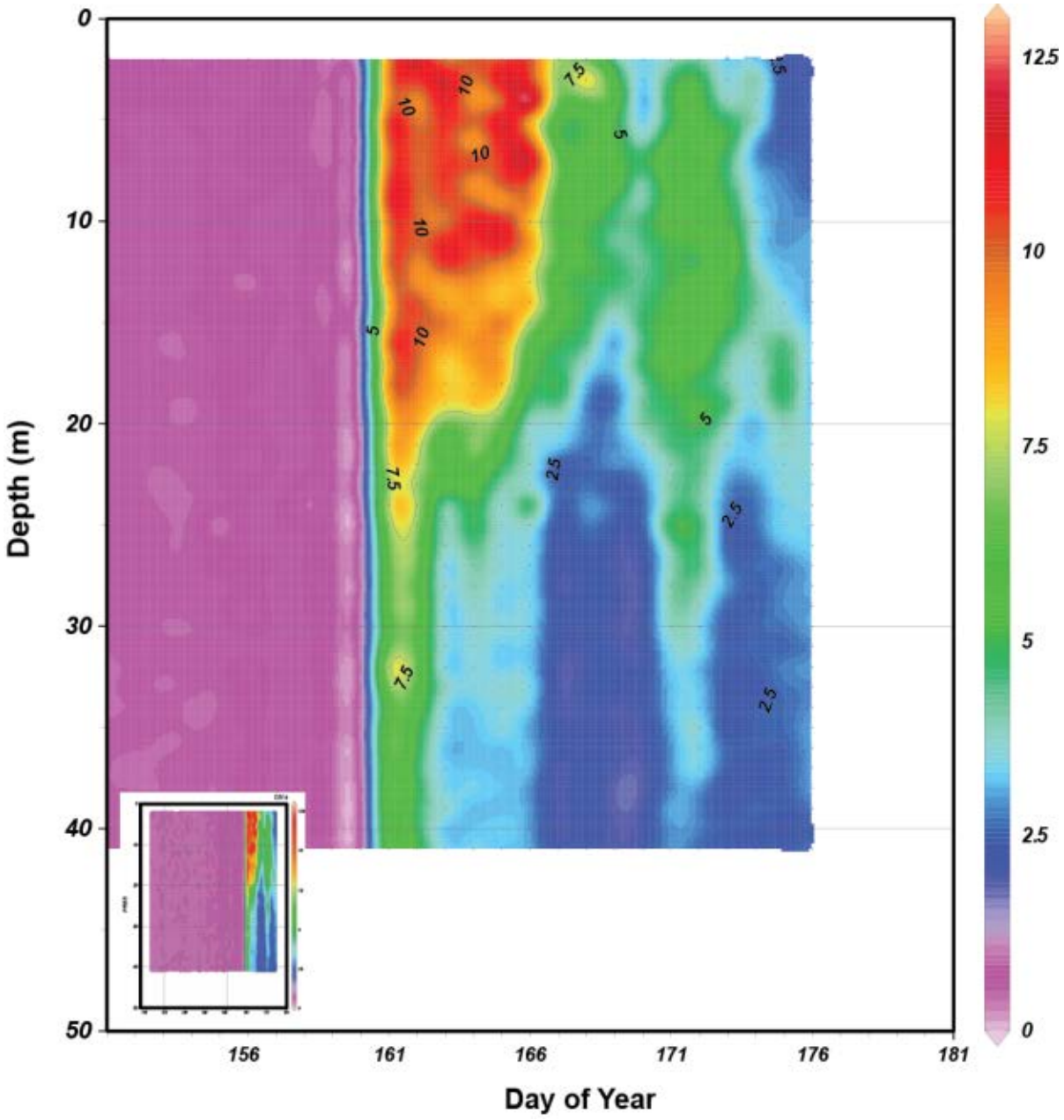

Figure 3.22: Time series of water column Chl *a* concentration (mg m^{-3}) from daily CTD casts during the month of June (Arctic-ICE 2011). Inset in lower left is of the entire water column and data series.

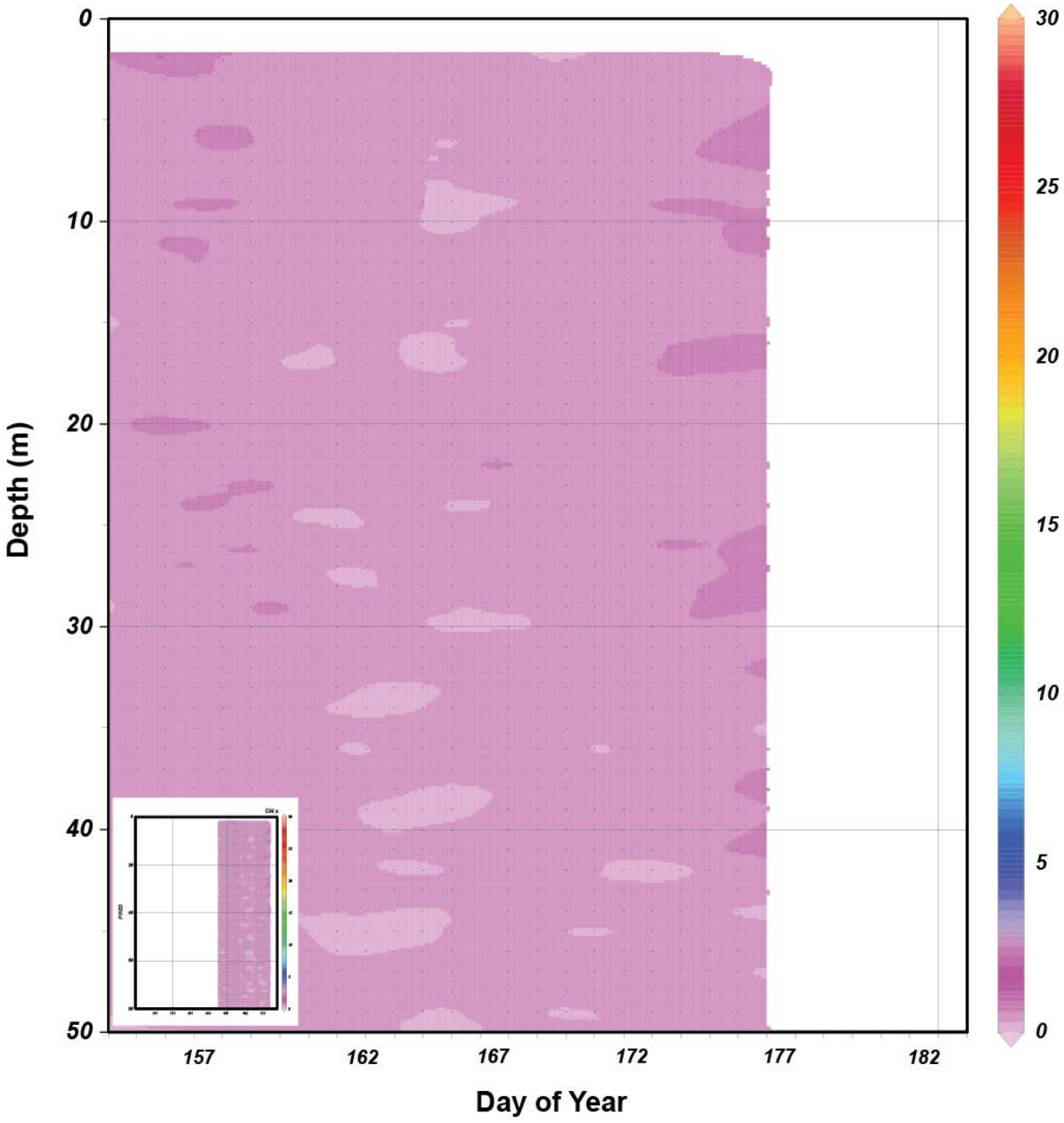

Figure 3.23: Time series of water column Chl *a* concentration (mg m^{-3}) from daily CTD casts during the month of June (Arctic-ICE 2012). Inset in lower left is of the entire water column and data series.

3.1 Long-Term Variability in Under-Ice Phytoplankton

To meet the second objective of my thesis, "To compare and contrast the timing of the under-ice bloom and controlling processes between different years", historical data were collected from a variety sources (see Chapter 2) and collated with the Arctic-ICE data discussed above.

3.1.1 Chlorophyll a Concentration

Chlorophyll *a* concentration data were obtained through databases maintained by academia, governments, and some peer-reviewed and grey literature publications (BioChem database; ARCNUT database; C-ICE'01 Field Summary Report; Michel et al. 2003; Michel et al. 2006; Apollonio and Matrai, 2011; NOAA World Ocean Database, 2013). Notable years of the historical datasets included 1983 in which no bloom occurred and 1986 in which a substantial bloom (287 [BioChem] and 278 [ArcNut] mg m^{-2}) took place under the ice. However, it should be noted that in 1983, there was a paucity of samples collected, and that measurements ended on June 7. The 1986 BioChem sampling showed the highest concentration of Chl *a* integrated over the upper 30 m of the water column at 539 mg m^{-2}. Additionally this was the latest bloom in our entire data set. For each year, presented in Figures 3.24-3.41, I estimated the date of bloom onset. Due to variability in the dataset's temporal coverage, setting strict criteria for bloom onset date was difficult. As the bloom would not develop under a dry snow cover/winter scenario, and to not select an erroneous onset date with that of ice algae sloughing from the sea ice and settling down into the water column, I used the following criteria: (1) snow melt was well underway and (2) Chl *a* concentration started increasing beyond baseline concentrations prior to the bloom

onset. Due to gaps in the temporal time series datasets during the melt period, I chose the middle date in between data points where a bloom was determined to commence. In some years, this gap was large and therefore, confidence in identifying the correct date of bloom onset was less and duly noted for these years.

3.1.2 Summary of Historical Data

Apollonio and Matrai (2011) presented four years of under ice Chl *a* concentration data in the water column; the 1956 dataset did not provide enough temporal information to determine the timing of a bloom. Therefore, I removed 1956 from my analyses. However, it was clear that primary production was taking place under the ice during this year in Allen Bay. Peak Chl *a* concentration during the 1956 study was 37.1 mg m^{-2} (not shown).

Data from the years 1961, 1962, and 1963 from Jones Sound under landfast ice did provide enough data to determine bloom timing (Apollonio and Matrai, 2011). The 1961 dataset from Environment Canada showed that daily averaged temperatures reached above 0 °C on June 18. All snow had diminished as of June 7. Sampling in 1961 began on June 25 with baseline values of 1.1 mg m^{-2}. July 9 was determined to be bloom onset with a peak of 84.8 mg m^{-2} reached on July 20 (Figure 3.24).

The 1962 dataset from Environment Canada showed that daily averaged temperatures reached above 0 °C on June 5. All snow had diminished as of June 27. The 1962 dataset had an initial sampling date of June 15 with a baseline value of 13.3 mg m^{-2}. Bloom onset during this study was determined to be June 25 with a peak value of 122 mg m^{-2} reached on July 2 (Figure 3.25). Similar to 1961, a second peak occurred under the ice days later on July 11 reaching 119 mg m^{-2}.

The 1963 dataset from Environment Canada showed that daily averaged temperatures reached above 0 °C on June 19. All snow had diminished as of July 11. Initial sampling for the 1963 dataset took place on June 19 and showed a baseline value of 8.8 mg m^{-2}. Bloom onset was determined to be June 27, after which a rapid accumulation of biomass occurred, peaking at 134 mg m^{-2} on July 9 (Figure 3.26).

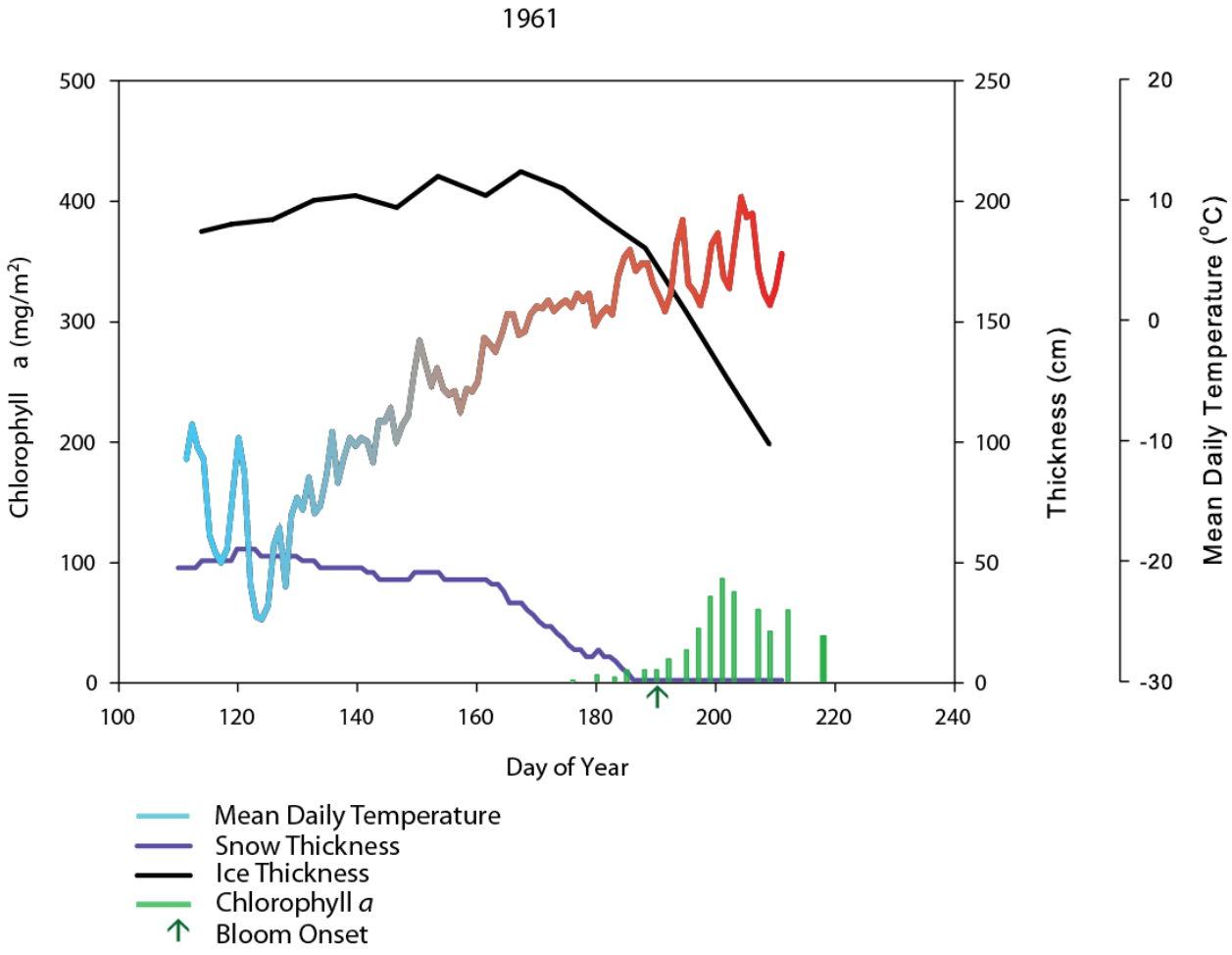

Figure 3.24 A complete graph of 1961 showing ice and snow thickness, chlorophyll a, bloom onset, and mean daily air temperature. Environmental variables collected from Environment data historical archive. Chlorophyll data is from Apollonio and Matrai (2011).

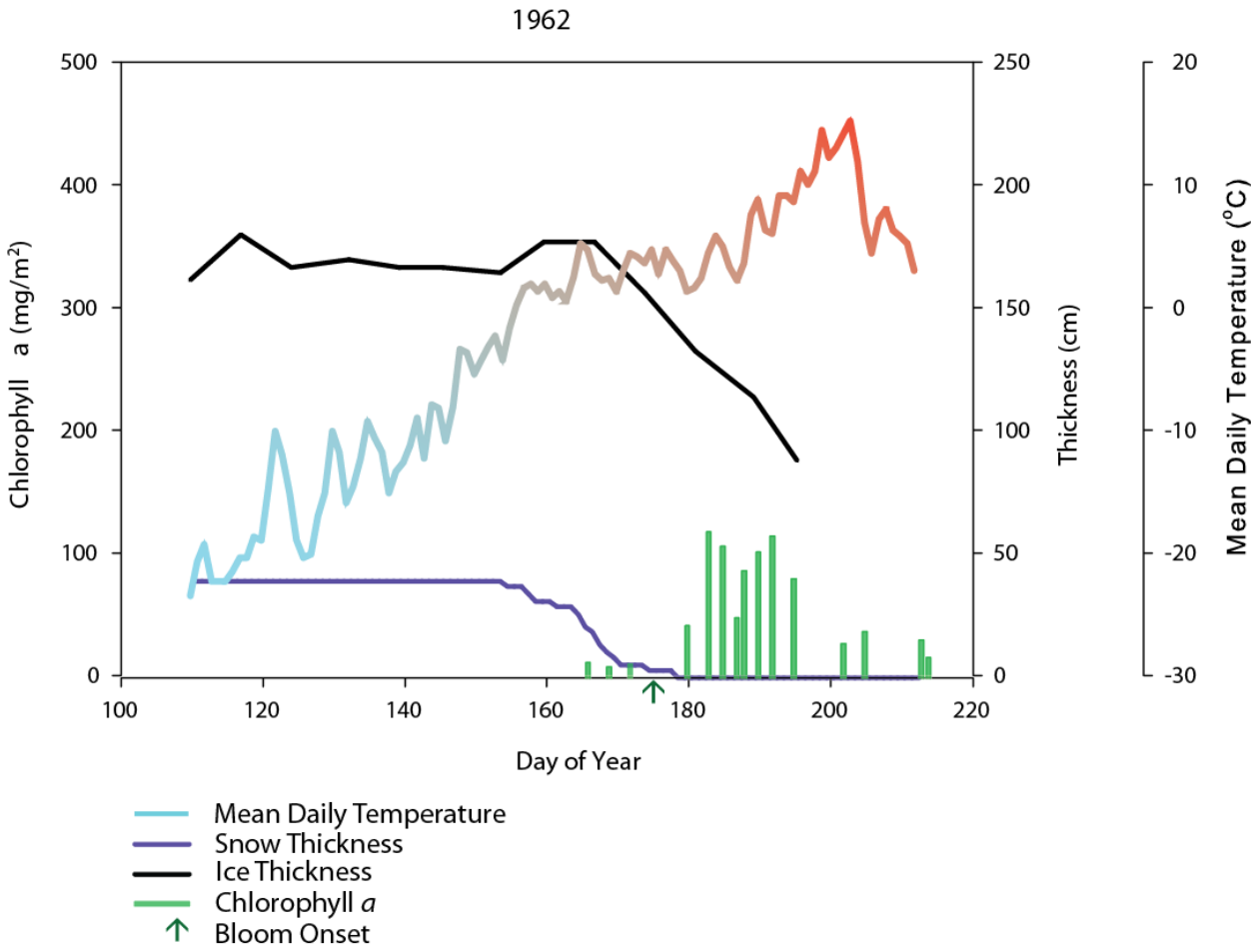

Figure 3.25: A complete graph of 1962 showing ice and snow thickness, chlorophyll a, bloom onset, and mean daily air temperature. Environmental variables collected from Environment data historical archive. Chlorophyll data is from Apollonio and Matrai (2011).

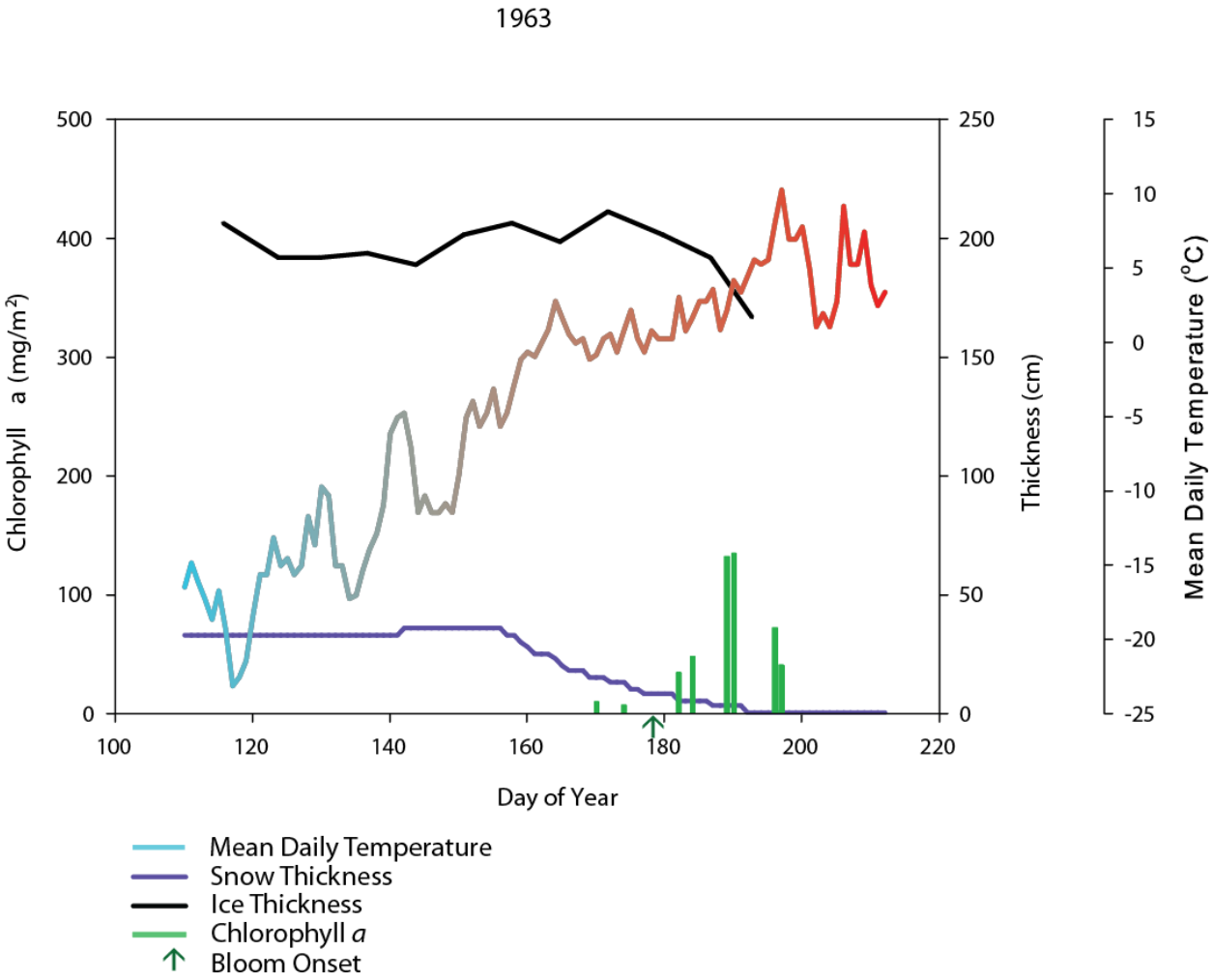

Figure 3.26: A complete graph of 1963 showing ice and snow thickness, chlorophyll *a*, bloom onset, and mean daily air temperature. Environmental variables collected from Environment data historical archive. Chlorophyll data is from Apollonio and Matrai (2011).

The rest of the blooms sampled were all from the Resolute Bay region. The 1984 dataset from Environment Canada showed that daily averaged temperatures reached above 0 °C on June 5. All snow had diminished as of June 12. The bloom initiated on July 1, and peaked on July 21 at 440 mg m^{-2}, four days after ice break-up (ArcNut database) (Figure 3.27).

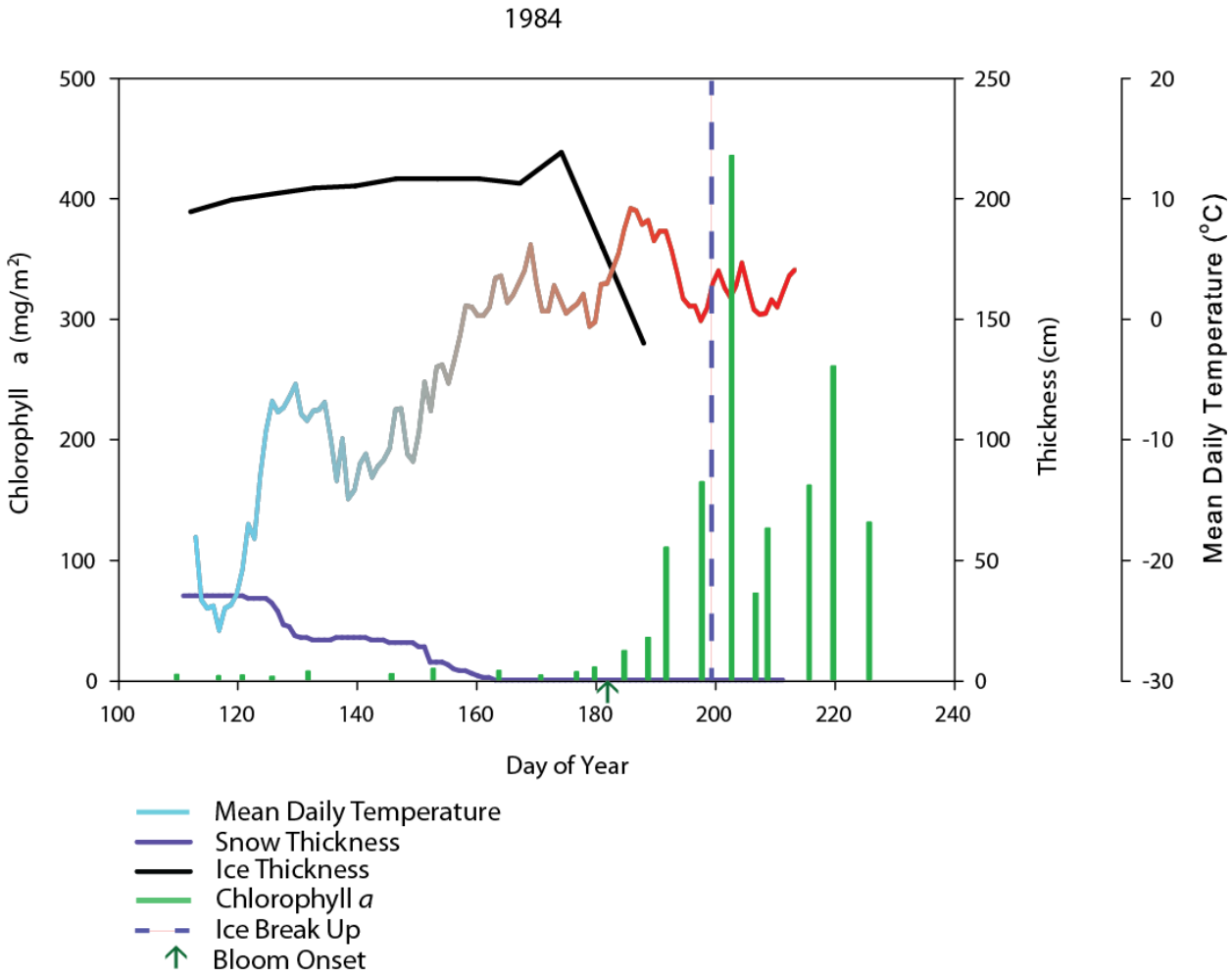

Figure 3.27: A complete graph of 1984 showing ice and snow thickness, chlorophyll *a*, bloom onset, ice break-up, and mean daily air temperature. Environmental variables collected from Environment data historical archive. Ice break-up determined from Canadian Ice Service charts. Chlorophyll data is from the ArcNut database.

The year 1985 had two concurrent studies ongoing in similar areas. Mean temperatures stayed above 0 °C on June 2. All snow had diminished as of June 7 (Environment Canada). The

bloom initiated on July 5 for both studies in the region, and both studies peaked on July 8 at values of 255 (BioChem) and 190 mg m^{-2} (ArcNut), twenty-two days prior to ice break-up (Figure 3.28).

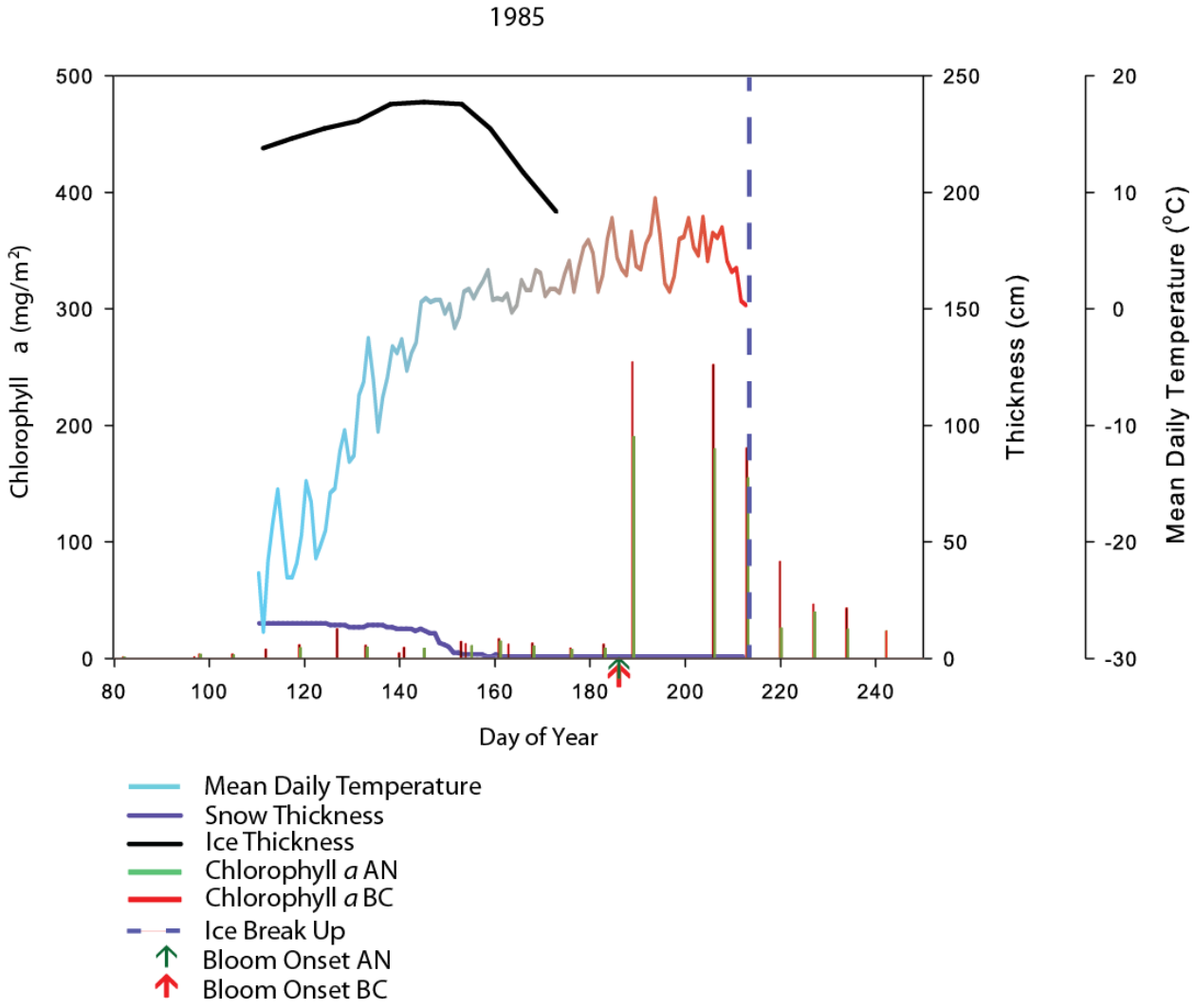

Figure 3.28: A complete graph of 1985 showing ice and snow thickness, chlorophyll *a*, bloom onset, ice break-up, and mean daily air temperature. Environmental variables collected from Environment data historical archive. Ice break-up determined from Canadian Ice Service charts. Chlorophyll data is from the ArcNut and BioChem databases.

Similar to 1985, the year 1986 also had two concurrent studies. Mean daily temperatures surpassed 0 °C on June 22, somewhat late compared to previous years. This date was not

statistically different from the rest data using a two-sample t-test at a confidence interval of 95%. Snow diminished as of July 4 with a major rain event taking place on June 30. Both studies showed extremely interesting results with respect to the number of Chl *a* concentration peaks encountered prior to ice break-up on August 7. Bloom commencement for the BioChem (BC) study took place on July 8, while the ArcNut (AN) study took place on July 10. The "BC" study showed a first peak (44.3 mg m^{-2}) taking place on May 20 and then decreased back to 0 mg m^{-2}. This initial peak occurred prior to snow melt onset and therefore, did not make the criteria for phytoplankton bloom onset as it was likely associated with sloughing of ice algae. An additional peak was observed on June 12 with concentrations reaching 117 mg m^{-2} and a final peak on August 10 at 539 mg m^{-2}. Similar to the BC study, the AN dataset had multiple Chl *a* concentration peaks around the same dates. The largest peak of the AN data set was 278 mg m^{-2} on July 28. However, the BC dataset showed a larger under-ice peak of 287 mg m^{-2} on July 22 (Figure 3.29).

For 1987, mean temperatures stayed above 0 °C following June 9, with a slight dip on June 15. All snow had diminished as of June 13. Sampling in the water column started early in the 1987 dataset on March 31 with base Chl *a* concentrations at 0.8 mg m^{-2}. After the suspected ice algae had sloughed off the ice bottom on approximately April 29, the water column attained a baseline concentration of 7.4 mg m^{-2}. This value was similar to that observed in other years of the historical dataset. Bloom commencement was conservatively estimated with low confidence as July 9, the mid date between the mid-value of 71.0 mg m^{-2} on July 27 and the previous measurement of 6.0 mg m^{-2} on June 21. The highest peak concentration of 143.0 mg m^{-2} was reached 3 days prior to ice break-up on August 1 (Figure 3.30).

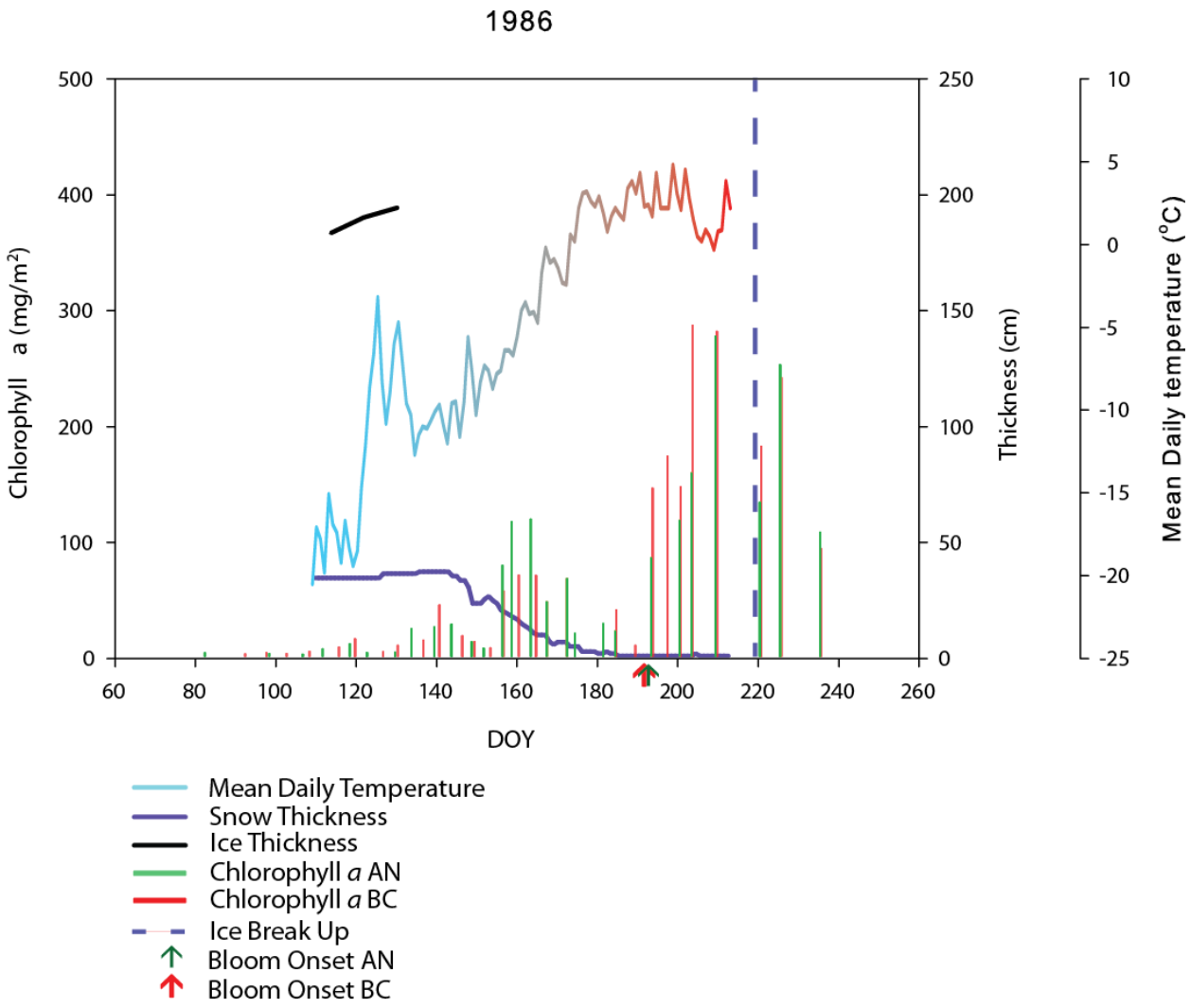

Figure 3.29: A complete graph of 1986 showing ice and snow thickness, chlorophyll *a*, bloom onset, ice break-up, and mean daily air temperature. Environmental variables collected from Environment data historical archive. Ice break-up determined from Canadian Ice Service charts. Chlorophyll data is from the ArcNut and BioChem databases.

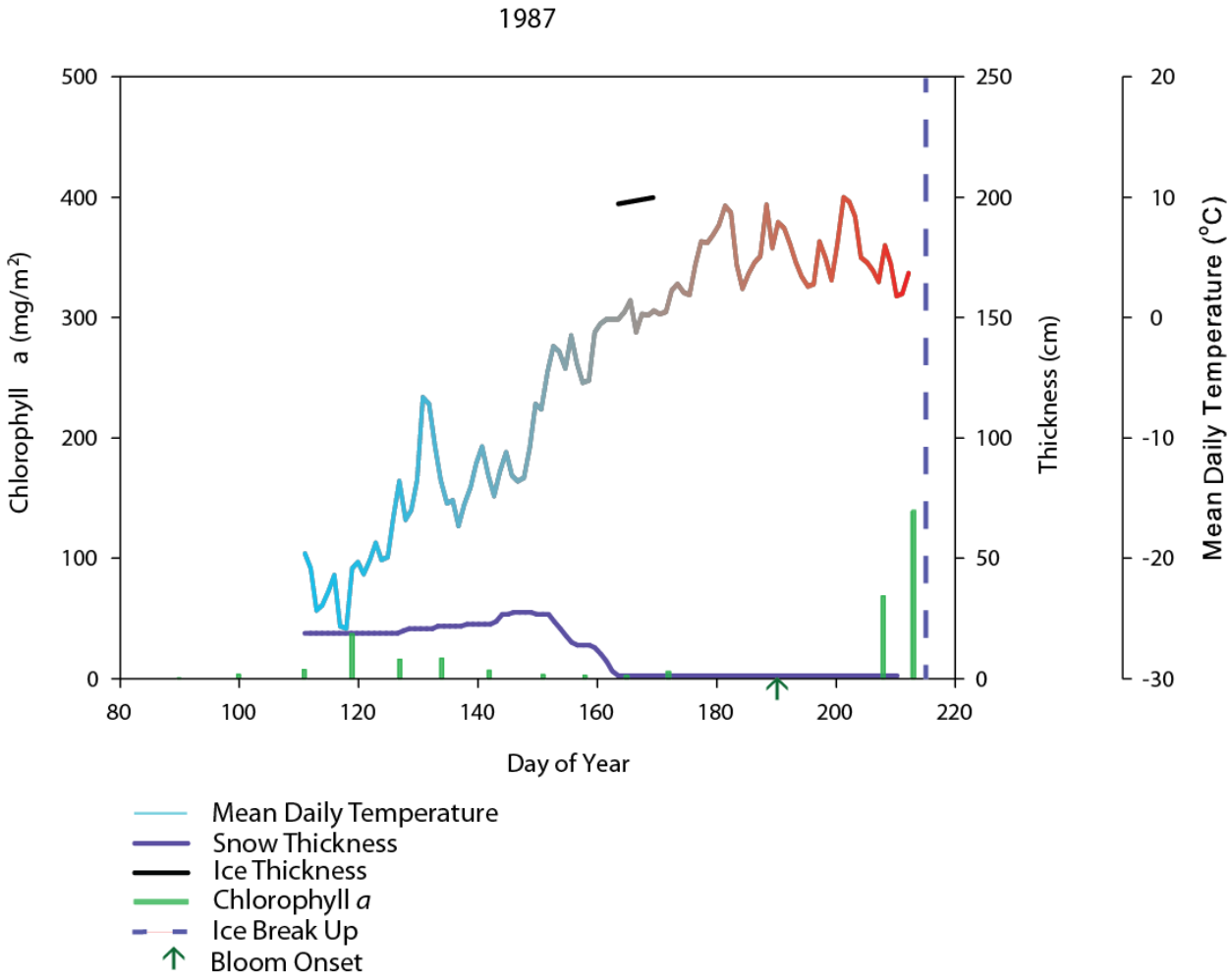

Figure 3.30: A complete graph of 1987 showing ice and snow thickness, chlorophyll *a*, bloom onset, ice break-up, and mean daily air temperature. Environmental variables collected from Environment data historical archive. Ice break-up determined from Canadian Ice Service charts. Chlorophyll data is from the BioChem database.

In the 1988 dataset, mean temperatures reached above 0 °C on June 25 and the snow cover had completely melted as of June 28. During 1988, sampling in the water column initiated on May 31 with baseline Chl *a* concentrations at approximately 10.6 mg m^{-2}. Bloom initiation was conservatively estimated with low confidence as July 16. Similar to 1987 there was a gap in sampling of over 30 days. The previously recorded value of 15.6 mg m^{-2} was measured on June

27, with the peak concentration of 192.1 mg m^{-2} recorded on August 5. Ice break-up occurred on August 4 (Figure 3.31).

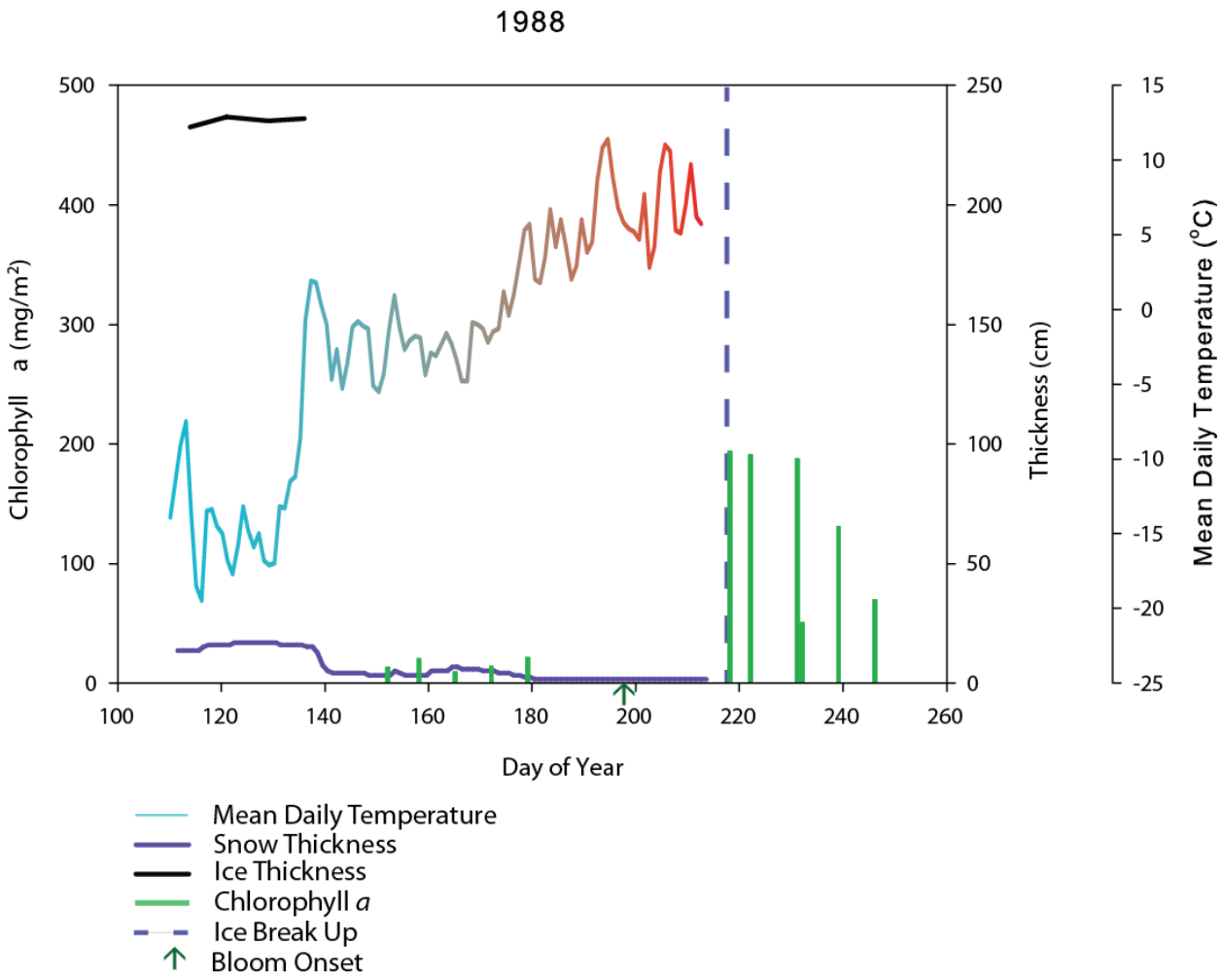

Figure 3.31: A complete graph of 1988 showing ice and snow thickness, chlorophyll *a*, bloom onset, ice break-up, and mean daily air temperature. Environmental variables collected from Environment data historical archive. Ice break-up determined from Canadian Ice Service charts. Chlorophyll data is from the BioChem database.

In the 1989 dataset, mean temperatures reached above 0 °C on June 18 and the snow cover had completely melted as of June 30. In 1989 sampling took place after the bloom had already initiated. The initial recorded value on July 15 of 126 mg m^{-2} was two days after ice break-up and continued to accumulate, peaking at a concentration of 242 mg m^{-2} on July 26. No

initial bloom date could be determined; however, the presence of a substantial concentration of biomass in the water column two days after the ice broke up strongly suggests that the bloom had largely developed under the ice cover (Figure 3.32).

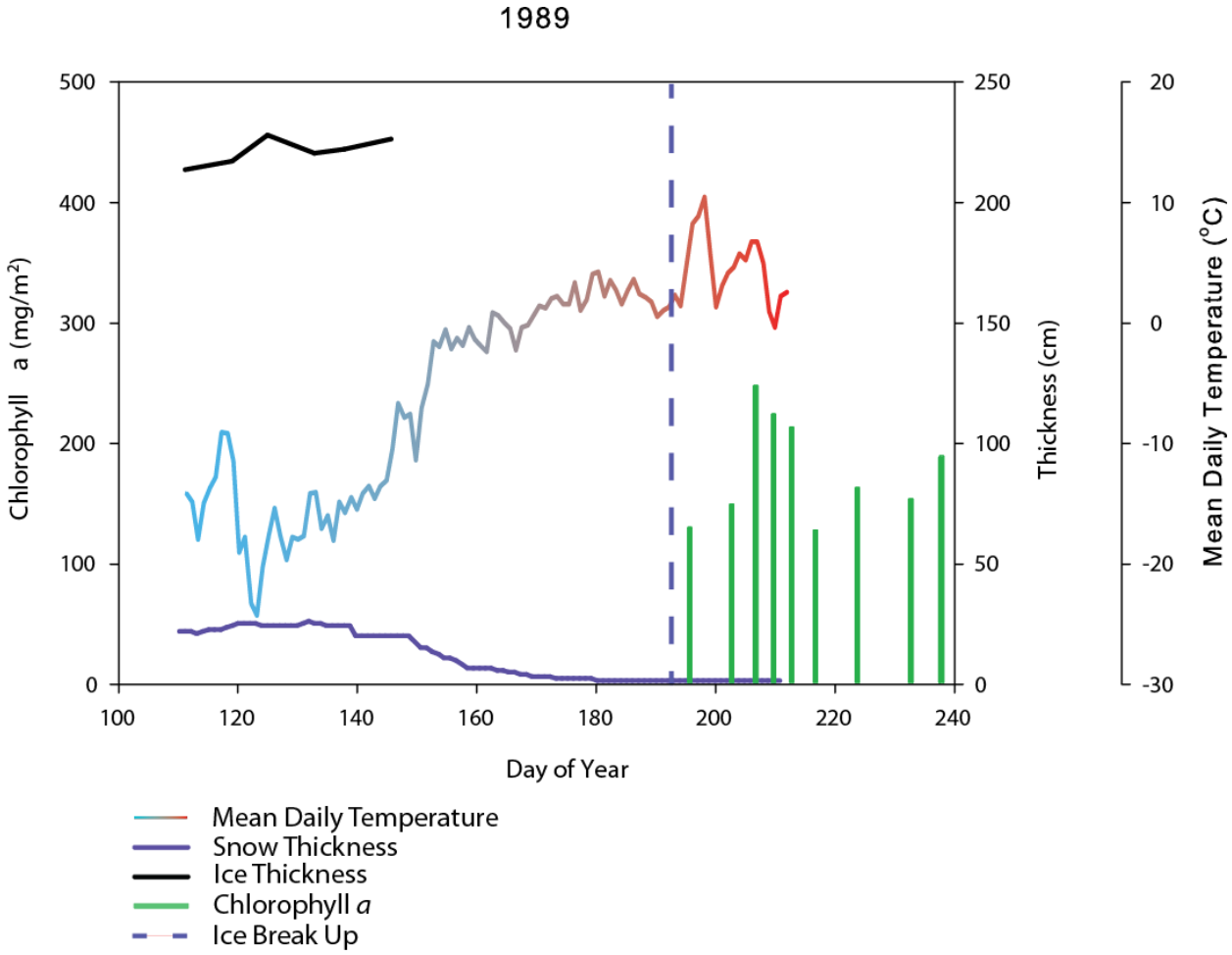

Figure 3.32: A complete graph of 1989 showing ice and snow thickness, chlorophyll *a*, bloom onset, ice break-up, and mean daily air temperature. Environmental variables collected from Environment data historical archive. Ice break-up determined from Canadian Ice Service charts. Chlorophyll data is from the ArcNut database.

In the 1990 dataset, mean temperatures reached above 0 °C on June 15 and the snow cover had completely melted as of June 25. The 1990 dataset was similar to that of 1989 where sampling began on July 9 and was found to have an initial sampling Chl *a* concentration of 60.0 mg m^{-2}. Due to the fact that this concentration was well above the baseline concentrations of

that for previous years and snow melt was advanced, the bloom onset had occurred prior to the start of the dataset. However, the date of onset could not have been long before the start and therefore, I estimated, with low confidence, a bloom onset date one day prior to this on July 8. With that said, the phytoplankton bloom had clearly commenced prior to ice break-up on July 26 with concentrations reaching 200 mg m^{-2} on July 13 with a peak concentration observed on July 27 at 225 mg m^{-2}, one day after break-up (Figure 3.33).

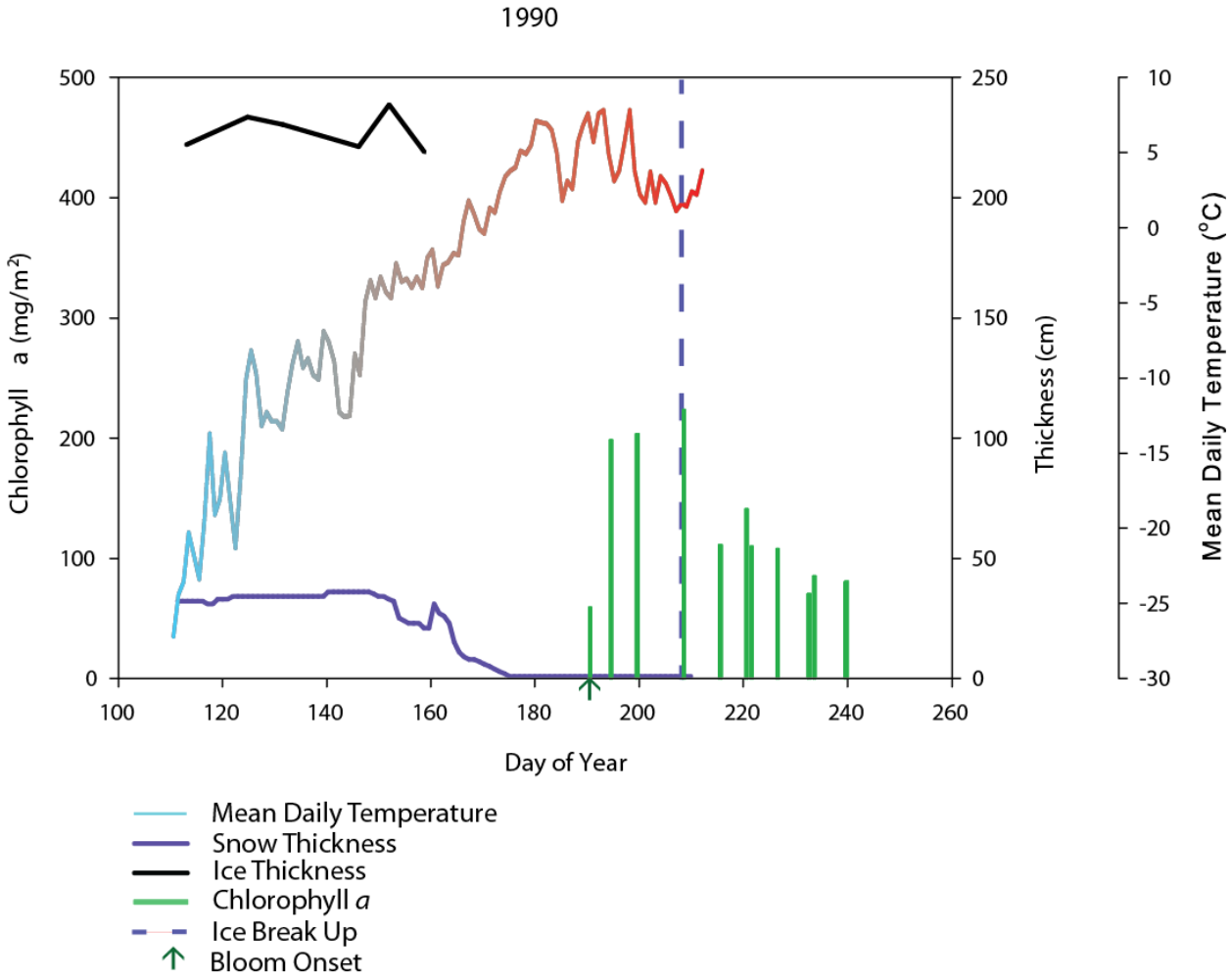

Figure 3.33: A complete graph of 1990 showing ice and snow thickness, chlorophyll *a*, bloom onset, ice break-up, and mean daily air temperature. Environmental variables collected from Environment data historical archive. Ice break-up determined from Canadian Ice Service charts. Chlorophyll data is from the ArcNut database.

In the 1991 dataset, mean temperatures reached above 0 °C on June 7 and the snow cover had completely melted as of June 26. The 1991 dataset had an initial sampling date of June 3 with an integrated concentration of 12.7 mg m^{-2}. Between June 12 and July 2, concentrations dropped to 4.7 mg m^{-2}. Bloom commencement was estimated as July 6, the middle point between the July 2 observation and a concentration of 141 mg m^{-2} observed on July 10. Peak values were reached on July 21 at 144 mg m^{-2}; three days after ice break-up (Figure 3.34).

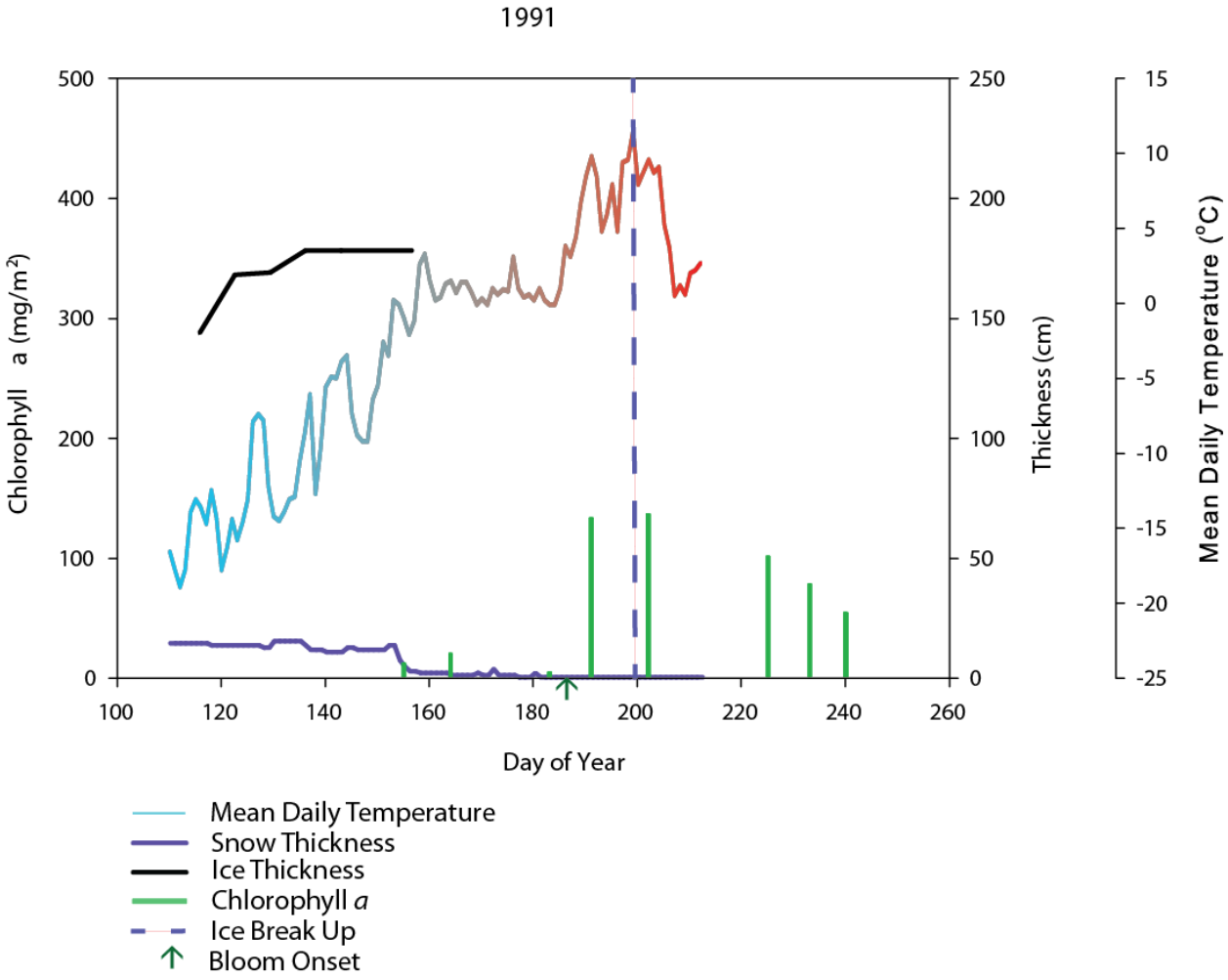

Figure 3.34: A complete graph of 1991 showing ice and snow thickness, chlorophyll *a*, bloom onset, ice break-up, and mean daily air temperature. Environmental variables collected from Environment data historical archive. Ice break-up determined from Canadian Ice Service charts. Chlorophyll data is from the ArcNut database.

In the 1992 dataset, mean temperatures reached above 0 °C on June 21 and the snow cover had completely melted as of July 2. 1992 had an initial sampling date of May 1 with a baseline value of 3.4 mg m^{-2}. A slight increase to 27.0 mg m^{-2} was recorded on May 21 and was suspected to be ice algae sloughing from the ice bottom with a gradual decline to baseline values again. Bloom onset was not determined. Fortier et al. (2002) noted that the percent Chl *a* in suspended pigments was low. This suggested that this last increase seen on June 23 with a maximum concentration of 166 mg m^{-2} was likely not a bloom. Furthermore, the recorded peak was well before the snowmelt had concluded. Additionally, there were no signs of decline so peak bloom concentrations could be obtained for this year. Prior to June 23, a medium sized spike of biomass was recorded in the water column. Concentrations reached a maximum of 94.6 mg m^{-2} on June 6 with a decrease in the biomass going to baseline values again. Ice break-up was determined to be on July 23 (Figure 3.35).

In the 1994 dataset, mean temperatures reached above 0 °C on June 14 and the snow cover had completely melted as of June 18. 1994 had an initial sampling date of May 6 with baseline values at approximately 13.0 mg m^{-2}. A slight increase was observed at 31.6 mg m^{-2}; however, this increase was suspected to be associated with sloughing of ice algae from the ice bottom. Bloom onset was estimated as June 7. Water column biomass accumulated at a steady rate until a peak value of 354 mg m^{-2} on June 26 was obtained, long before ice-breakup occurred on July 14 (Figure 3.36).

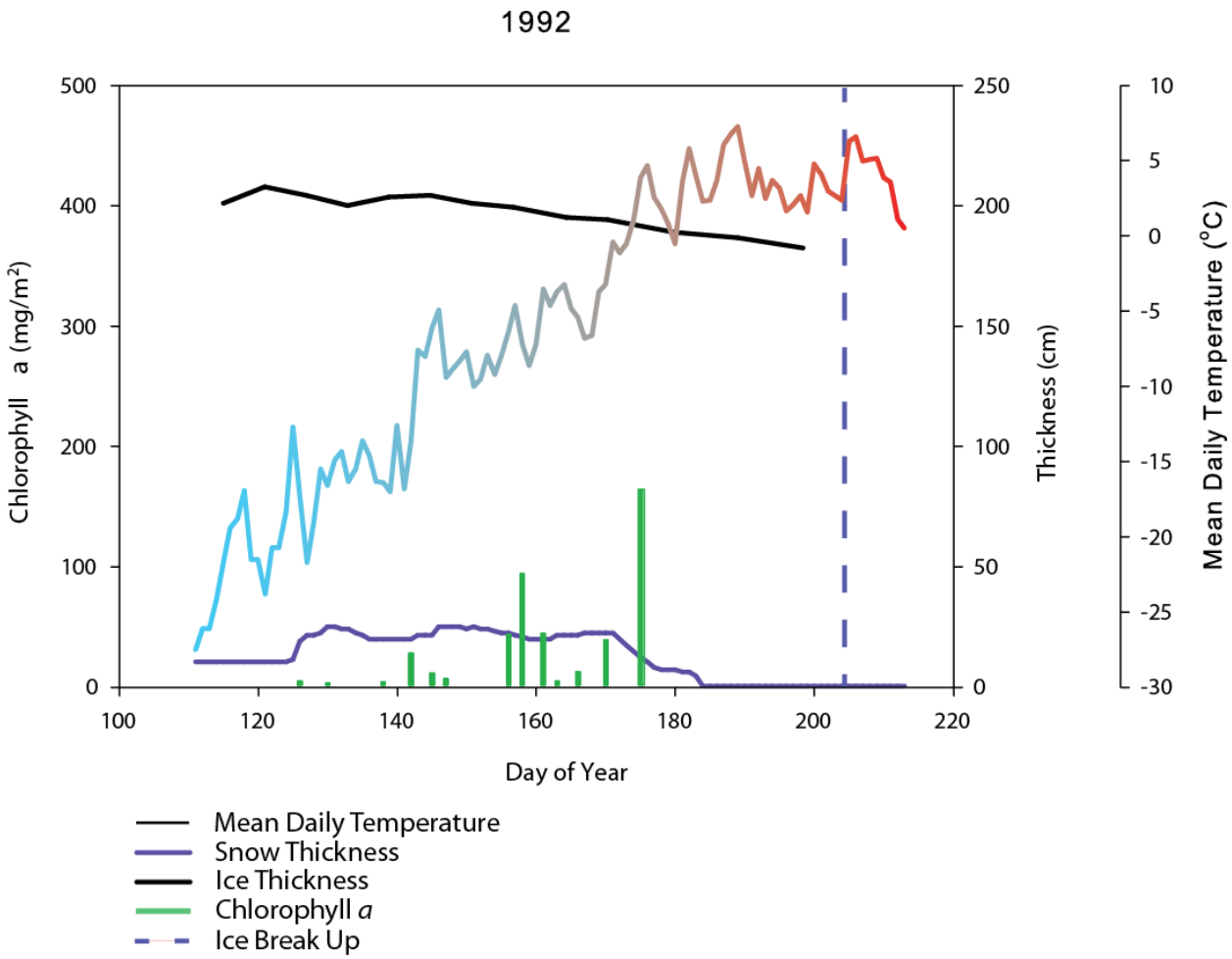

Figure 3.35: A complete graph of 1992 showing ice and snow thickness, chlorophyll *a*, ice break-up, and mean daily air temperature. Environmental variables collected from Environment data historical archive. Ice break-up determined from Canadian Ice Service charts. Chlorophyll data is from the Fortier et al. (2002).

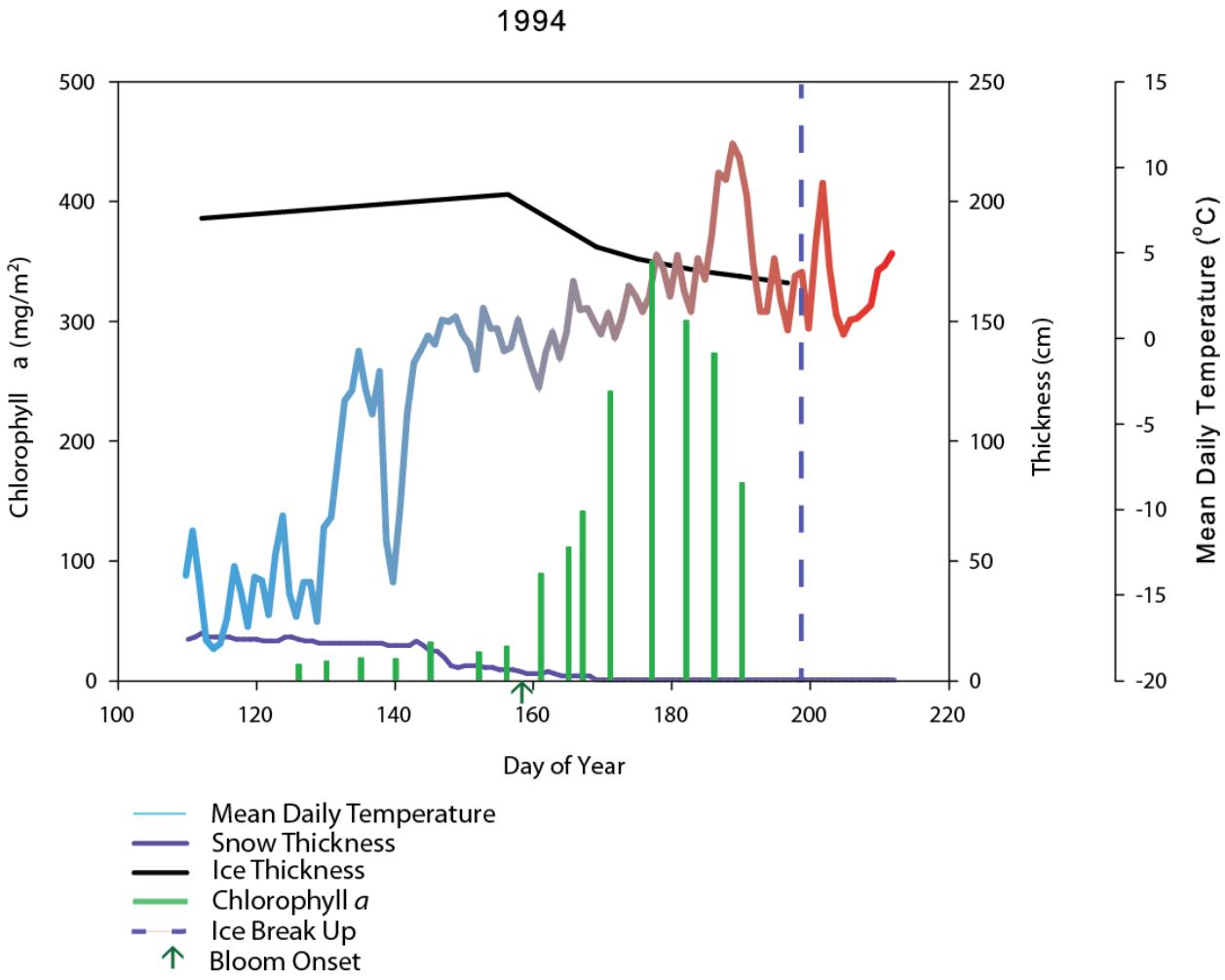

Figure 3.36: A complete graph of 1994 showing ice and snow thickness, chlorophyll *a*, bloom onset, ice break-up, and mean daily air temperature. Environmental variables collected from Environment data historical archive. Ice break-up determined from Canadian Ice Service charts. Chlorophyll data is from the Fortier et al. (2002).

In the 1995 dataset, mean temperatures reached above 0 °C on June 11 and the snow cover had completely melted as of June 19. Initial sampling took place on May 5 with baseline values hovering around 11.5 mg m^{-2}. Bloom onset was estimated as June 13, rising from below 32.5 to 94.1 mg m^{-2} in just over 5 days. The accumulation rate of biomass in the water column was relatively slow until July 2 when a significant increase was observed resulting in an integrated biomass 444 mg m^{-2} on July 6. Ice break-up was determined to be August 31 (Figure 3.37).

In the 2001 dataset, mean temperatures reached above 0 °C on June 12 and the snow cover had completely melted as of July 1. 2001 was initially sampled on May 9 with baseline Chl *a* concentrations being recorded at 3.15 mg m^{-2}. Variability during the initial melt period was attributed to ice algae sloughing from the ice bottom. Bloom onset was determined to be July 4 with the highest concentrations observed on the final day of sampling (July 6) at 52.9 mg m^{-2}. Ice break up was on August 6 (Figure 3.38).

In the 2010 dataset, mean temperatures reached above 0 °C on June 8 and the snow cover had completely melted as of June 16. 2010 was initially sampled on May 10 with baseline Chl *a* concentrations being recorded at 3.30 mg m^{-2} integrated over the top 25 m using discrete sampling in the water column. Bloom onset was determined to be June 9 with the highest concentrations observed on the final day of sampling (June 21) at 339 mg m^{-2} using discrete sampling integrated over the upper 30 m of the water column. Ice break up was on July 12 (Figure 3.39).

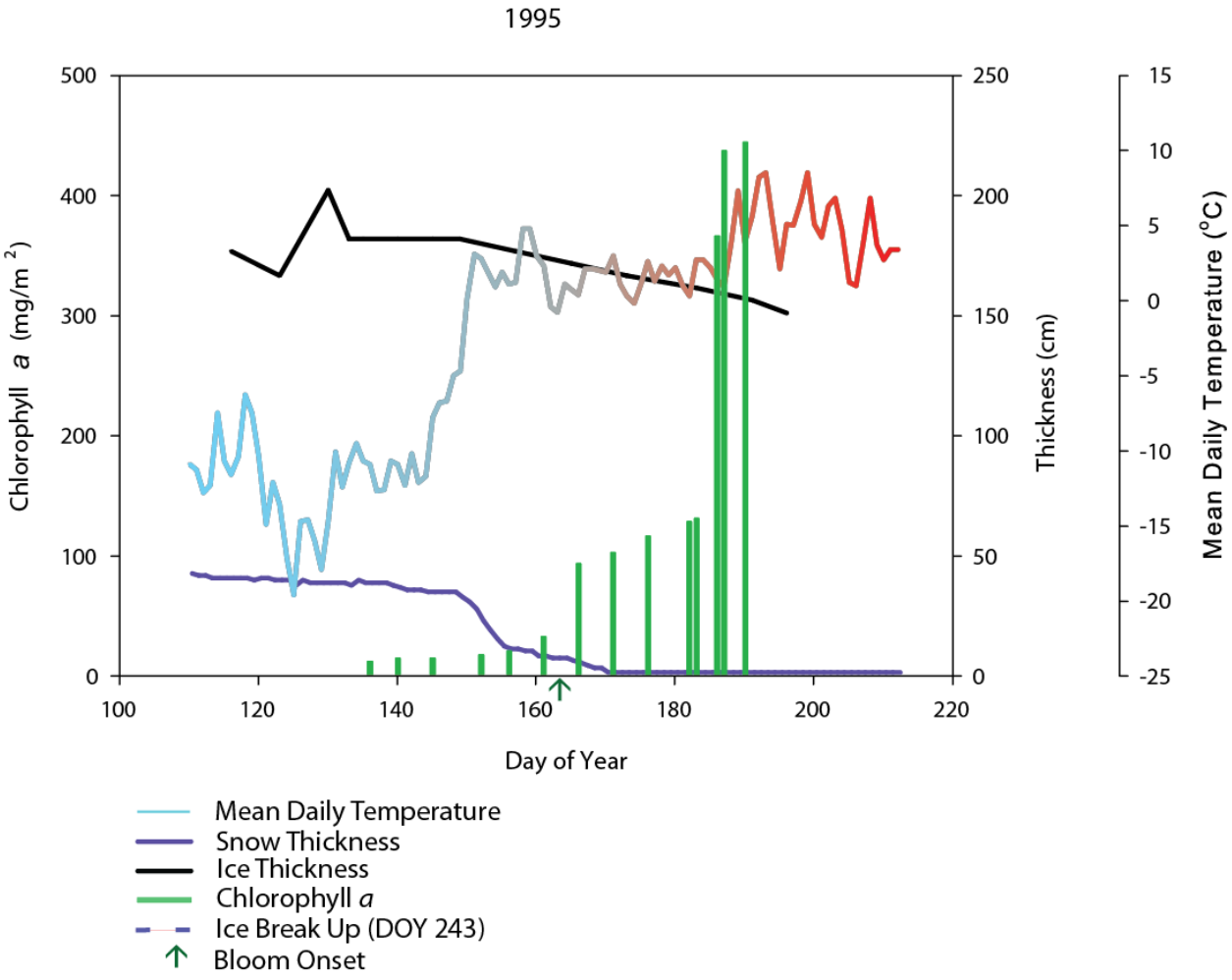

Figure 3.37: A complete graph of 1995 showing ice and snow thickness, chlorophyll a, bloom onset, ice break-up, and mean daily air temperature. Environmental variables collected from Environment data historical archive. Ice break-up determined from Canadian Ice Service charts. Chlorophyll data is from the Fortier et al. (2002).

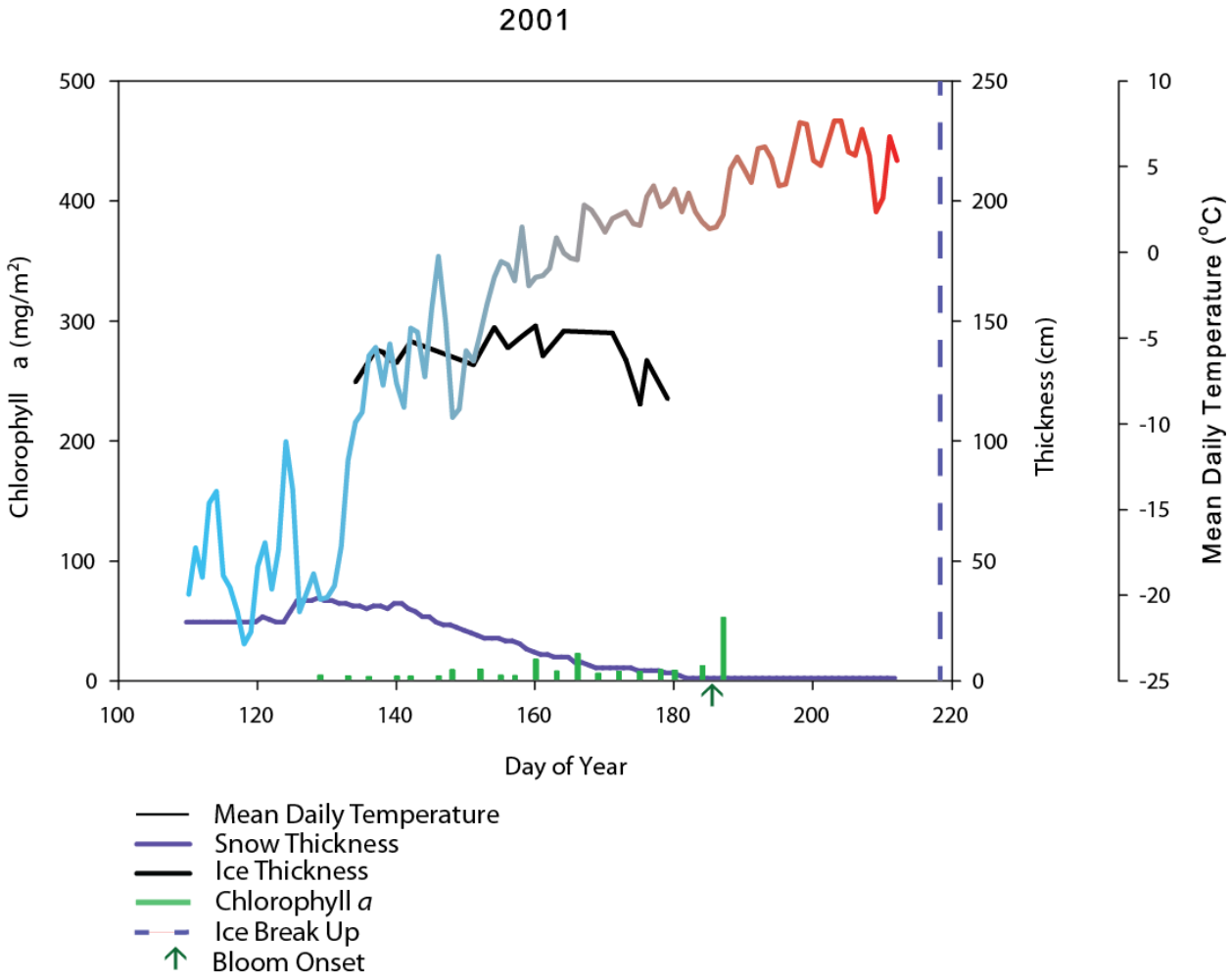

Figure 3.38: A complete graph of 2001 showing ice and snow thickness, chlorophyll *a*, bloom onset, ice break-up, and mean daily air temperature. Ice and snow thickness were collected from C-ICE, (2001) and other Environmental variables collected from Environment data historical archive. Ice break-up determined from Canadian Ice Service charts. Chlorophyll data is from the Michel et al. (2003).

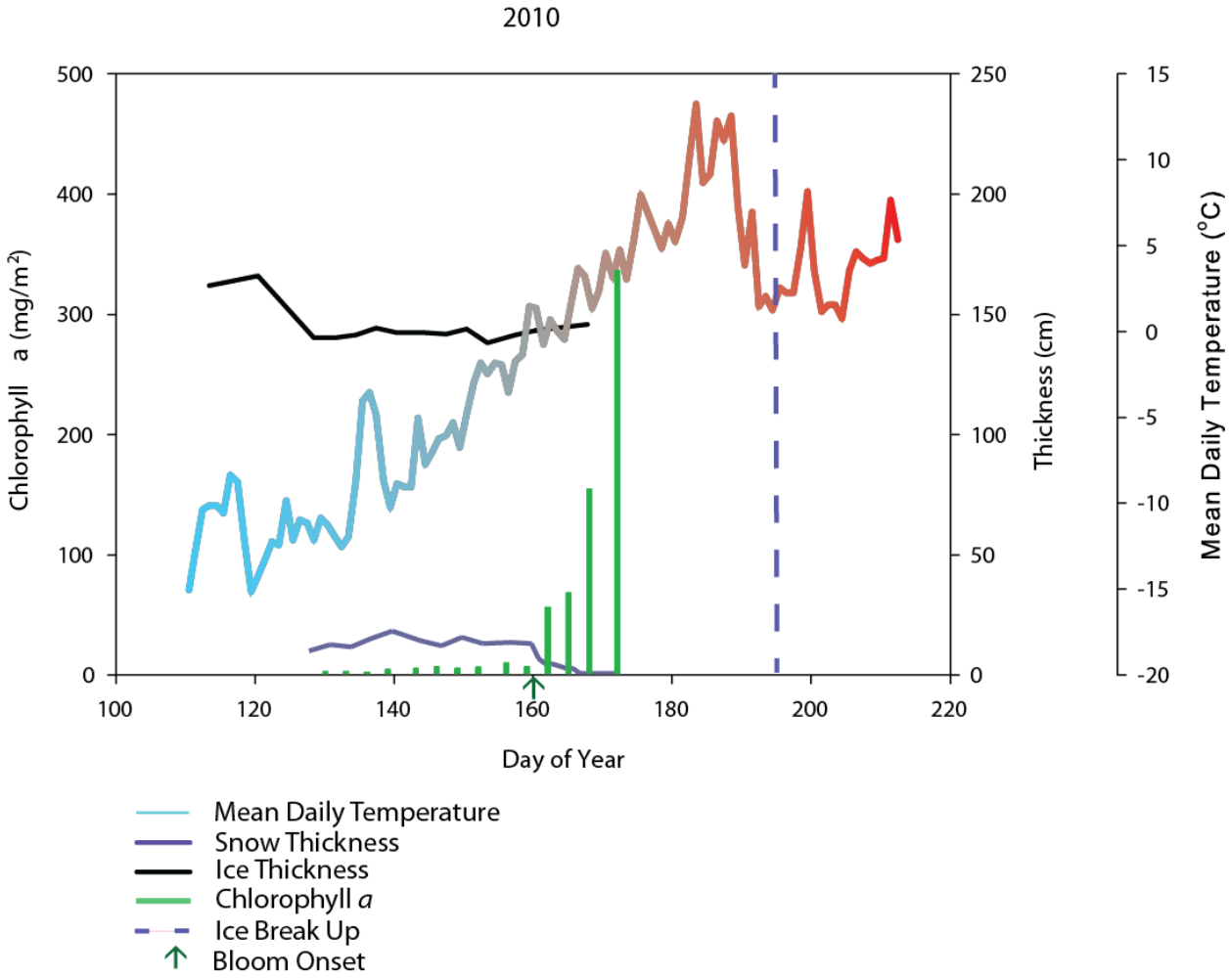

Figure 3.39: A complete graph of 2010 showing ice and snow thickness, chlorophyll *a*, bloom onset, ice break-up, and mean daily air temperature. Environmental variables collected from Environment data historical archive and Arctic-ICE campaign. Ice break-up determined from Canadian Ice Service charts. Chlorophyll data is from Arctic-ICE (2010).

In the 2011 dataset, mean temperatures reached above 0 °C on June 6 and the snow cover had completely melted as of June 17. 2011 was initially sampled on April 26 with baseline Chl *a* concentrations being recorded at 1.65 mg m^{-2} using discrete sampling over the top 20 m of the water column. Bloom onset was determined to be June 9 with the highest concentrations observed on June 11 at 182 mg m^{-2} using discrete sampling. Ice break up was on June 27 (Figure 3.40).

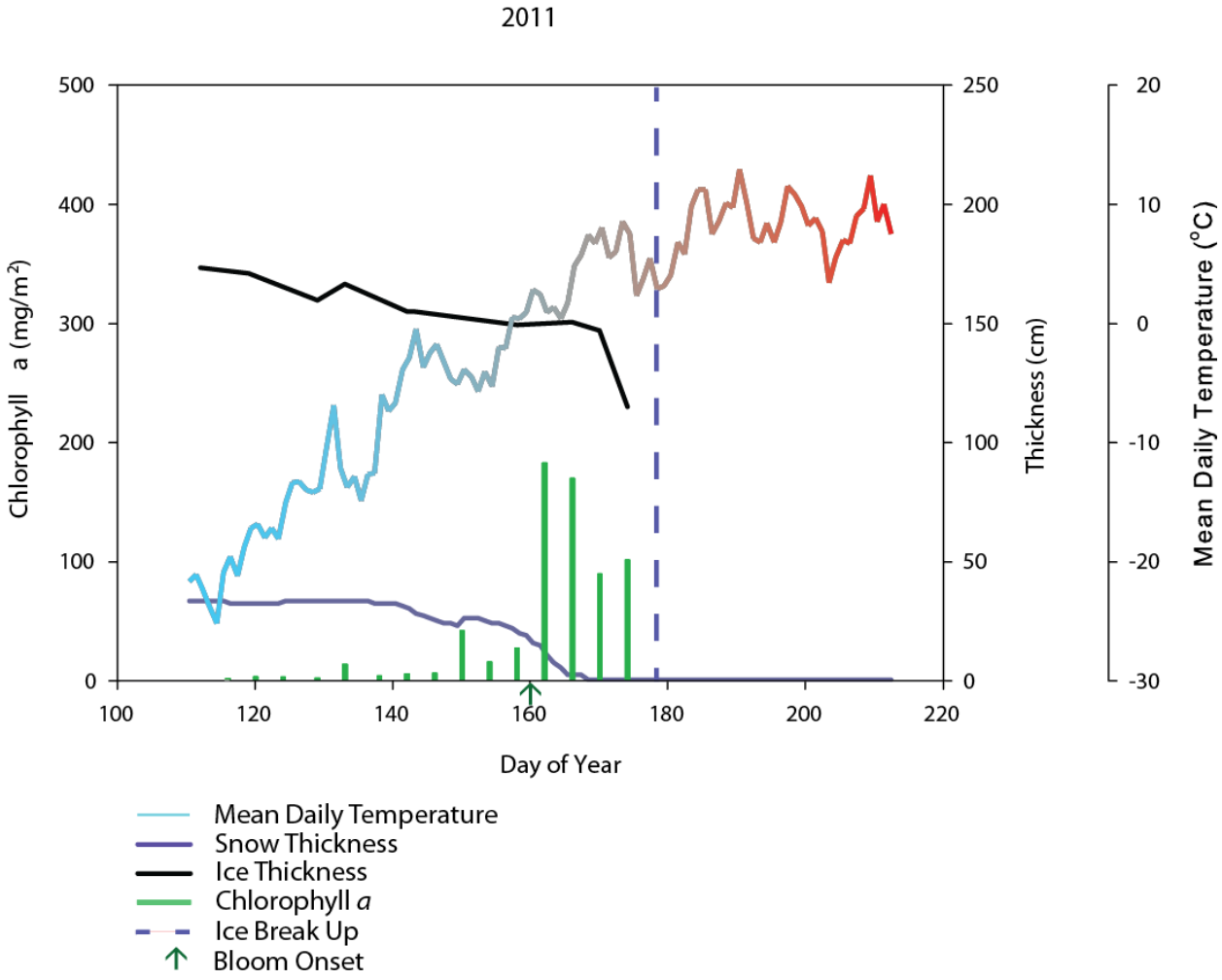

Figure 3.40: A complete graph of 2011 showing ice and snow thickness, chlorophyll *a*, bloom onset, ice break-up, and mean daily air temperature. Environmental variables collected from Environment data historical archive and Arctic-ICE campaign. Ice break-up determined from on-ice observations. Chlorophyll data is from Arctic-ICE (2011).

In the 2012 dataset, mean temperatures reached above 0 °C on May 29 and the snow cover had completely melted as of June 12. 2012 was initially sampled on May 18 with baseline Chl *a* concentrations being recorded at 4.92 mg m^{-2} in the water column using discrete sampling. Bloom onset was not determined with the highest concentrations observed on the final day of sampling (June 23) at 16.7 mg m^{-2} using discrete sampling over the top 25 m. Ice break up was on July 16 (Figure 3.41).

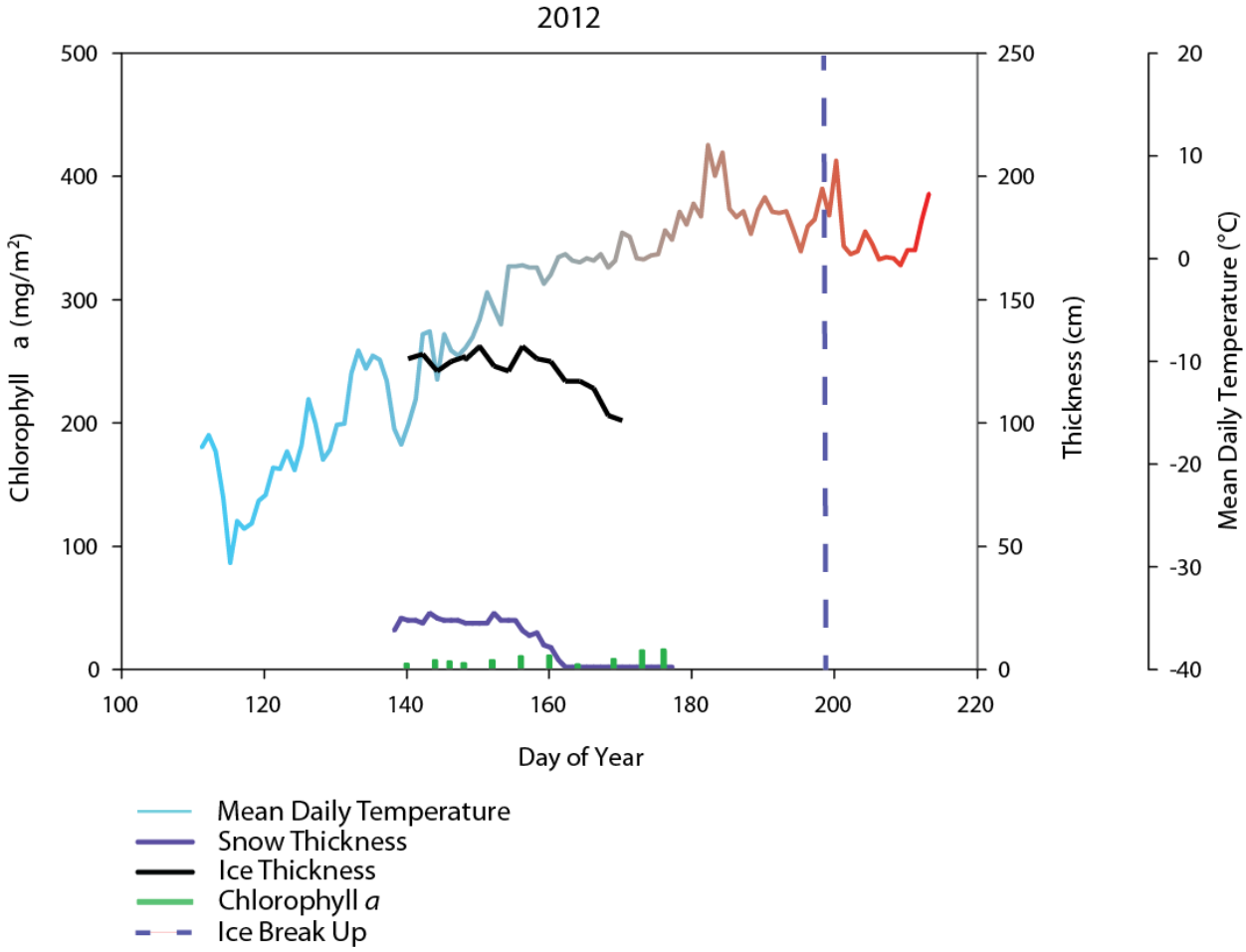

Figure 3.41: A complete graph of 2012 showing ice and snow thickness, chlorophyll *a*, bloom onset, ice break-up, and mean daily air temperature. Environmental variables collected from Environment data historical archive and Arctic-ICE campaign. Ice break-up determined from Canadian Ice Service charts. Chlorophyll data is from Arctic-ICE (2012).

Table 3.1 summarizes important dates and information obtained from Figures 3.24-3.41. The historical data presented showed a total of 11 blooms taking place with high certainty of bloom onset determination. The blooms commenced under landfast ice concentrations of 9/10ths or greater. In fact, the results suggest that onset of the regional spring bloom occurred before ice-breakup in all the datasets examined.

Paired data from those compiled in Table 3.1 were averaged for the three variables, demonstrating that bloom onset tended to occur around June 27 (day 178), the average date 0 cm snow depth was reached on June 25 (day 176), and the average date of ice break-up was July 28 (day 209). The date of 0 cm snow was considered to be when snow had melted completely from the ice. Therefore, on average, the bloom commenced 2 days after snowmelt was complete, and a month prior to ice-break-up. Furthermore, an analysis of variance, which provided a pair-wise paired Holm-Sidak test, between these three variables shows that bloom onset and date of complete snowmelt were not statistically different ($n = 17$; $p = 0.289$); whereas date of ice break-up was significantly different from both bloom onset ($n = 14$; $p < 0.001$) and snow depth ($n = 17$; $p < 0.001$).

Table 3.1: Summary table of maximum recorded integrated chlorophyll a concentrations through discrete depth samples, the depth over which data were integrated, and the dates of maximum Chl *a* observation, bloom onset (including relative certainty of bloom onset date), ice break-up, and 0 cm snow depth being reached.

Year	Max Chl *a* (mg m^{-2})	Integration Depth (m)	Date of Max Chl *a* (DOY)	Bloom Onset (DOY)	Bloom Certainty	Ice Break-Up (DOY)	Date of 0 cm Snow (DOY)
1961	84.8	10	201	190	HIGH	N/A	187
1962	122	15	183	176	LOW	N/A	178
1963	134	15	190	178	LOW	N/A	192
1983	2.78*	25	121	N/A	N/A	198	N/A
1984	440	20	203	184	HIGH	199	164
1985 (BC)	255	30	189	186	LOW	211	185
1985 (AN)	190	30	189	186	LOW	211	185
1986 (BC)	539	30	222	189	HIGH	219	185
1986 (AN)	278	30	209	191	HIGH	219	185
1987	215	30	230	190	LOW	216	164
1988	192	30	218	198	LOW	217	180
1989	242*	30	207	N/A	N/A	194	181
1990	225	30	208	189	HIGH	207	176
1991	144	30	202	187	LOW	199	177
1992	166*	15	175	N/A	N/A	205	184
1994	354	30	177	158	HIGH	195	169
1995	451	30	190	164	HIGH	243	170
2001	52.9	25	187	185	HIGH	218	182
2010	339	30	172	160	HIGH	193	167
2011	182	20	162	160	HIGH	178	168
2012	16.7*	25	175	N/A	N/A	198	164

* - 1983, 1989, 1992, and 2012 were not included in final analysis as bloom onset was not determined.

Chapter Four: **Discussion**

The two objectives of my thesis were to (1) determine the biophysical processes controlling the timing of under-ice phytoplankton production in Resolute Bay, NU; and (2) compare and contrast the timing of the under-ice bloom and controlling processes between different years. In this chapter, I discuss the results of my thesis in light of these two main elements. To do so, I have split the chapter into two sections: (1) the first part discusses results from the three year Arctic-ICE field campaign in an effort to better understand the formation mechanisms behind under-ice blooms; and (2) the second part discusses the historical data from the 1960's until present day to see whether under-ice blooms are more of a recent phenomenon or are a response to a changing climate.

4.0 Arctic-ICE Field Campaign

In Chapter 3, I presented results from the three-year biophysical dataset collected during the Arctic-ICE campaigns, which are discussed below to examine factors mitigating the timing of under-ice phytoplankton production in Resolute Bay, NU. While some of the physical and environmental observations were similar among all three years, the outcomes were variable. For example, nutrient concentrations and timing of melt onset were fairly consistent throughout the three years; however, the timing and development of the bloom varied.

4.0.1 Nutrient Concentrations

All nutrient concentrations for the years 2010, 2011, and 2012 were initially at comparable levels with each other and with those reported in Michel et al. (2006) and Apollonio et al. (2002). The region near Resolute is typically ample in nitrate+nitrite, silicic acid, and

phosphate concentrations before any substantial water column production occurs (Michel et al., 2006). The nutrient rich supply originates from waters of Pacific origin that traverse the Canadian Archipelago at depth and tend to mix to the surface in Barrow Strait near Resolute due to topographic relief (Michel et al., 2006). Post-bloom nutrient concentrations from the Arctic-ICE 2011 dataset, and likely peak bloom from 2010, were in agreement with those reviewed in Jones and Coote (1980), Cota et al. (1990), and Michel et al. (2006), suggesting that nutrients were exhausted in surface waters during these years. That is, substantial new production had occurred in the under-ice water column during both years. However, in 2012 no bloom developed during the observation period and nutrient concentrations in the upper water column had remained close to pre-bloom levels.

4.0.2 Melt Onset and Progression

During the three years of Arctic-ICE, the dates of melt onset were similar; however, the rate of melt differed during 2011 in comparison to 2010 and 2012. In 2010 and 2012, snow melt onset was steady, despite different snow covers on the icescape with the lowest snow depths observed during 2012. In 2010, melt onset started on approximately June 6 when a decrease in albedo occurred. The albedo declined at a steady rate that was inversely similar to the increase in transmitted PAR. Similarly, 2012 showed a steady decline in albedo that commenced on June 4, matched with an increase in PAR transmitted to the water column. In 2011, snow melt onset was determined according to the date of rapid decline in albedo, which started on June 9. A major rain event on June 10 resulted in surface albedo reaching 0.3 by June 11, only 2 days after melt onset. In contrast, surface albedo reached 0.3 on June 16 and 13 in 2010 and 2012, respectively, demonstrating a much slower melt progression of 10 and 9 days.

Although Perovich (1996) demonstrated that transmitted PAR should increase in the water column with a decrease in surface albedo during melt, this was not seen in 2011. The discrepancy can be explained by the amount of phytoplankton biomass in the water column that significantly attenuated transmitted light. Similarly, the decrease in PAR transmitted to depth following June 16 in 2010 was associated with the increasing accumulation of phytoplankton biomass in the water column and its associated absorption of PAR.

In 2010 the steady melt progression regulated the amount of light transmitted to the water column at a rate that allowed for the relatively slow development of the bloom in comparison to 2011. It is important to note that the bloom of 2010 was dominated by pelagic centric diatom species (>65% of total protists) with the ice algae bloom terminating approximately two weeks prior to the under-ice bloom onset (Mundy et al., 2014). Therefore, it appears that the lack of major rain events in 2010 and the resulting regular melt evolution of the system permitted the development of a true phytoplankton bloom.

In 2011, as previously mentioned, snow melt reached advanced stages mere days after its onset, thus decreasing albedo and theoretically increasing light transmission. Additionally, the rain events on June 10 and 12 were responsible for the termination of the ice algal bloom (Campbell et al., 2014). Galindo et al. (2014) noted that the under-ice phytoplankton bloom consisted predominantly of ice-associated pennate diatom species. This provided strong evidence that the bloom was seeded by the sloughed ice algae sinking in the water column at the time of bloom onset. It is also important to note that the ice algal bloom taxonomic composition differed from that of the under-ice bloom. As discussed in Galindo et al. (2014), key species were for the ice-algal bloom consisted of *Nitzschia frigida* (Grunow) (21-56% in 2011) and *Navicula pelagica* (Cleve) (ca. 7% of pennate diatoms in 2011). However, key species for the under-ice

bloom were: *Fossula arctica* (ca. 50-80%), *Fragilariopsis cylindrus* (Grunow) (ca. 2-19%), *Fragilariopsis oceanica* (Cleve, Hasle) (ca. 2-15%), *Navicula septentrionalis* (Grunow) (ca. 2-13%) and *Nitzschia frigida* (Grunow) (ca. 2%). Furthermore, Chl *a* concentrations integrated over the water column were one order of magnitude greater than that observed in the sea ice, Therefore, the observations support that separate blooms indeed occurred between the ice environment and the water column. It is noted that sea ice diatoms are known to rapidly settle in the water column once sloughed from the ice cover (Michel et al., 1996) and therefore, the taxonomic composition of the bloom in 2011 may have also influenced the duration of the bloom. That is, rapid settling of the large sea ice diatoms may have caused a relatively early termination to the under-ice bloom in that year.

Interestingly, a similar trend to what was documented for 2011 was also observed in the 1986 historical dataset. In terms of ice algae concentrations, 1986 was quite unique with some of the highest ice algae biomass concentrations ever reported for the Arctic, reaching concentrations of 250 to 330 mg m^{-2} in the ice bottom (Smith et al. 1990; Welch and Bergman, 1989). In both of these studies, the ice algae bloom sloughed from the ice towards the end of May (Figure 4.1). However, provided integrated Chl *a* concentrations in the sea ice were greater than the first two integrated water column peaks on May 20 and June 12, it is likely that these first peaks were associated with sloughing events of bottom ice algae from the sea ice. Furthermore, provided the June 12 peak occurred a week or so after the ice algal sloughing event, it may have been a rapid phytoplankton bloom seeded by the sloughed ice algae as observed in 2011. It is significant to note that this potential early ice algae seeded bloom reached a peak and declined quite rapidly as was observed in 2011. The depletion of surface nutrients (2 to 5 m) observed during 2011 is thus of significance, as the ice algae bloom appeared to exhaust the surface nutrients prior to the

occurrence of a more drawn out bloom as that observed in 2010. Leu et al. (2011) discussed the importance of primary production timing with life cycle stages of secondary producers. Therefore, the rapid bloom observed in 2011 could have strongly affected trophic transfer of energy with potential cascading consequences on the ecosystem.

Although 2012 showed similar melt and PAR transmission characteristics to that of 2010, a phytoplankton bloom never developed. It is suspected that the increased levels of Chl *a* at the end of sampling were the initial phase of bloom onset, but this was impossible to conclude with any certainty.

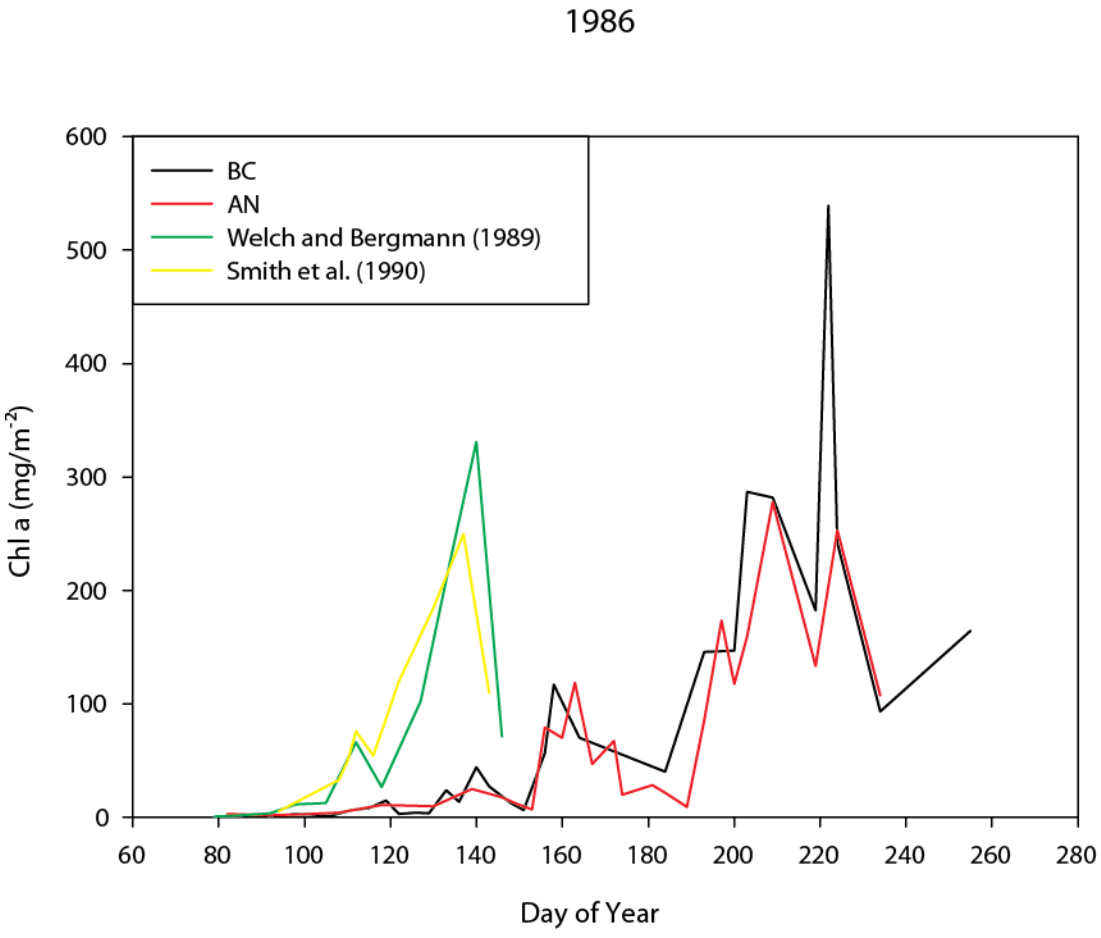

Figure 4.1: Time series of integrated chlorophyll (Chl) a concentrations in the bottom ice (data from Welch and Bergmann (1989) and Smith et al. (1990)) and water column (data from the ArcNut (AN) and BioChem (BC) datasets).

4.0.3 Stratification

Critical depth theory suggests that surface stratification plays a vital role in the initiation of spring blooms (Sverdrup, 1953). Figure 4.2 contrasts the development/existence of the surface mixed layer (observed through salinity profiles), with suspended Chl *a* concentrations (observed through Chl *a* profiles) during June in each of the three Arctic-ICE datasets.

Surface stratification was present as a weak surface halocline in both 2010 and 2011 on June 1 and 7/8 and surface stratification continued to strengthen and shoal throughout the rest of the observation periods. The June 11 water column of 2010 showed a gradual increase in surface stratification over the upper water column (observed as a salinity gradient of > 0.04 over the upper 20 m) as melt water collected underneath the ice cover and the bloom was just starting to commence. By June 11, 2011, drainage of freshwater from the rain event and associated snowmelt had led to strong stratification of the upper 20 m water column (salinity difference between the surface and 20 m was > 0.6) and the bloom was already well underway.

Weak surface stratification similar to that of 2010 was observed in 2012 on June 1. By June 11, however, the salinity gradient over the upper 20 m was < 0.01 and the vertical straight-line profile (i.e., a mixed layer) between 10 and 25 m depths suggested the presence of strong mixing forces under the ice homogenizing the water mass. These conditions contrasted with those observed in 2010 and 2011. By June 19, the upper 20 m water columns continued to be strongly stratified with the bloom well developed in 2010 and already declining in 2011, whereas only the upper 5 m water column had become strongly stratified due to melt waters by this time in 2012.

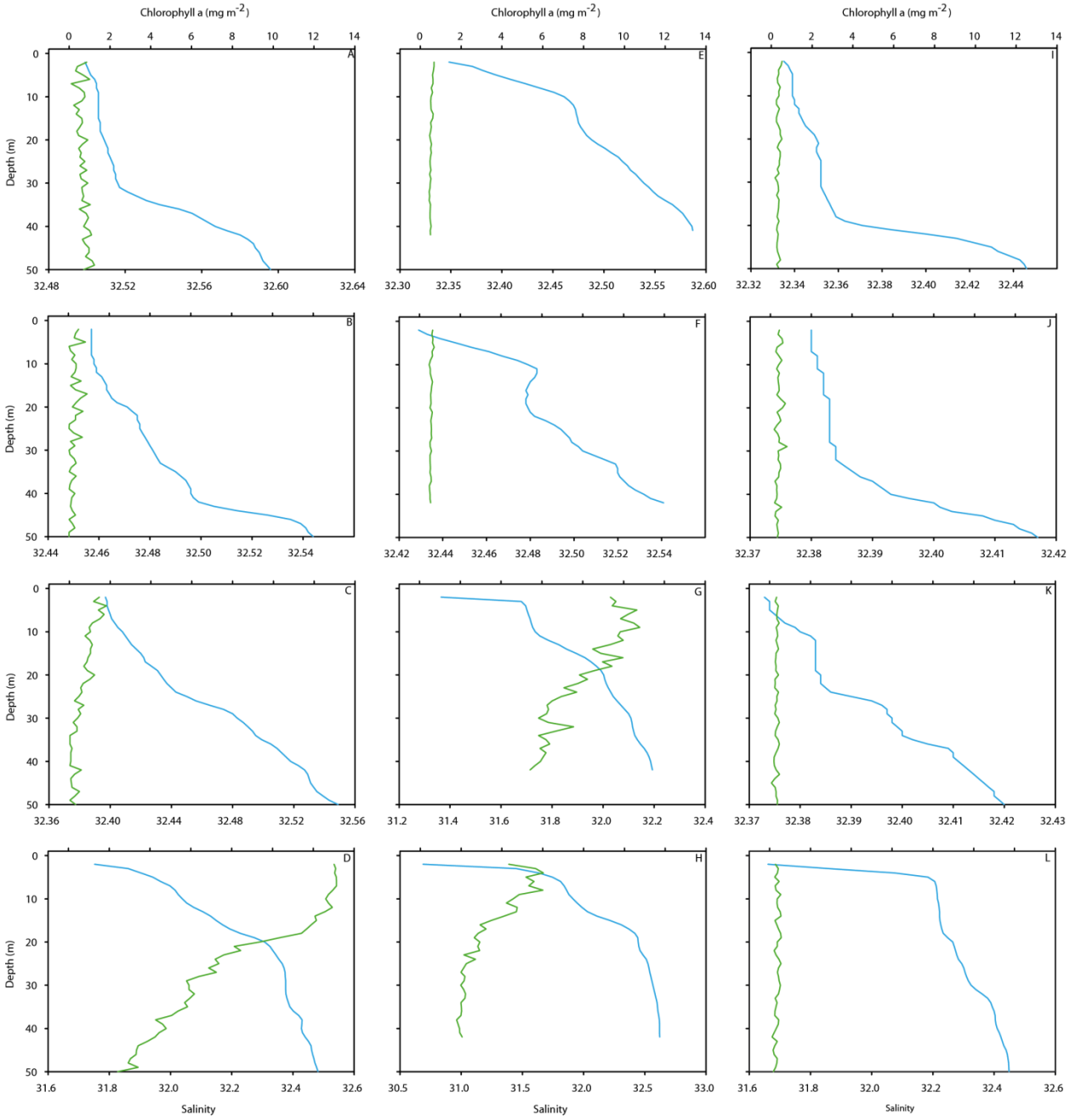

Figure 4.2: A comparison of the development of the surface mixed layer during the three Arctic-ICE field campaigns. Salinity is plotted in blue over 4 critical determined dates (Pre-melt (June 1) [A,E,I], bloom onset (June 8/7, 2010/2011, not applicable to 2012) [B,F,J], mid-point (June 11) [C,G,K], and advanced melt (June 19) [D,H,L]. Chl *a* concentration is standardized to the same scale and plotted in green.

Factors affecting the differences in stratification can be explained in part by the study of Landy et al. (2014) who examined melt progression during Arctic-ICE 2011 and 2012. Of particular note, drainage of surface melt was delayed during 2012. This was likely due to less of a hydraulic head, possibly associated with a thinner snow cover, and a less permeable ice cover associated with lower ice temperatures in 2012 (Landy et al., 2014). This lack of drainage led to a greater coverage of melt ponds on the surface (78% in 2012 versus 60% maximum in 2011; Landy et al., 2014). This can help explain, in part, the deeper penetration of transmitted PAR observed in 2012. That is, due to their low albedo, percent melt pond coverage controls the amount of light transmitted to the underlying water column (Ehn et al., 2011; Frey et al., 2011).

Drainage of the over-flooding occurred between June 15 and 17 in 2012, causing a slight decrease in pond coverage to 53% (Landy et al., 2014), which was matched by the observed stabilization of the depth PAR was transmitted to in the water column (Figure 3.10). Furthermore, the delay in drainage during 2012 likely contributed to the weak upper water column stratification until later in the period. This delay in stratification is suspected to have limited phytoplankton to acclimation and production in the euphotic zone above the critical depth.

In addition to delayed snowmelt drainage, the very deep and variable surface mixed layer is suspected as an important driving force behind the lack of a bloom observed in 2012. Figure 4.2 demonstrates that surface stratification never fully strengthened in 2012 relative to those of 2010 and 2011 until the end of the study. It is noted that strong under-ice currents, as evidenced by the rapid movement of sloughed ice algae clumps visible under the ice, were observed throughout the 2012 campaign (personal observation). It was confirmed that currents were less strong during 2010 and 2011 (C.J. Mundy, personal communication). Unfortunately current

velocities were not recorded in 2012. The observed strong currents in the region of the 2012 sampling campaign are likely linked to the opening of a tidally driven polynya situated close by (Hannah et al., 2009). In fact, the polynya started to open up off Sheringham Point by the end of the 2012 campaign, less than 5 km from our study site. Additionally, tidally driven currents in the vicinity of Barrow strait and near the edge of Allen Bay are notably strong, reaching 50-150 cm s^{-1} (Prinsenberg and Bennett, 1989; McLaughlin et al., 2006). It is most likely that strong currents kept the water column mixing to depth and therefore, conditions never satisfied the critical depth theory for bloom development during the sampling period.

Table 4.1 summarizes the observations and conclusions related to bloom development during the three-year Arctic-ICE field program. As observed during the three years in the Arctic-ICE field campaigns, decreased snow cover and eventual melt pond onset, allowed enough light to penetrate the water column for a bloom to occur. These observations agree with Apollonio et al. (2002), Mundy et al. (2014), and Palmer et al. (2013). Furthermore, stratification was an important factor required in the critical depth theory for bloom development to be met. In the under-ice water column, this was observed by consistent salinity gradients over the upper 20 m in 2010 and 2011. Essentially, very shallow or 0 cm surface mixed layer depths were observed. Therefore, once transmitted PAR increased in the underlying water column, the critical depth would have been below the mixed layer depth, satisfying the theory. However, under-ice mixing forces were evidenced to possibly influence the delay of consistent surface stratification during 2012 and therefore, bloom onset.

Table 4.1: Summary table of Arctic-ICE observations and conclusions.

	2010	2011	2012
Bloom Onset Date	160	160	N/A
Type of Bloom	Dominated by pelagic centric diatoms	Seeded and dominated by ice-associated diatoms	N/A
Driving Force	Regular melt progression with consistent stratification strengthened by ice melt	Rain event - rapid melt progression resulted in strong surface stratification	Mixing and late surface drainage delayed strong surface stratification
Ice-Algal Bloom	Sloughed 2 weeks prior to bloom onset	Sloughed during bloom onset	Sloughed 2 weeks prior to end of study

Additionally, the measurements of nutrient concentrations agree with Tremblay et al. (2008) and Martin et al. (2010) who state a nitrogen limited environment quickly emerges above the nutricline and is a strong candidate for the eventual demise of the under-ice bloom when it occurs. The development of a SCM in 2011, and the decrease in surface nutrient concentrations observed in both 2010 and 2011, introduces the possibility that in some years, nutrients in the upper water column can be depleted prior to ice break-up. This point is of particular importance when considering the applicability, or rather lack-there-of, for making primary production estimates for the Arctic Ocean from satellite data, which require an ice-free ocean (e.g., Arrigo et al., 2008).

4.1 Long Term Trends and Variability

4.1.1 Timing of Bloom Onset

Perovich et al. (1996) determined that the snow depth is the chief variable in determining light penetration to the water column. Through a modelling study, Palmer et al. (2013) suggested that in addition to complete snowmelt, melt ponds needed to cover 10% of the surface in order

for a bloom to commence. In contrast, Mundy et al. (2014) suggested that blooms could develop under a melting snow cover prior to melt pond development, but dependent on surface stratification of the water column. The lack of statistical difference between the dates of bloom onset and complete snow melt suggest that the bloom development is dependent on an advanced snow melt stage, but does not necessarily imply the requirement of melt pond development. This conclusion does slightly contrast Palmer et al. (2013); however, it is important to note that the conclusions made by Palmer et al. (2013) were based on a phytoplankton growth model for first-year ice in the Chukchi Sea. Therefore, the discrepancy observed suggest that parameterizations associated with radiative transfer and, or light limitation of phytoplankton in the model of Palmer et al. (2013) may need to be re-visited.

It is clear in the results that under-ice phytoplankton blooms have been a regular phenomenon in the Canadian Arctic. Therefore, they are not a more recent observation representing a direct response to climate change. However, this is not to say that the blooms are not being affected by the changing sea ice climate. In the next sub-section, I explore the associations of bloom onset with various climate related variables.

4.1.2 Association of Bloom Onset with Climate Related Trends

An examination of the historical ice and snow thickness data, compiled from Environment Canada and Canadian Ice Service datasets, shows that maximum ice thickness increased from the late 1950s to the start of the 1990s, then started to decrease from the early 1990s onward (Figure 4.4). Furthermore, the date of complete snowmelt has been significantly decreasing over the entire period (Figure 4.5). Both datasets support a recent warming and earlier melt onset since at least the mid 1990s. Lindsay and Zhang (2005) noted that the late 1980's and

1990's could be considered a tipping point in Arctic climate. Positive feedbacks associated with increasing open water and thinning ice was suggested to create a new era for the ice-ocean system in the Arctic (Lindsay and Zhang, 2005). The decreasing trend in maximum first-year ice thickness in the Resolute Bay, Nunavut, region from the mid 1990s onwards is thus interpreted as being associated with this general tipping point change in climate across the Arctic. It is also significant to note that the most recent data of the region demonstrate some of the thinnest first-year ice covers and earliest melt onset dates observed since the early 1960's.

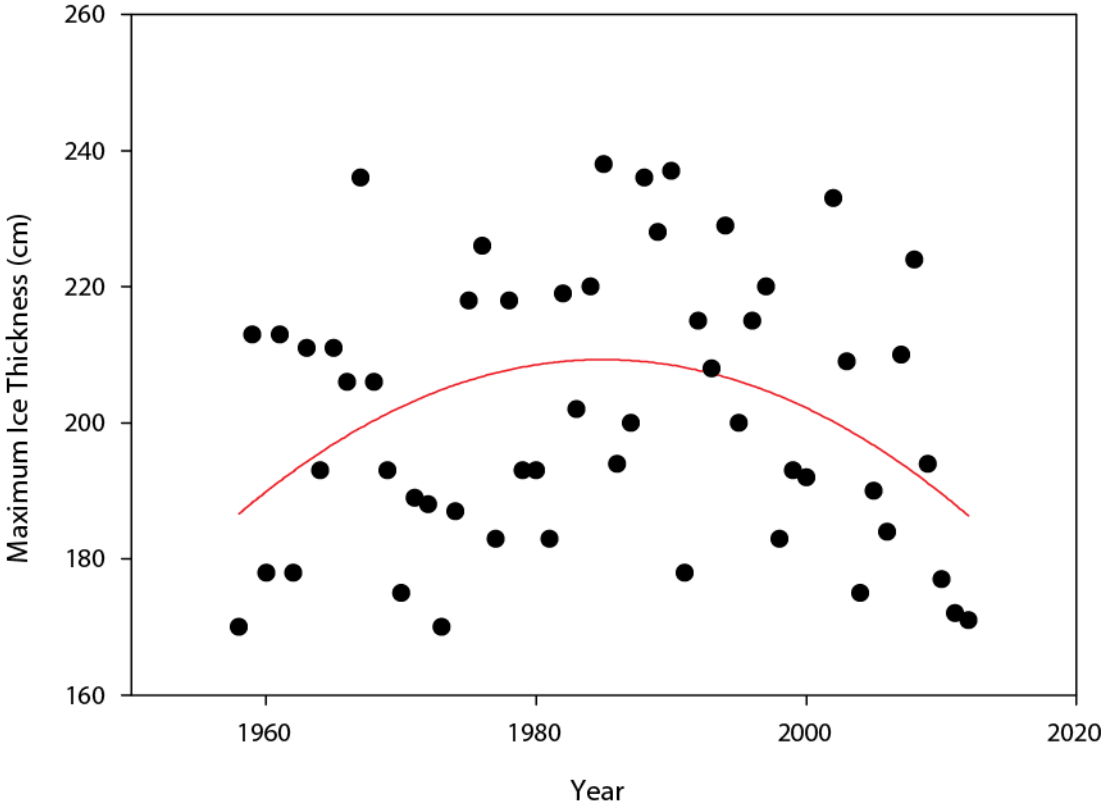

Figure 4.3: Maximum ice thickness by year in Resolute Bay, NU. The red line represents a best-fit polynomial trend with an equation of the form: f=-123039.86+124.19*x-0.031*x^2 (n = 54; p = 0.029; R^2 = 0.129). Data are from Environment Canada historical archives.

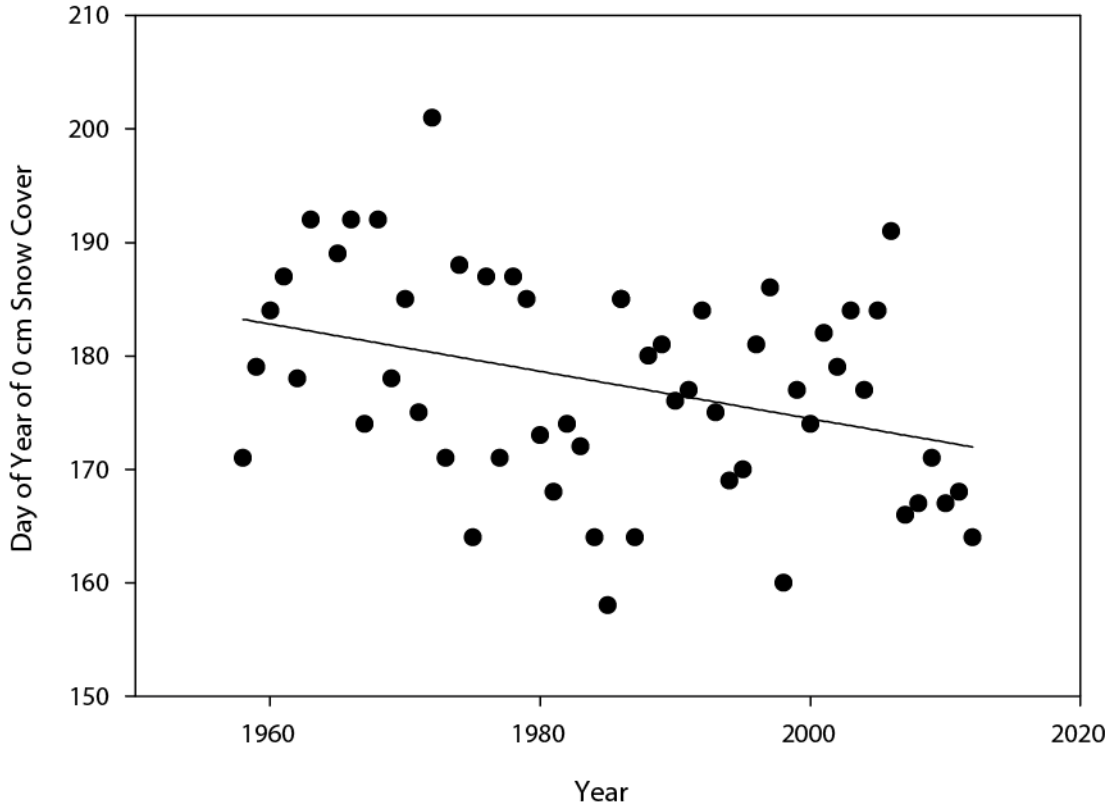

Figure 4.4: Date of complete snow melt on the ice in Resolute Bay (Note: 1963 was tested and found to be an outlier and thus was removed from the analyses). The black line represents a best-fit linear relationship of the form: f = 591.46-0.21*x (n = 55; p = 0.008; R^2 = 0.123). Data are from Environment Canada historical archives.

Correlation analyses were conducted between historical time series datasets to explore if significant relationships existed (Table 4.2). A Spearman two-tailed test was used to test the significance of correlations at an α-level of 0.05. Bloom onset showed a strong correlation with air temperature reaching 0 ºC (n = 17, p = 0.001, r = 0.707). Maximum snow depth showed significant correlations with air temperature reaching 0 ºC (n = 55, p = 0.009, r = 0.349) and date of 0 snow (n = 55, p = 0.025, r = 0.302). Lastly, date of 0 snow and air temperature reaching 0 ºC demonstrated the most significant correlation of the entire dataset (n = 59, p < 0.001, r = 0.704).

Relationships between air temperature and snowmelt are well documented in the literature (Jin et al., 1994; Perovich, 1996; Curry et al., 1996; Iacozza and Barber, 2001; Zhang et

al., 2008). The positive correlation between air temperature reaching 0 ºC and complete snowmelt highlights the seasonal melt progression of the system. As ambient air temperatures slowly warm the snowpack in spring, snow grains increase in size and moisture collects causing albedo to decrease. The lowered albedo allows for more light to penetrate and be absorbed within the snowpack resulting in a positive feedback, which further accelerates melt. The correlation with maximum snow depth is not as straight forward to explain. Snow depth tends to increase during spring near Resolute Bay, Nunavut (Figure 5 in Leu et al., 2014), which is likely related to the tendency for precipitation events during spring in the Arctic (Warren et al. 1999). Therefore, an earlier spring melt would not allow as much snow to accumulate on the ice surface in a particular year. Furthermore, all things being equal, a thinner snow cover should result in an earlier date of complete snow melt. Surprisingly, no significant correlation was observed with date of ice break-up as the same positive feedback described above induces ice melt.

Apollonio and Matrai (2011) supported a possible linkage between snow depth in spring and the timing of maximum water column production, suggesting that a deeper snow cover could delay bloom onset. However, no correlation was observed between maximum snow depth and bloom onset timing in the historical dataset. Discussed earlier, bloom onset was found to be a function of snow melt that mitigated transmission of PAR to the underlying water column and melt water stratification. The significant positive correlations between bloom onset and date of air temperature reaching 0 ºC and between air temperature reaching 0 ºC and complete snowmelt, support this statement. These results strongly link timing of under-ice phytoplankton blooms to snow melt onset.

Table 4.2: Correlation matrix of Spearman 2-tailed test for collected and determined variables from Environment Canada and Chl *a* databases.

			Snow Max (Annual)	Ice Max (Annual)	Date of 0 Snow	Date of Ice Break-Up	Air Temp
Spearman	Bloom Onset	*r*	-.141	.242	.297	.420	.707**
		p-value	.616	.366	.247	.135	.001
		n	15	16	17	14	17
	Snow Max (Annual)	*r*		-.149	.302*	-.252	.349**
		p-value		.279	.025	.346	.009
		n		55	55	16	55
	Ice Max (Annual)	*r*			.010	.240	.123
		p-value			.940	.353	.366
		n			56	17	56
	Date of 0 Snow	*r*				.316	.704**
		p-value				.201	.000
		n				18	59
	Date of Ice Break-up	*r*					.181
		p-value					.471
		n					18

**** Correlation is significant at the 0.01 level (2-tailed).**
*** Correlation is significant at the 0.05 level (2-tailed).**

With a basic linear trend analyses, Figure 4.6 illustrates blooms in the region are happening slightly earlier as time progresses (1 day yr^{-1}; n = 16; R^2 = 0.20). Removing the low confidence bloom onset dates improves the trend slightly (n= 10; R^2 = 0.442; Figure 4.6). However, the fit does not appear to be linear according to the non normal distribution of residuals around the trend. In reality, there appears to be a relatively stable bloom onset date until after mid 1990, when bloom onset has become earlier on average.

An intriguing question arises of whether some sort of a tipping point has been met in more recent years for bloom onset. The apparent shift in earlier bloom onset could be related to the weak trend of an earlier date of complete snow melt combined with the switch in ice thickness trend that occurred during the 1990s. Furthermore, there is a decreasing trend over time in maximum snow depth (Figure 4.6). The earlier melt of snow and thinning snow and ice cover

would allow for an earlier and greater transmission of light into the water column in spring. Additionally, earlier melt would contribute towards surface stratification of the water column, further assisting the conditions required for bloom onset. Unfortunately, the dataset does not allow further interpretation. In order to better understand the response of under-ice phytoplankton blooms to a warming climate, we require more and long-term time-series studies of the under-ice environment over the winter-spring-summer transitions to better document the driving processes of the spring phytoplankton bloom in the Canadian Arctic.

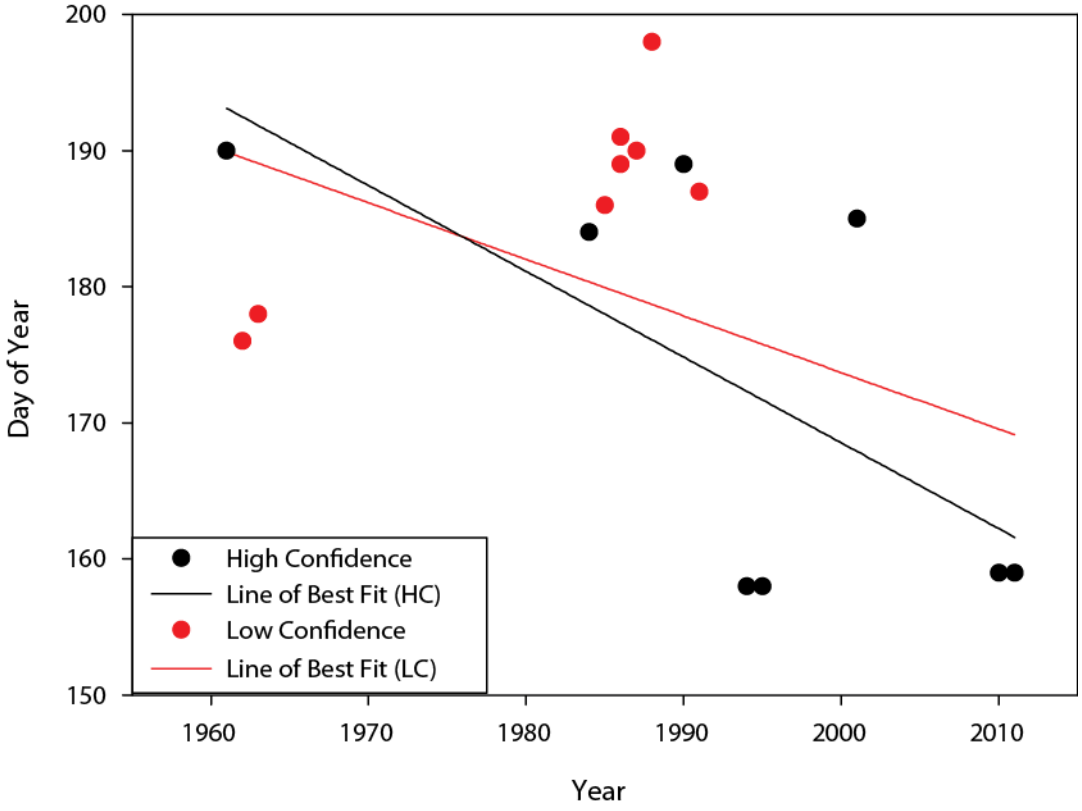

Figure 4.5: Line of best fit for only "high certainty" bloom onset dates shown in black (n = 10; R^2 =0.442). Line of best fit including "low certainty" bloom onset dates shown in red, (n = 16; R^2 = 0.20).

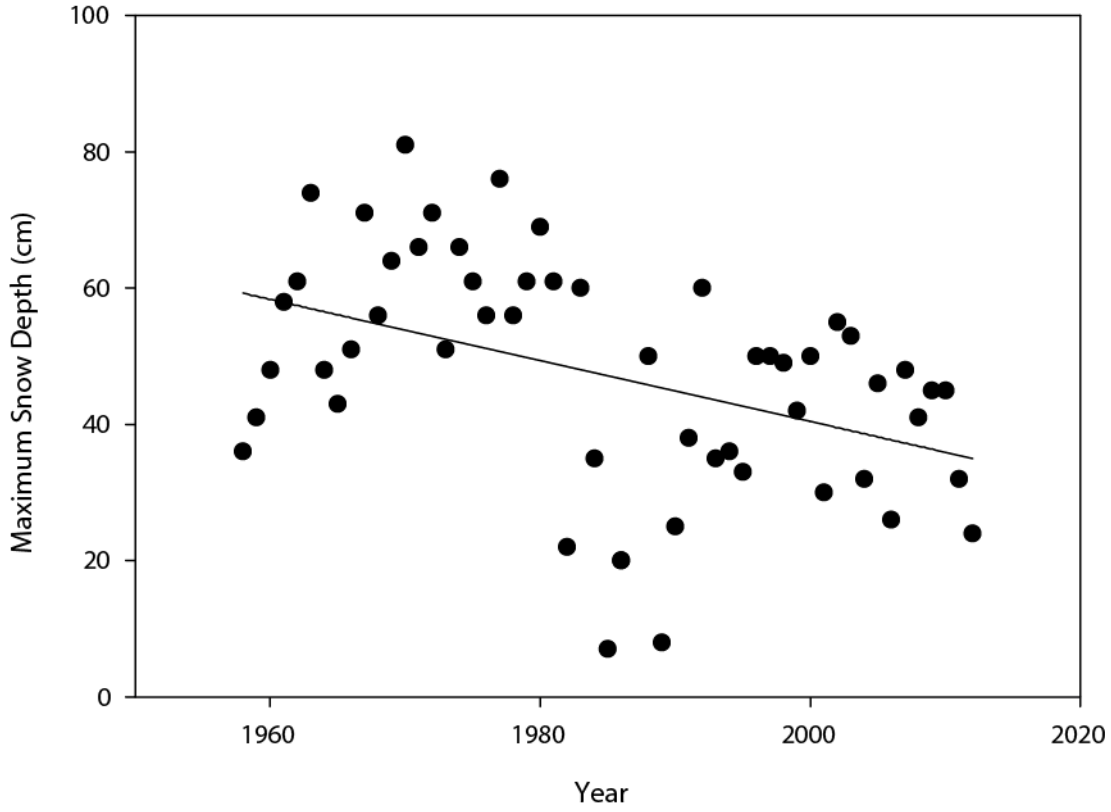

Figure 4.6: Time series of maximum snow depth observed on-ice near Resolute Bay, NU. The equation plotted has the form f=937.2 –0.448*x (*n* = 55; *p* = 0.0012; R^2 = 0.1814). Data are from Environment Canada historical archives.

Chapter Five: **Conclusions and Future Work**

In this chapter I summarize findings from my thesis and discuss in relation to my two main objectives. I conclude with a short discussion on how the scientific community could proceed forward to continue the advancement of knowledge in relation to our understanding of phytoplankton blooms in the ice-covered Arctic, and to Arctic oceanography in general.

5.0 Summary and Conclusions

My thesis set out to complete two objectives: (1) identification of the biophysical processes controlling the timing of under-ice blooms near Resolute Bay, NU in the central Canadian Arctic; and (2) To compare and contrast the timing of the under-ice bloom and controlling processes between different years.

Towards objective (1), I found that the development of under-ice blooms during the Arctic-ICE program conformed well to critical depth theory. Key forcing variables behind bloom timing under landfast ice were: (1) increased light transmission through the ice cover, which was ultimately controlled by snow melt and the formation of melt ponds on the ice surface; and (2) strengthening of surface stratification by snow and ice melt drainage into the water column. Both factors (1) and (2) were intimately linked to the rate of melt. This fact was particularly evident for 2011 where a rain event rapidly accelerated bloom development. It is significant to note that the rapid melt progression also appeared to influence taxonomic composition of the bloom, which may have further influenced bloom duration. That is, a bloom dominated by typical centric diatoms developed with the regular melt progression of 2010, whereas the rapid melt progression of 2011 appeared to influence the development of an ice-associated pennate diatom

bloom in the water column. I speculated that pennate diatoms could sink faster in the water column and thus influenced an earlier peak biomass as observed in 2011.

In contrast, a later date of surface drainage influenced a delay in surface stratification during 2012. Furthermore, under-ice mixing forces likely further delayed development of surface stratification and ultimately causing the lack of a bloom observation during the 2012 study period.

The contrasting lack of bloom development in 2012, yet similar melt progression characteristics is of critical importance with respect to prediction of under-ice bloom timing using only surface observations such as melt onset timing and melt pond coverage. The variability of the three-years of Arctic-ICE field campaigns highlights the need for actual under-ice observations of both physical and biological parameters into the future. Small independent studies that have historically been conducted do not allow for easy multi-variable data collection. Collaboration between researchers, institutions, and industry is key to large inter-disciplinary studies.

The historical dataset showed that under-ice blooms are a regular and recurring phenomena in the central Canadian Arctic. Evidence suggested that all blooms observed commenced prior to ice break-up and near the date when snow cover had reached 0 cm levels.

A correlation between the dates of bloom onset and air temperatures reaching 0°C strongly suggest a link of bloom timing with melt onset. A further concern of change is related to the suggestion that under-ice production will increase as a function of changing ice type in the central Arctic (Mundy et al., 2009; Arrigo et al., 2012; Palmer et al, 2014). More specifically, changes from thick MYI to thin FYI, where MYI has higher albedo and scattering properties than FYI for every season, including melt (Nicolaus et al., 2012), will increase transmission of

PAR to the underlying ocean. Indeed, it is likely that the historical coverage of thick MYI has resulted in a euphotic zone too shallow to allow blooms to develop, thus resulting in historically low phytoplankton production observations (English, 1961; Gosselin et al., 1997). My conclusion of under-ice blooms being a regular phenomena under FYI in the Canadian Arctic supports the suggestions of others potential that as the central Arctic changes ice regimes from MYI to FYI with warming ambient air and ocean temperatures providing a longer open water season (Maslanik et al., 2007; Barber et al., 2009, Stroeve et al., 2012), under-ice production will increase and shift earlier in its timing.

As primary producers form the base of most marine food webs, a change in the timing of spring blooms can directly impact vital components such as transfer of energy through trophic levels, along with the quantity and quality of biomass production (Søreide et al., 2010; Leu et al., 2011). That is, a shift in bloom timing could lead to a mismatch of grazer production with primary production, causing a cascading effect through the food web (Søreide et al., 2010). Therefore, the accelerated decrease in sea ice extent and thickness (Stoeve et al., 2007; Comiso et al., 2008) will have consequences that could affect the Arctic food web structure and function (Leu et al., 2011). It is likely we are beyond the tipping point of preventing major changes in the Arctic from occurring (ACIA, 2005). However, the establishment of long-term monitoring programs throughout the Arctic will allow us to see the changes and hopefully work in parallel with them rather than against in the future.

5.1 Recommendations

I have reflected on my experience through the undertaking of this Masters work and concluded on the following list of what I believe to be important points required to further our

understanding of primary producers in the Arctic ice-covered ecosystem. Furthermore, I discuss how further work to collate datasets, such as that presented in my thesis, is required to improve the transfer of knowledge between scientists, industry, policy makers, and the general public.

A first point is that annual biological, chemical, and physical studies are of the utmost importance. A regular sampling program should be established based on a consistent time interval of at least once per week to provide improved insights on bloom timing and the mechanisms that contribute to their formation. This aggressive sample collection could be achieved through community based monitoring programs by training and hiring local people from northern communities. Data collection should include, but not be limited to: physical environment variables (snow depth, ice thickness, air temperature, precipitation, albedo, and light measurements); physical water column data by way of moorings and discrete sampling, including frequent CTD casts; and discrete environmental and biological water samples including measurements for nutrient concentrations as well as biomass and taxonomic determination.

Taking a whole ecosystem approach when studying biophysical variables will help to better understand the Arctic marine ecosystem. Currently, most studies are regional specific. However, biological species at the third or higher trophic levels can be quite mobile and habitat use can span the entire Canadian Arctic (whales for example).

Many approaches have recently been employed and developed to map out trophic levels and food web dynamics. These typically include some kind of tracer such as lipids (Falk-Petersen et al., 2009; Søreide et al., 2010), pigments (Morata et al., 2011), stable isotopes (Hobson and Welch 1992; Kurle and Worthy 2001;Hobson et al. 2002; Layman et al. 2007; Pineault et al., 2013), combination of stable isotopes and lipids (Falk-Petersen et al., 2009;

Søreide et al., 2010; Wang et al., 2014) and more recently, highly branched isoprenoids (T. Brown, personal communication). A combination of these approaches could help decipher the important role primary production and its timing play in the marine ecosystem structure and function. Furthermore, the above annual studies should become part of a framework for a long running temporal monitoring program across the Pan-Arctic region.

Another point is the need to better examine the fate of the spring bloom and what happens after the blooms demise when, for example, subsurface chlorophyll maxima (SCM) develop. Implications of the SCM for biogeochemical fluxes, food webs, and accuracy of remote sensing blooms are vital, yet understudied. Martin et al. (2002) noted that SCMs, structure, function, and significance have not yet been established. Martin et al., (2002) also noted that the determination of baseline concentrations of Chl *a* and productivity measurements for water column communities of primary producers is necessary for Arctic environment ecological assessments.

My research has established a limited baseline of Chl *a* concentration in the ice-covered system of the Canadian Arctic. The limited nature of this dataset highlights the need for a more thorough study throughout the entire Pan-Arctic region. Still, as most studies are limited to less than 5 years in a region, and are often a seasonal sampling campaign, it is near impossible to gain a proper perspective understanding of events with limited contributions of samples. The development of new Arctic stations, such as the Canadian High Arctic Research Station (CHARS), provides promise of long-term time series monitoring in the Canadian Arctic. The hope should be to follow closely in the footsteps of the regular oceanographic monitoring programs already underway across the Arctic, such as the long-term time series monitoring program employed by the Greenland Climate Research Centre (http://www.natur.gl/en/climate-research-centre/). Furthermore, stations such as MARS (McGill Arctic Research Station

http://www.mcgill.ca/mars/mars-mcgill-arctic-research-station), which have been established since 1960, have great potential to couple the long running terrestrial data with marine sampling programs. Furthermore, I strongly believe that open collaboration is the key to succeeding in the future.

Finally, the science community is at odds within itself. The competitive funding scheme and limited collaboration within the science community has created an environment which limits the advancements that could be made through more collaborative efforts. A fundamental shift within the global science community needs to occur in order to work as a team. The science community is making progress towards this ideology through things such as: open access journals, some inter-university partnerships, and public access databases, such as the ones utilized in this thesis. However, we, as global citizens, need to fund natural and applied sciences at an economic loss on a global scale, with the knowledge that this loss is offset by societal and environmental gains. Furthermore, the addition of a comprehensive open access database, updated on an annual basis, would allow collaborative sharing of information between researchers, industry, and the public. It could be advanced further with industry partnership. This would help foster a better working relationship and allow for innovation to excel.

Chapter Six: **References**

ACIA (Arctic Climate Impact Assessment) (2005). Arctic climate impact assessment: scientific report. Cambridge University Press, Cambridge

Ackley, S.F. and C.W. Sullivan. (1994). Physical control on the development and characteristics of Antarctic sea ice biological communities – a review and synthesis. Deep-Sea Res. I., 41, 1583-1604.

Aiken, J., Moore, G. F., Trees, C. C., Hooker, S. B., and Clark, D. K. (1996). The SeaWiFS CZCS-type pigment algorithm. Oceanographic Literature Review,43(3), 315-316.

Alexander, V., and Niebauer, H. J. (1981). Oceanography of the eastern Bering Sea ice-edge zone in spring. Limnol. Oceanogr, 26(6), 1111-1125.

Allison, I., R.E. Brandt and S.G. Warren (1993). East Antarctic sea ice: Albedo, thickness distribution, and Snow Cover. Journal of Geophysical Research, 98(C7), 12-417.

Antoine, D., André, J. M., and Morel, A. (1996). Oceanic primary production: 2. Estimation at global scale from satellite (coastal zone color scanner) chlorophyll. Global biogeochemical cycles, 10(1), 57-69.

Apollonio, S. (1965). Chlorophyll in Arctic sea-ice. Arctic 18:118–122

Apollonio, S., Pennington, M., and Cota, G. F. (2002). Stimulation of phytoplankton photosynthesis by bottom-ice extracts in the Arctic. Polar Biology, 25(5), 350-354.

Apollonio, S., and Matrai, P. (2011). Marine primary production in the Canadian Arctic, 1956, 1961–1963. Polar biology, 34(5), 767-774.

Arctic Nutrient Database 1904-2000 (ARCNUT) [Cota, G., and Pomeroy, L.] (http://data.eol.ucar.edu/codiac/dss/id=62.015), Accessed: March 1, 2013

Arrigo, K.R. (2003). Primary production in sea ice. IN Sea Ice: An Introduction to its Physics, Chemistry, Biology and Geology, D.N. Thomas and G.S. Dieckmann (Eds). Blackwell Science Ltd., Oxford, UK. pp. 143-183.

Arrigo, K.R. and Sullivan, C.W. (1992). The influence of salinity and temperature covariation on the photophysiological characteristics of Antarctic sea ice microalgae. J. Phycol., 28, 746-756.

Arrigo K.R., van Dijken G., Pabi, S., (2008). Impact of a shrinking Arctic ice cover on marine primary production. Geophys Res Lett 35: L19603.

Arrigo, K. R., Perovich, D. K., Pickart, R. S., Brown, Z. W., van Dijken, G. L., Lowry, K. E., and Swift, J. H. (2012). Massive phytoplankton blooms under Arctic sea ice. Science, 336(6087), 1408-1408.

Arsalane, W., Rousseau, B., and Duval, J. C. (1994). Influence of the pool size of xanthophyll cycle on the effects of light stress in a diatom: Competition between photoprotection and photoinhibition. Photochemistry and photobiology, 60(3), 237-243.

Barber, D. G., Reddan, S. P., and LeDrew, E. F. (1995). Statistical characterization of the geophysical and electrical properties of snow on landfast first-year sea ice. Journal of Geophysical Research, 100(C2), 2673-2686.

Barber, D. G., Galley, R., Asplin, M. G., De Abreu, R., Warner, K. A., Pućko, M., and Julien, S. (2009). Perennial pack ice in the southern Beaufort Sea was not as it appeared in the summer of 2009. Geophysical Research Letters,36(24), L24501.

Bartlett, J. S., Ciotti, Á. M., Davis, R. F., and Cullen, J. J. (1998). The spectral effects of clouds on solar irradiance. Journal of Geophysical Research: Oceans (1978–2012), 103(C13), 31017-31031.

Behrenfeld, M. J., and Kolber, Z. S. (1999). Widespread iron limitation of phytoplankton in the South Pacific Ocean. Science, 283(5403), 840-843.

Bishop, J. K., and Rossow, W. B. (1991). Spatial and temporal variability of global surface solar irradiance. Journal of Geophysical Research: Oceans (1978–2012), 96(C9), 16839-16858.

Bourgault, D., Hamel, C., Cyr, F., Tremblay, J. É., Galbraith, P. S., Dumont, D., and Gratton, Y. (2011). Turbulent nitrate fluxes in the Amundsen Gulf during ice-covered conditions. Geophysical Research Letters, 38(15), L15602.

Braarud, T. (1935). The" Øst" Expedition to the Denmark Strait 1929. 2. The phytoplankton and its conditions of growth:(including some qualitative data from the Arctic in 1930). Dybwad in Komm..

Brown, K., Galindo, V, Mundy, C.J., (2010). Arctic-ICE (Arctic – Ice-Covered Ecosystem in a Rapidly Changing Environment) 2010 Field Report A sea ice-based study in Resolute Passage, NU, Canada. 113 p.

Brown, T. A., Belt, S. T., Philippe, B., Mundy, C. J., Massé, G., Poulin, M., and Gosselin, M. (2011). Temporal and vertical variations of lipid biomarkers during a bottom ice diatom bloom in the Canadian Beaufort Sea: further evidence for the use of the IP 25 biomarker as a proxy for spring Arctic sea ice. Polar biology, 34(12), 1857-1868.

Brzezinski, M. A. (2004). The Si: C: N Ratio of Marine diatoms: Interspecific variability and the effect of some environmental variables. Journal of Phycology, 21(3), 347-357.

Carmack, E. C., Macdonald, R. W., and Jasper, S. (2004). Phytoplankton productivity on the Canadian Shelf of the Beaufort Sea. Marine Ecology Progress Series, 277, 37-50.

Carmack, E., Barber, D., Christensen, J., Macdonald, R., Rudels, B., and Sakshaug, E. (2006). Climate variability and physical forcing of the food webs and the carbon budget on panarctic shelves. Progress in Oceanography, 71(2), 145-181.

Carmack, E., and Wassmann, P. (2006). Food webs and physical–biological coupling on pan-Arctic shelves: unifying concepts and comprehensive perspectives. Progress in Oceanography, 71(2), 446-477.

Campbell, K., Galindo, V, Landy, J. (2011). Arctic-ICE (Arctic – Ice-Covered Ecosystem in a Rapidly Changing Environment) 2011 Field Report A sea ice-based study in Allen Bay, NU, Canada. 126 p.

Campbell, K (2012). Analysis of sea ice microalgae biomass variability using transmitted irradiance. Thesis, University of Manitoba.

Campbell, K., Mundy, C. J., Barber, D. G., and Gosselin, M. (2014). Characterizing the sea ice algae chlorophyll a–snow depth relationship over Arctic spring melt using transmitted irradiance. Journal of Marine Systems.

Change, I. P. O. C. (1995). IPCC Second Assessment. Secretaria do IPCC, Organização Mundial de Metereologia, Genebra.

Clarke, G. L., Ewing, G. C., and Lorenzen, C. J. (1970). Spectra of backscattered light from the sea obtained from aircraft as a measure of chlorophyll concentration. Science, 167(3921), 1119-1121.

Coale, K. H., Johnson, K. S., and Fitzwater, S. E. (1996). An ecosystem-scale iron fertilization experiment in the equatorial Pacific Ocean. Nature, 383, 10.

Colbeck, S. C. (1982). An overview of seasonal snow metamorphism. Reviews of Geophysics and Space Physics, 20(1), 45-61.

Comiso, J. C., Parkinson, C. L., Gersten, R., and Stock, L. (2008). Accelerated decline in the Arctic sea ice cover. Geophysical Research Letters, 35(1), L01703.

Conover, R. J., and Gustavson, K. R. (1999). Sources of urea in arctic seas: zooplankton metabolism. Marine Ecology Progress Series, 179, 41-54.

Cota GF, Prinsenberg SJ, Bennett EB, Loder JW, Lewis MR, Anning JL, Watson NHF, Harris LR (1987). Nutrient fluxes during extended blooms of Arctic ice algae. J Geophys Res 92:1951–1962

Cota GF, Horne EPW (1989). Physical control of arctic ice algal production. Mar Ecol Prog Ser 52:111–121

Cota, G.F., L. Legendre, M. Gosselin and R.G. Ingram. (1991). Ecology of bottom ice algae: I. Environmental controls and variability. J. Mar. Sys., 2, 257-277.

Cota G., Pomeroy, L. (2013). Cota-Pomeroy Arctic Nutrient Database. Retrieved November 18, 2013 From: http://data.eol.ucar.edu/codiac/dss/id=62.015

Cross, W. E. (1982). Under-ice biota at the Pond Inlet ice edge and in adjacent fast ice areas during spring. Arctic, 13-27.

Cullen, J. J. (1982). The deep chlorophyll maximum: comparing vertical profiles of chlorophyll a. Canadian Journal of Fisheries and Aquatic Sciences, 39(5), 791-803.

Cullen, J. J., Franks, P. J., Karl, D. M., and Longhurst, A. (2002). Physical influences on marine ecosystem dynamics. The sea, 12, 297-336.

Curry, J. A., Schramm, J. L., Rossow, W. B., and Randall, D. (1996). Overview of Arctic cloud and radiation characteristics. Journal of Climate, 9(8), 1731-1764.

Cushing, D. H. (1990). Plankton production and year-class strength in fish populations: an update of the match/mismatch hypothesis. Advances in marine biology, 26, 249-293.

Demmig-Adams, B., and Adams Iii, W. W. (1992). Photoprotection and other responses of plants to high light stress. Annual review of plant biology, 43(1), 599-626.

Derksen, C., Piwowar, J., and LeDrew, E. (1997). Sea-ice melt-pond fraction as determined from low level aerial photographs. Arctic and Alpine Research, 345-351.

Drobot, S., and Anderson, M., (2001). Snow Melt Onset Over Arctic Sea Ice from SMMR and SSM/I Brightness Temperatures. (1979 to 2007). Boulder, Colorado USA: National Snow and Ice Data Center.

Ehn, J. K., Mundy, C. J., Barber, D. G., Hop, H., Rossnagel, A., and Stewart, J. (2011). Impact of horizontal spreading on light propagation in melt pond covered seasonal sea ice in the Canadian Arctic. Journal of Geophysical Research, 116, C00G02.

Eicken, H., Bock, C., Wittig, R., Miller, H., and Poertner, H. O. (2000). Magnetic resonance imaging of sea-ice pore fluids: methods and thermal evolution of pore microstructure. Cold Regions Science and Technology, 31(3), 207-225.

Eicken, H., Grenfell, T. C., Perovich, D. K., Richter-Menge, J. A., and Frey, K. (2004). Hydraulic controls of summer Arctic pack ice albedo. J. Geophys. Res, 109 (C08007).

Else, B. G. T., Papakyriakou, T. N., Raddatz, R., Galley, R. J., Mundy, C. J., Barber, D. G. Barber, Swystun, K., and Rysgaard, S. (2014). Surface energy budget of landfast sea ice during the transitions from winter to snowmelt and melt pond onset: The importance of net longwave radiation and cyclone forcings. Journal of Geophysical Research: Oceans.

English, T. S. (1961). Some biological oceanographic observations in the central North Polar Sea drift station Alpha, 1957-1958 (No. 13). Arctic Institute of North America.

Falk-Petersen, S., Hopkins, C. C. E., and Sargent, J. R. (1990). Trophic relationships in the pelagic, Arctic food web. In Trophic relationships in the marine environment. Proceedings of 24th European Marine Biology Symposium(pp. 315-333).

Falk-Petersen, S., Hagen, W., Kattner, G., Clarke, A., and Sargent, J. (2000). Lipids, trophic relationships, and biodiversity in Arctic and Antarctic krill.*Canadian Journal of Fisheries and Aquatic Sciences*, *57*(S3), 178-191.

Falkowski, P. G. (1994). The role of phytoplankton photosynthesis in global biogeochemical cycles. Photosynthesis Research, 39(3), 235-258.

Falkowski, P. G. (1997). Evolution of the nitrogen cycle and its influence on the biological sequestration of CO 2 in the ocean. Nature, 387(6630), 272-275.

Falkowski, P. G. (2000). Rationalizing elemental ratios in unicellular algae.Journal of Phycology, 36(1), 3-6.

Falkowski, P. G. (2002). The ocean's invisible forest. Scientific American,287(2), 54-61.

Falkowski, P. G., and Raven, J. A. (2013). Aquatic photosynthesis. Princeton University Press.

Fetterer, F., and Untersteiner, N. (1998). Observations of melt ponds on Arctic sea ice. Journal of Geophysical Research, 103(C11), 24821-24835.

Fofonoff, P., and R. C. Millard Jr. (1983), Algorithms for computation of fundamental properties of seawater, UNESCO Tech. Pap. Mar. Sci., 44, 53 p.

Fortier, M., Fortier, L., Michel, C., and Legendre, L. (2002). Climatic and biological forcing of the vertical flux of biogenic particles under seasonal Arctic sea ice. Marine Ecology Progress Series, 225(1), 16.

Frey, K. E., Perovich, D. K., and Light, B. (2011). The spatial distribution of solar radiation under a melting Arctic sea ice cover. Geophysical Research Letters,38(22), L22501.

Fukuchi, M., Watanabe, K., Tanimura, A., Hoshiai, T., Sasaki, H., Satoh, H., and Yamaguchi, Y. (1989, September). A phytoplankton bloom under sea ice recorded with a moored system in lagoon Saroma Ko, Hokkaido, Japan. InProc. NIPR Symp. Polar Biol (Vol. 2, pp. 9-15).

Gargett, A., and Marra, J. O. H. N. (2002). Effects of upper ocean physical processes (turbulence, advection and air-sea interaction) on oceanic primary production. The sea, 12, 19-49.

Galindo, V., Levasseur, M., Mundy, C. J., Gosselin, M., Tremblay, J. É., Scarratt, M., ... and Lizotte, M. (2014). Biological and physical processes influencing sea ice, under-ice algae, and dimethylsulfoniopropionate during spring in the Canadian Arctic Archipelago. Journal of Geophysical Research: Oceans.

Garrido, J. L., Otero, J., Maestro, M. A., and Zapata, M. (2000). The Main Nonpolar Chlorophyll c From Emiliania Huxleyi (Prymnesiophycecae) Ia a Chlorophyll c2-Monogalactosyldiacylglyceride Ester: A Mass Spectrometry Study. Journal of Phycology, 36(3), 497-505.

Glud RN, Rysgaard S, Kühl M, Hansen JW (2007). The sea ice in Young Sound: implications for carbon cycling. In:Rysgaard S, Glud RN (eds) Carbon cycling in Arctic marine ecosystems. Case study: Young Sound. Medd Grønland. Bioscience 58: 62−85

Golden, K. M., Ackley, S. F., and Lytle, V. I. (1998). The percolation phase transition in sea ice. Science, 282(5397), 2238-2241.

Gordon, H. R., Clark, D. K., Mueller, J. L., and Hovis, W. A. (1980). Phytoplankton pigments from the Nimbus-7 Coastal Zone Color Scanner: comparisons with surface measurements. Science, 210(4465), 63-66.

Gradinger, R. (1996). Occurrence of an algal bloom under Arctic pack ice.Marine ecology progress series. Oldendorf, 131(1), 301-305.

Gran, H. H. (1931). On the conditions for the production of plankton in the sea. Rapp. Proc. Verb. Cons. Int. Explor. Mer, 75, 37-46.

Gran, H. H., and Braarud, T. (1935). A quantitative study of the phytoplankton in the Bay of Fundy and the Gulf of Maine (including observations on hydrography, chemistry and turbidity). Journal of the Biological Board of Canada, 1(5), 279-467.

Grasshoff, K., Kremling, K., and Ehrhardt, M. (Eds.). (2009). Methods of seawater analysis. John Wiley & Sons.

Grebmeier, J. M., Smith Jr, W. O., and Conover, R. J. (1995). Biological processes on Arctic continental shelves: ice-ocean-biotic interactions. Coastal and Estuarine studies, 49, 231-261.

Gregg, W. W., and Carder, K. L. (1990). A simple spectral solar irradiance model for cloudless maritime atmospheres. LIMNOLOGY, 35.

Grenfell, T.C. and G.A. Maykut (1977). The optical properties of ice and snow in the Arctic Basin. Journal of Glaciology, 18: 445–463.

Grenfell, T. C., and Perovich, D. K. (1984). Spectral albedos of sea ice and incident solar irradiance in the southern Beaufort Sea. Journal of Geophysical Research, 89(C3), 3573-3580.

Grenfell, T. C., Barber, D. G., Fung, A. K., Gow, A. J., Jezek, K. C., Knapp, E. J., and Tanis, F. (1998). Evolution of electromagnetic signatures of sea ice from initial formation to the establishment of thick first-year ice. Geoscience and Remote Sensing, IEEE Transactions on, 36(5), 1642-1654.

Hagen, W., and Auel, H. (2001). Seasonal adaptations and the role of lipids in oceanic zooplankton. Zoology, 104(3), 313-326.

Hanesiak, J. M., Barber, D. G., De Abreu, R. A., and Yackel, J. J. (2001). Local and regional albedo observations of arctic first-year sea ice during melt ponding. Journal of geophysical research, 106(C1), 1005-1016.

Hannah, C. G., Dupont, F., and Dunphy, M. (2009). Polynyas and Tidal Currents in the Canadian Arctic Archipelago. Arctic, 62(1).

Harrison, W. G., and Cota, G. F. (1991). Primary production in polar waters: relation to nutrient availability. Polar Research, 10(1), 87-104.

Hecky, R. E., and Kilham, P. (1988). Nutrient limitation of phytoplankton in freshwater and marine environments: a review of recent evidence on the effects of enrichment. Limnology and Oceanography, 33(4), 796-822.

Hobson, K. A. (1992). Determination of trophic relationships within a high Arctic marine food web using $\delta^{13}C$ and $\delta^{15}N$ analysis. Mar. Ecol. Prog. Ser., 84, 9-18.

Hobson, K., Fisk, A., Karnovsky, N., Holst, M., Gagnon, J., and Fortier, M. (2002). A stable isotope ($\delta^{13}C$, $\delta^{15}N$) model for the North Water food web: implications for evaluating trophodynamics and the flow of energy and contaminants. Deep Sea research- Part II-Topical Studies in Oceanography, 49(22):5131-5150.

Holligan, P. M. (1987). The physical environment of exceptional phytoplankton blooms in the Northeast Atlantic. Rapports et Proces Verbaux des Reunions Conseil International pour l'Exploration de la Mer, 187, 9-18.

Holligan, P. M. (1992). Do marine phytoplankton influence global climate?. InPrimary productivity and biogeochemical cycles in the sea (pp. 487-501). Springer US.

Horner, R.A., (1985). Sea Ice Biota. CRC Press Inc., Florida.

Horner RA (1989). Arctic sea-ice biota. In: Herman Y (ed) The Arctic seas: climatology, oceanography, geology and biology. Van Nostrand Reinhold, New York, pp 123–146

Iacozza, J., Barber, D.G., (2001). Ablation patterns of snow cover over smooth first-year sea ice in the Canadian Arctic. Hydrol. Proc. 15, 3559-3569.

Jassby, A. D., and Platt, T. (1976). Mathematical formulation of the relationship between photosynthesis and light for phytoplankton.

Jeffrey, S.W., Mantoura, R.F.C., and Wright, S.W., (2005). Phytoplankton pigments in oceanography: guidelines to modern methods. UNESCO Publishing. Paris (France).

Johnston, M., and Frederking, R. (2001). Decay of First-Year Sea Ice: A Second Season of Field Measurements, 2001.

Jones, E.P., and Coote, A.R., (1980). Nutrient distributions in the Canadian Archipelago: indicators of summer water mass and flow characteristics. Can. J. Fish. Aquat. Sci. 37:589-599

Jones, E. P., J. H. Swift, L. G. Anderson, M. Lipizer, G. Civitarese, K. K. Falkner, Gerhard Kattner, and F. McLaughlin. (2003). Tracing pacific water in the north atlantic ocean. Journal of Geophysical Research: Oceans (1978–2012) 108, C4 .

Jin, Z., Stamnes, K., Weeks, W. F., and Tsay, S. C. (1994). The effect of sea ice on the solar energy budget in the atmosphere-sea ice-ocean system: A model study. Journal of Geophysical Research: Oceans (1978–2012), 99(C12), 25281-25294.

Jin, M., Deal, C., Wang, J., Alexander, V., Gradinger, R., Saitoh, S. I., Stabeno, P. (2007). Ice-associated phytoplankton blooms in the southeastern Bering Sea. Geophysical Research Letters, 34(6), L06612.

Kay, J. E., L'Ecuyer, T., Gettelman, A., Stephens, G., and O'Dell, C. (2008). The contribution of cloud and radiation anomalies to the 2007 Arctic sea ice extent minimum. Geophysical Research Letters, 35(8), L08503.

Kirk, J. T. O. (1994). Light and photosynthesis in aquatic ecosystems. Cambridge university press.

Knap, A. H., Michaels, A., Close, A. R., Ducklow, H., and Dickson, A. G. (1996). Protocols for the joint global ocean flux study (JGOFS) core measurements. JGOFS, Reprint of the IOC Manuals and Guides No. 29, UNESCO 1994, 19.

Kok, B. (1956). On the inhibition of photosynthesis by intense light. Biochimica et biophysica acta, 21(2), 234-244.

Krause, G. H., and Weis, E. (1991). Chlorophyll fluorescence and photosynthesis: the basics. Annual review of plant biology, 42(1), 313-349.

Kurle, C. and Worthy, G. (2001). Stable isotope assessment of temporal and geographic differences in feeding ecology of northern fur seals (*callorhinus ursinus*) and their prey. *Ecologia*, 126(2):254-265.

Kwok R, Cunningham GF, Wensnahan M, Rigor I, Zwally HJ, Yi D (2009). Thinning and volume loss of the Arctic Ocean sea ice cover: 2003−2008. J Geophys Res 114: C07005.

Lalli, C. M., and Parsons, T. R. (1997). Biological oceanography: an introduction. Butterworth-Heinemann.

Landy, J., Gale, M., Crabeck, O., (2012). Arctic-ICE (Arctic –Ice-Covered Ecosystem) 2012 Field Report A sea ice-based study in Resolute Passage, NU, Canada. 171 p.

Langleben, M. P. (1967). Albedo measurements of an Arctic ice cover from high towers. McGillL Univ Montreal (Quebec) Dept. of Physics.

Layman, C., Arrington, D., Montana, C., and Post, D. (2007). Can stable isotope ratios provide for community-wide measures of trophic structure? *Ecology*, 88(1):42-48.

Legendre, L., Ingram, R. G., and Poulin, M. (1981). Physical control of phytoplankton production under sea ice (Manitounuk Sound, Hudson Bay). Canadian Journal of Fisheries and Aquatic Sciences, 38(11), 1385-1392.

Legendre, L. (1990). The significance of microalgal blooms for fisheries and for the export of particulate organic carbon in oceans. Journal of Plankton Research, 12(4), 681-699.

Legendre, L., Gosselin, M., (1991). In situ spectroradiometric estimation of microalgal biomass in first-year sea ice. Polar Biol. 11, 113-115.

Lehninger, A. L. (1975). Biochemistry: the molecular basis of cell structure and functions. Worth, New York, 659.

Leu, E., Wiktor, J., Søreide, J. E., Berge, J., and Falk-Petersen, S. (2010). Increased irradiance reduces food quality of sea ice algae. Marine Ecology Progress Series, 411, 49-60.

Leu, E., Søreide, J. E., Hessen, D. O., Falk-Petersen, S., and Berge, J. (2011). Consequences of changing sea-ice cover for primary and secondary producers in the European Arctic shelf seas: timing, quantity, and quality. Progress in Oceanography, 90(1), 18-32.

Leu, E., Mundy, C.J., Campbell, K., Gabrielsen, T., Gosselin, M., Juul-Pedersen, T., Gradinger, R. (subm: 2014) Arctic spring awakening - steering principles behind the phenology of vernal ice algae blooms. Prog Oceanogr

Lindsay, R. W., and Zhang, J. (2005). The thinning of Arctic sea ice, 1988-2003: Have we passed a tipping point?. Journal of Climate, 18(22), 4879-4894.

Long, S. P., Humphries, S., and Falkowski, P. G. (1994). Photoinhibition of photosynthesis in nature. Annual review of plant biology, 45(1), 633-662.

Longhurst, A., Sathyendranath, S., Platt, T., and Caverhill, C. (1995). An estimate of global primary production in the ocean from satellite radiometer data. Journal of Plankton Research, 17(6), 1245-1271.

MacIntyre, H. L., Kana, T. M., and Geider, R. J. (2000). The effect of water motion on short-term rates of photosynthesis by marine phytoplankton. Trends in plant science, 5(1), 12-17.

Mann, K., and Lazier, J. (2009). Dynamics of marine ecosystems: biological-physical interactions in the oceans. John Wiley and Sons.

Margalef, R. (1978). Life-forms of phytoplankton as survival alternatives in an unstable environment. Oceanologica acta, 1(4), 493-509.

Markus, T., Stroeve, J. C., and Miller, J. (2009). Recent changes in Arctic sea ice melt onset, freezeup, and melt season length. Journal of Geophysical Research: Oceans (1978–2012), 114(C12).

Marsden, R. F., Paquet, R., and Ingram, R. G. (1994). Currents under land-fast ice in the Canadian Arctic Archipelago Part 1: Vertical velocities. Journal of marine research, 52(6), 1017-1036.

Markus, T., Stroeve, J. C., and Miller, J. (2009). Recent changes in Arctic sea ice melt onset, freezeup, and melt season length. Journal of Geophysical Research, 114(C12), C12024.

Maslanik, J. A., Fowler, C., Stroeve, J., Drobot, S., Zwally, J., Yi, D., and Emery, W. (2007). A younger, thinner Arctic ice cover: Increased potential for rapid, extensive sea-ice loss. Geophysical Research Letters, 34(24), L24501.

McCarthy, J. J. (2002). Biological responses to nutrients. The Sea, 12, 219-244.

McLaughlin, F., Carmack, E., Macdonald, R., Weaver, A. J., and Smith, J. (2002). The Canada Basin, 1989–1995: Upstream events and far-field effects of the Barents Sea. Journal of Geophysical Research, 107(C7), 3082.

McLaughlin, F. A., E. C. Carmack, R. W. Macdonald, H. Melling, J. H. Swift, P. A. Wheeler, B. F. Sherr, and E. B. Sherr. (2004). The joint roles of Pacific and Atlantic-origin waters in the Canada Basin, 1997–1998. Deep Sea Research Part I: Oceanographic Research Papers, 51(1), 107-128.

McLaughlin, F. A., Carmack, E. C., Ingram, R. G., Williams, W., and Michel, C. (2006). Oceanography of the Northwest passage. The Sea, 14, 1213-1244.

Michel, C., A. Riedel, and C.J. Mundy. (2003). Biological Investigation of First-Year Sea Ice near Resolute Bay, Nunavut, Spring to Early Summer 2001. Can. Data Rep. Hydrogr. Ocean Sci. 160: vi + 29 p.

Michel, C., Ingram, R. G., and Harris, L. R. (2006). Variability in oceanographic and ecological processes in the Canadian Arctic Archipelago. Progress in Oceanography, 71(2), 379-401.

Miller, C. B., and Wheeler, P. A. (2012). Biological Oceanography. Wiley-Blackwell.

Mobley, C. D. (1995). The optical properties of water. Handbook of optics, 2.

Morata, N., Poulin, M., and Renaud, P. E. (2011). A multiple biomarker approach to tracking the fate of an ice algal bloom to the sea floor. *Polar biology, 34*(1), 101-112.

Mundy, C. J., Barber, D. G., and Michel, C. (2005). Variability of snow and ice thermal, physical and optical properties pertinent to sea ice algae biomass during spring. Journal of Marine Systems, 58(3), 107-120.

Mundy, C.J., Gosselin, M., Ehn, J.K., Gratton, Y., Rossnagel, A.L., Barber, D.G., Martin, J. Tremblay, J.-E., Palmer, M., Arrigo, K., Darnis, G., Fortier, L., Else, B., and Papakyriakou, T.N. (2009). Contribution of under-ice primary production to an ice-edge upwelling phytoplankton bloom in the Canadian Beaufort Sea. Geophysical Research Letter. 36, L17601.

Müller, P., Li, X. P., and Niyogi, K. K. (2001). Non-photochemical quenching. A response to excess light energy. Plant Physiology, 125(4), 1558-1566.
Nelson, D. L., Lehninger, A. L., and Cox, M. M. (2008). Lehninger principles of biochemistry. Macmillan.

Nghiem, S. V., Rigor, I. G., Perovich, D. K., Clemente-Colón, P., Weatherly, J. W., and Neumann, G. (2007). Rapid reduction of Arctic perennial sea ice.Geophysical Research Letters, 34(19), L19504.

Nicolaus, M., Katlein, C., Maslanik, J., and Hendricks, S. (2012). Changes in Arctic sea ice result in increasing light transmittance and absorption. Geophysical Research Letters, 39(24).

Niyogi, K. K., Björkman, O., and Grossman, A. R. (1997). The roles of specific xanthophylls in photoprotection. Proceedings of the National Academy of Sciences, 94(25), 14162-14167.

O'Reilly, J. E., Maritorena, S., Mitchell, B. G., Siegel, D. A., Carder, K. L., Garver, S. A., Kahru, M., and McClain, C. (1998). Ocean color chlorophyll algorithms for SeaWiFS. Journal of Geophysical Research: Oceans (1978–2012), 103(C11), 24937-24953.

Overland, J. E., Wang, M., and Salo, S. (2008). The recent Arctic warm period.Tellus A, 60(4), 589-597.

Pabi, S., van Dijken, G. L., and Arrigo, K. R. (2008). Primary production in the Arctic Ocean, 1998–2006. Journal of Geophysical Research: Oceans (1978–2012), 113(C8).

Palmer, M.A., van Dijken, G.L., Mitchell, G., Seegers, B.J., Lowry, K.E., Mills, M.M., Arrigo, K.R., (2013). Light and nutrient control of photosynthesis in natural phytoplankton populations from the Chukchi and Beaufort seas, Arctic Ocean Limnol. Oceanogr., 58(6), 2185–2205

Papakyriakou, T. N. (1999). An examination of relationships among the energy balance, surface properties and climate over snow covered sea ice during the spring season. University of Waterloo.

Parsons TR, Maita Y, Lali CM (1984). A manual of chemical and biological methods for seawater analysis. Pergamon Press

Partensky, F., Blanchot, J., and Vaulot, D. (1999). Differential distribution and ecology of Prochlorococcus and Synechococcus in oceanic waters: a review. Bulletin-Institut Oceanographique Monaco-Numero Special -, 457-476.

Perovich DK, Cota GF, Grenfell TC, Maykut GA (1993). Bio-optical observations of first-year arctic sea ice. Geophys Res Lett 20:1059–1062

Perovich, D. K. (1996). The Optical Properties of Sea Ice (No. MONO-96-1). COLD REGIONS RESEARCH AND ENGINEERING LAB HANOVER NH.

Perovich, D. K. and A. J. Gow (1996B), A quantitative description of sea ice inclusions, J. Geophys. Res., 101(C8), 18327-18343

Perovich, D. K., Grenfell, T. C., Light, B., and Hobbs, P. V. (2002a). Seasonal evolution of the albedo of multiyear Arctic sea ice. Journal of Geophysical Research, 107(C10), 8044.

Perovich, D. K., Tucker III, W. B., and Ligett, K. A. (2002b). Aerial observations of the evolution of ice surface conditions during summer. Journal of Geophysical Research, 107(C10), 8048.

Peterson, B. J., McClelland, J., Curry, R., Holmes, R. M., Walsh, J. E., and Aagaard, K. (2006). Trajectory shifts in the Arctic and subarctic freshwater cycle. Science, 313(5790), 1061-1066.

Petzold, D. E., (1977). An estimation technique for snow surface albedo. Climat. Bull., 21, 1-11.

Pineault, S., Tremblay, J. É., Gosselin, M., Thomas, H., and Shadwick, E. (2013). The isotopic signature of particulate organic C and N in bottom ice: Key influencing factors and applications for tracing the fate of ice-algae in the Arctic Ocean. *Journal of Geophysical Research: Oceans*, *118*(1), 287-300.

Polashenski, C., Perovich, D., and Courville, Z. (2012). The mechanisms of sea ice melt pond formation and evolution. Journal of Geophysical Research, 117(C1), C01001.

Pope, R. M., and Fry, E. S. (1997). Absorption spectrum (380–700 nm) of pure water. II. Integrating cavity measurements. Applied optics, 36(33), 8710-8723.

Polyakov, I. V., Beszczynska, A., Carmack, E. C., Dmitrenko, I. A., Fahrbach, E., Frolov, I. E., and Walsh, J. E. (2005). One more step toward a warmer Arctic. Geophysical Research Letters, 32(17), L17605.

Prieur, L., and Sathyendranath, S. (1981). An optical classification of coastal and oceanic waters based on the specific spectral absorption curves of phytoplankton pigments, dissolved organic matter, and other particulate materials. Limnology and Oceanography, 26(4), 671-689.

Prinsenberg, S. J., and Bennett, E. B. (1987). Mixing and transports in Barrow Strait, the central part of the Northwest Passage. Continental Shelf Research,7(8), 913-935.

Prinsenberg, S. J., and Grant Ingram, R. (1991). Under-ice physical oceanographic processes. Journal of Marine Systems, 2(1), 143-152.

Rampal, P., Weiss, J., and Marsan, D. (2009). Positive trend in the mean speed and deformation rate of Arctic sea ice, 1979–2007. Journal of Geophysical Research, 114(C5), C05013.

Raven P.H., Evert R.F., Eichhorn S.E. (2005). Biology of Plants, (7th ed.). New York: W.H. Freeman and Company Publishers. pp. 124–127. ISBN 0-7167-1007-2.

Redfield, A. C., Ketchum, B. H., and Richards, F. A. The influence of organisms on the composition of sea-water, Hill MN, The Sea vol. 2, 1963, 26-77. Inter Science, New York.

Riebesell, U., and Wolf-Gladrow, D. A. (2002). Supply and uptake of inorganic nutrients. Phytoplankton productivity: carbon assimilation in marine and freshwater ecosystems, 109-140.

Robinson, D., Arrigo, K., Iturriaga, R., Sullivan, C., (1995). Microalgal light-harvesting in extreme low-light environments in McMurdo Sound, Antarctica. J. Phycol. 31, 508-520.
Romanov, I. P. (2001). Atlas of ice and snow of the Arctic Basin and Siberian shelf seas. A. Tunik (Ed.). Backbone Publishing Company.

Rowan, K. S. (1989). Photosynthetic pigments of algae. CUP Archive.

Rysgaard S, Nielsen TG, Hansen BW (1999). Seasonal variation in nutrients, pelagic primary production and grazing in a high-Arctic coastal marine ecosystem, Young Sound, Northeast Greenland. Mar Ecol Prog Ser 179: 13−25

Sakshaug, E., and Skjoldal, H. R. (1989). Life at the ice edge. Ambio (Sweden).

Sakshaug, E. (2004). Primary and secondary production in the Arctic Seas, in The Organic Carbon Cycle in the Arctic Ocean, edited by R. Stein and R. W. Macdonald, pp. 57–81, Springer-Verlag, Berlin.

Sathyendranath, S., Longhurst, A., Caverhill, C. M., and Platt, T. (1995). Regionally and seasonally differentiated primary production in the North Atlantic. Deep Sea Research Part I: Oceanographic Research Papers, 42(10), 1773-1802.

Schauer, U., Loeng, H., Rudels, B., Ozhigin, V. K., and Dieck, W. (2002). Atlantic water flow through the Barents and Kara Seas. Deep Sea Research Part I: Oceanographic Research Papers, 49(12), 2281-2298.

Schweiger, A. J. (2004). Changes in seasonal cloud cover over the Arctic seas from satellite and surface observations. Geophysical research letters, 31(12), L12207.

Schweiger, A. J., Zhang, J., Lindsay, R. W., and Steele, M. (2008). Did unusually sunny skies help drive the record sea ice minimum of 2007?. Geophysical Research Letters, 35(10), L10503.

Scott Pegau, W., and Paulson, C. A. (2001). The albedo of Arctic leads in summer. Annals of Glaciology, 33(1), 221-224.

Serreze, M. C., and Hurst, C. M. (2000). Representation of mean Arctic precipitation from NCEP-NCAR and ERA reanalyses. Journal of Climate, 13(1), 182-201.

Sherr, E. B., Sherr, B. F., and Hartz, A. J. (2009). Microzooplankton grazing impact in the Western Arctic Ocean. Deep Sea Research Part II: Topical Studies in Oceanography, 56(17), 1264-1273.

Simmonds, I., Burke, C., and Keay, K. (2008). Arctic climate change as manifest in cyclone behavior. Journal of Climate, 21(22), 5777-5796.

Smith, W. O., and Sakshaug, E. (1990). Autotrophic processes in polar regions. Polar Oceanography. Part B. Academic Press, San Diego, 477-525.

Søreide, J. E., Leu, E. V. A., Berge, J., Graeve, M., and Falk-Petersen, S. T. I. G. (2010). Timing of blooms, algal food quality and Calanus glacialis reproduction and growth in a changing Arctic. Global Change Biology, 16(11), 3154-3163.

Strass, V. H., and Nöthig, E. M. (1996). Seasonal shifts in ice edge phytoplankton blooms in the Barents Sea related to the water column stability. Polar Biology, 16(6), 409-422.

Stroeve, J. C., Serreze, M. C., Holland, M. M., Kay, J. E., Malanik, J., and Barrett, A. P. (2012). The Arctic's rapidly shrinking sea ice cover: a research synthesis. Climatic Change, 110(3-4), 1005-1027.

Sverdrup, H. U. (1953). On Conditions for the Vernal Blooming of Phytoplankton J. Cons. int. Explor. Mer 18(3): 287-295

Takahashi, T., Sutherland, S. C., Wanninkhof, R., Sweeney, C., Feely, R. A., Chipman, D. W., and De Baar, H. J. (2009). Climatological mean and decadal change in surface ocean pCO2, and net sea–air CO2 flux over the global oceans. Deep Sea Research Part II: Topical Studies in Oceanography, 56(8), 554-577.

Thomas, D. N., and Dieckmann, G. S. (Eds.). (2009). Sea ice. Wiley-Blackwell.

Tremblay, J. É., Simpson, K., Martin, J., Miller, L., Gratton, Y., Barber, D., and Price, N. M. (2008). Vertical stability and the annual dynamics of nutrients and chlorophyll fluorescence in the coastal, southeast Beaufort Sea. Journal of Geophysical Research: Oceans (1978–2012), 113(C7).

Tschudi, M. A., Curry, J. A., and Maslanik, J.A. (2001). effect on surface albedo during FIRE/SHEBA. Journal of geophysical research, 106(D14), 15-335.

Untersteiner, N. (1968). Natural desalination and equilibrium salinity profile of perennial sea ice. Journal of Geophysical Research, 73(4), 1251-1257.

Vézina, A. F., Demers, S., Laurion, I., Sime-Ngando, T., Kim Juniper, S., and Devine, L. (1997). Carbon flows through the microbial food web of first-year ice in Resolute Passage (Canadian High Arctic). Journal of marine systems, 11(1), 173-189.

Wang. M., and Overland, J. E. (2009). A sea ice free summer arctic within 30 years? Geophys Res Lett 36: L07502.

Wang, S. W., Budge, S. M., Gradinger, R. R., Iken, K., and Wooller, M. J. (2014). Fatty acid and stable isotope characteristics of sea ice and pelagic particulate organic matter in the Bering Sea: tools for estimating sea ice algal contribution to Arctic food web production. *Oecologia*, *174*(3), 699-712.

Warren, S. G. and Wiscombe, W. J. (1981). A model for the spectral albedo of snow. I: Snow containing atmospheric aerosols. J. Atmos. Sci., 37, 2735-2745.

Warren, S. G., Rigor, I. G., Untersteiner, N., Radionov, V. F., Bryazgin, N. N., Aleksandrov, Y. I., and Colony, R. (1999). Snow depth on Arctic sea ice. Journal of Climate, *12*(6), 1814-1829.

Weeks, W. F., and Ackley, S. F. (1982). The growth, structure, and properties of sea ice (No. CRREL-MONO-82-1). Cold Regionss Research and Engineering Lab Hanover NH.

Wiktor, J. (1999). Early spring microplankton development under fast ice covered fjords of Svalbard, Arctic. Oceanologia.

Woodgate, R. A., Aagaard, K., and Weingartner, T. J. (2005). Monthly temperature, salinity, and transport variability of the Bering Strait through flow.Geophysical Research Letters, 32(4).

Woodgate, R. A., Aagaard, K., and Weingartner, T. J. (2006). Interannual changes in the Bering Strait fluxes of volume, heat and freshwater between 1991 and 2004. Geophysical Research Letters, 33(15), L15609

Wright, S. W., Jeffrey, S. W., and Mantoura, R. F. C. (Eds.). (2005). Phytoplankton pigments in oceanography: guidelines to modern methods. Unesco Pub..

Zapata, M., Rodriguez, F., and Garrido, J. L. (2000). Separation of chlorophylls and carotenoids from marine phytoplankton: a new HPLC method using a reversed phase C8 column and pyridine-containing mobile phases. Marine Ecology Progress Series, 195, 29-45.

Zhang, T., Stamnes, K., and Bowling, S. A. (1996). Impact of clouds on surface radiative fluxes and snowmelt in the Arctic and subarctic. Journal of Climate, 9(9), 2110-2123.

Appendix A: Day of Year Chart Conversion

Non-Leap Year												
DATE	**JAN**	**FEB**	**MAR**	**APR**	**MAY**	**JUN**	**JUL**	**AUG**	**SEP**	**OCT**	**NOV**	**DEC**
1	1	32	60	91	121	152	182	213	244	274	305	335
2	2	33	61	92	122	153	183	214	245	275	306	336
3	3	34	62	93	123	154	184	215	246	276	307	337
4	4	35	63	94	124	155	185	216	247	277	308	338
5	5	36	64	95	125	156	186	217	248	278	309	339
6	6	37	65	96	126	157	187	218	249	279	310	340
7	7	38	66	97	127	158	188	219	250	280	311	341
8	8	39	67	98	128	159	189	220	251	281	312	342
9	9	40	68	99	129	160	190	221	252	282	313	343
10	10	41	69	100	130	161	191	222	253	283	314	344
11	11	42	70	101	131	162	192	223	254	284	315	345
12	12	43	71	102	132	163	193	224	255	285	316	346
13	13	44	72	103	133	164	194	225	256	286	317	347
14	14	45	73	104	134	165	195	226	257	287	318	348
15	15	46	74	105	135	166	196	227	258	288	319	349
16	16	47	75	106	136	167	197	228	259	289	320	350
17	17	48	76	107	137	168	198	229	260	290	321	351
18	18	49	77	108	138	169	199	230	261	291	322	352
19	19	50	78	109	139	170	200	231	262	292	323	353
20	20	51	79	110	140	171	201	232	263	293	324	354
21	21	52	80	111	141	172	202	233	264	294	325	355
22	22	53	81	112	142	173	203	234	265	295	326	356
23	23	54	82	113	143	174	204	235	266	296	327	357
24	24	55	83	114	144	175	205	236	267	297	328	358
25	25	56	84	115	145	176	206	237	268	298	329	359
26	26	57	85	116	146	177	207	238	269	299	330	360
27	27	58	86	117	147	178	208	239	270	300	331	361
28	28	59	87	118	148	179	209	240	271	301	332	362
29	29		88	119	149	180	210	241	272	302	333	363
30	30		89	120	150	181	211	242	273	303	334	364
31	31		90		151		212	243		304		365

Leap Year												
DATE	**JAN**	**FEB**	**MAR**	**APR**	**MAY**	**JUN**	**JUL**	**AUG**	**SEP**	**OCT**	**NOV**	**DEC**
1	1	32	61	92	122	153	183	214	245	275	306	336
2	2	33	62	93	123	154	184	215	246	276	307	337
3	3	34	63	94	124	155	185	216	247	277	308	338
4	4	35	64	95	125	156	186	217	248	278	309	339
5	5	36	65	96	126	157	187	218	249	279	310	340
6	6	37	66	97	127	158	188	219	250	280	311	341
7	7	38	67	98	128	159	189	220	251	281	312	342
8	8	39	68	99	129	160	190	221	252	282	313	343
9	9	40	69	100	130	161	191	222	253	283	314	344
10	10	41	70	101	131	162	192	223	254	284	315	345
11	11	42	71	102	132	163	193	224	255	285	316	346
12	12	43	72	103	133	164	194	225	256	286	317	347
13	13	44	73	104	134	165	195	226	257	287	318	348
14	14	45	74	105	135	166	196	227	258	288	319	349
15	15	46	75	106	136	167	197	228	259	289	320	350
16	16	47	76	107	137	168	198	229	260	290	321	351
17	17	48	77	108	138	169	199	230	261	291	322	352
18	18	49	78	109	139	170	200	231	262	292	323	353
19	19	50	79	110	140	171	201	232	263	293	324	354
20	20	51	80	111	141	172	202	233	264	294	325	355
21	21	52	81	112	142	173	203	234	265	295	326	356
22	22	53	82	113	143	174	204	235	266	296	327	357
23	23	54	83	114	144	175	205	236	267	297	328	358
24	24	55	84	115	145	176	206	237	268	298	329	359
25	25	56	85	116	146	177	207	238	269	299	330	360
26	26	57	86	117	147	178	208	239	270	300	331	361
27	27	58	87	118	148	179	209	240	271	301	332	362
28	28	59	88	119	149	180	210	241	272	302	333	363
29	29	60	89	120	150	181	211	242	273	303	334	364
30	30		90	121	151	182	212	243	274	304	335	365
31	31		91		152		213	244		305		366
**** Leap Years In Study: 1984, 1988, 1992, 2012**												